

THE ROLES OF DNMT1 CYTOSINE METHYLTRANSFERASE PROTEINS IN  
GENOMIC REPROGRAMMING DURING MOUSE PREIMPLANTATION  
DEVELOPMENT.

By

Sarayu Ratnam

B.Sc, Stella Maris College, 1997

M.Sc, Madras University, 1999

Submitted to the Graduate Faculty of  
Graduate School of Public Health in partial fulfillment  
of the requirements for the degree of  
Doctor of Philosophy

University of Pittsburgh

2004

UNIVERSITY OF PITTSBURGH  
GRADUATE SCHOOL OF PUBLIC HEALTH

This dissertation was presented

by

Sarayu Ratnam

It was defended on

April 1, 2004

and approved by

Dr. Robert Ferrell, Ph.D.  
Associate Professor  
Department of Human Genetics  
Graduate School of Public Health

Dr. Urvashi Surti, Ph.D.  
Associate Professor  
Department of Cellular and Molecular Pathology  
School of Medicine

Dr. Martin Schmidt, Ph.D.  
Associate Professor  
Department of Biochemistry and Molecular Genetics  
School of Medicine

Dr. J. Richard Chaillet, M.D., Ph.D.  
Dissertation Director  
Associate Professor  
Department of Biochemistry and Molecular Genetics  
School of Medicine

# THE ROLES OF DNMT1 CYTOSINE METHYLTRANSFERASE PROTEINS IN GENOMIC REPROGRAMMING DURING MOUSE PREIMPLANTATION DEVELOPMENT.

Sarayu Ratnam, PhD

University of Pittsburgh, 2004

Inheritance of DNA methylation on imprinted genes depends on the Dnmt1 (cytosine-5-) methyltransferase protein. Methylation patterns on imprinted genes are maintained by oocyte-specific Dnmt1 $\alpha$  isoform at the 8-cell stage of preimplantation development. Methylation patterns in postimplantation embryos are maintained by the Dnmt1 $\beta$  isoform. To determine if Dnmt1 $\beta$  can functionally replace Dnmt1 $\alpha$ , we expressed Dnmt1 $\beta$  in oocytes and discovered that Dnmt1 $\beta$  can maintain genomic imprints in the absence of Dnmt1 $\alpha$ . However, the ability of Dnmt1 $\beta$  to maintain imprinting is dependant on the level of oocyte Dnmt1 $\beta$ . Though Dnmt1 $\beta$  and Dnmt1 $\alpha$  have equivalent maintenance methyltransferase functions in oocytes, the unstable nature of oocyte Dnmt1 $\beta$ , in comparison to oocyte Dnmt1 $\alpha$ , leads to levels lower than what are required to maintain methylation at the 8-cell stage. We also determined that in cloned embryos, Dnmt1 $\alpha$  undergoes none of its expected trafficking to 8-cell stage nuclei. Instead, these embryos exhibit a mosaic pattern of Dnmt1 $\beta$  expression. Defects in intracellular trafficking of Dnmt1 $\alpha$  and misexpression of Dnmt1 $\beta$ , along with the intrinsic instability of Dnmt1 $\beta$ , might contribute to

aberrant DNA methylation in cloned embryos, thus raising concerns about the use of current cloning technologies for therapeutic cloning.

Molecular mechanisms involved in the formation of ovarian teratomas were also analyzed. Unfertilized oocytes arrest at the MII stage of meiotic maturation. After fertilization, oocytes continue into cell division. Premature activation of MII oocytes without fertilization, can lead to ovarian teratoma formation. To better understand mechanisms governing the prevention of spontaneous oocyte activation, we investigated the molecular defects leading to formation of ovarian teratomas in the *Tgkd* mouse model. *Tgkd* is a transgene insertional mutation that leads to reduced levels of the Inpp4b protein in MII oocytes of hemizygous *Tgkd* females. Wildtype GV oocytes have less Inpp4b protein than MII oocytes, and a significant decrease in Inpp4b is also seen after fertilization. Also, the dependence of ovarian teratoma formation on the mouse strain, emphasizes the role of a strain-specific modifier on chromosome 6, possibly IP<sub>3</sub>1. Thus, it is possible that oocyte Inpp4b normally suppresses spontaneous MII oocyte activation, possibly by reducing levels of IP<sub>3</sub>, an intermediate in the oocyte activation mechanism, that occurs following fertilization.

## **Acknowledgements**

I am very grateful to Dr. Richard Chaillet for having been a great advisor and given me the opportunity to work on some exciting projects in his lab. He has been a constant source of encouragement and support and his enthusiasm for research has always been an inspiration. I would also like to thank my committee members, Dr. Robert Ferrell, Dr. Urvashi Surti and Dr. Martin Schmidt for all their help and guidance rendered during my graduate school experience.

Special thanks to all the past and present members of the Chaillet lab who have made the lab a wonderful place to work in, especially, Bonnie Reinhart, Feng Ding and Kathryn Kumer who have always been very supportive both professionally and personally. Thanks to my collaborators Keith Latham and Jaquetta Trasler for all their help and suggestions with my projects. I also thank Tom Harper for his help with the confocal microscope.

I am extremely grateful to my parents, Bhanu and Sankar Ratnam and my brother Sharad Ratnam, for all their love and encouragement. They have always been there for me and none of this would have been possible without their constant faith and support. I am indebted to my aunt and uncle, Prabha and Sankar for having been my parents away from home and given me all the support I need.

Last, but definitely not the least, a big thanks to my wonderful husband, Kashyap Muthuraman for having been a source of constant encouragement. He has always been the comfort to come home to after a hard day at work.

## TABLE OF CONTENTS

1. Role of Dnmt1 cytosine methyltransferases in genomic imprinting during mouse preimplantation development.....	1
1.1. Introduction.....	1
1.1.1. Genomic imprinting in humans.....	1
1.1.2. Genomic imprinting in mice .....	8
1.1.2.1. Imprinted gene loci in the mouse.....	9
1.1.3. The imprinting mark.....	9
1.1.4. DNA Methylation.....	10
1.1.4.1. DNA methylation during mammalian development.....	14
1.1.4.2. DNA methylation and imprinting.....	17
1.1.5. DNA Methyltransferases .....	18
1.1.5.1. Dnmt1 methyltransferase .....	18
1.1.5.2. Dnmt3 methyltransferases.....	21
1.1.5.3. Dnmt2 methyltransferase .....	23
1.1.5.4. The isoforms of Dnmt1 protein .....	23
1.1.6. Cloning and methylation.....	27
1.1.6.1. Methylation reprogramming in cloned animals.....	29
1.1.6.2. Dnmt1 methyltransferase in cloned animals .....	30
1.1.7. Specific aims .....	31
1.1.7.1. Specific aim 1 .....	31
1.1.7.2. Specific Aim 2 .....	31
1.2. Results .....	33
1.2.1. Functional analysis of Dnmt1s protein in the presence of Dnmt1o protein .....	33
1.2.1.1. Expression of Dnmt1s protein in the <i>Dnmt1<sup>1s/1o</sup></i> females during oogenesis	40
1.2.1.2. Expression of the Dnmt1s protein in the <i>Dnmt1s-TG1</i> and <i>Dnmt1s-TG2</i> females during oogenesis .....	40
1.2.1.3. Localization and trafficking of the Dnmt1s protein during oogenesis and preimplantation development .....	41
1.2.1.4. Methylation of imprinted genes with forced expression of Dnmt1s protein.	46
1.2.2. Functional analysis of Dnmt1s protein in Dnmt1o-deficient mice .....	53
1.2.2.1. Expression of the Dnmt1s protein in the <i>Dnmt1s-TG1/ Dnmt1<sup>Δ1o</sup></i> females during oogenesis .....	53
1.2.2.2. Localization and trafficking of the Dnmt1s protein in Dnmt1o-deficient mice during oogenesis and preimplantation development.....	54

1.2.2.3.	Restoration of genomic imprinting in offspring derived from <i>Dnmt1s-TG1/Dnmt1<sup>Δlo</sup></i> mice.....	54
1.2.2.4.	Expression of imprinted genes in offspring derived from <i>Dnmt1s-TG1/Dnmt1<sup>Δlo</sup></i> females .....	65
1.2.2.5.	Analysis of genomic imprinting in embryos obtained from <i>Dnmt1s-TG2/Dnmt1<sup>Δlo</sup></i> females .....	66
1.2.2.6.	<i>Dnmt1o</i> versus <i>Dnmt1s</i> protein during preimplantation development.....	84
1.2.2.7.	Maintenance methyltransferase activity of oocyte-derived <i>Dnmt1s</i> and <i>Dnmt1o</i> proteins.....	85
1.2.2.8.	Stability of oocyte-derived <i>Dnmt1s</i> and <i>Dnmt1o</i> proteins during preimplantation development .....	89
1.2.3.	<i>Dnmt1</i> expression in cloned preimplantation embryos .....	92
1.2.3.1.	Aberrant expression of <i>Dnmt1s</i> protein in cloned preimplantation embryos	93
1.2.3.2.	Lack of <i>Dnmt1o</i> expression in the nuclei of 8-cell cloned embryos .....	100
1.2.3.3.	Quantitative analysis of aberrant <i>Dnmt1s</i> expression in nuclei of eight-cell stage embryos .....	104
1.3.	Materials and Methods .....	108
1.3.1.	Functional significance of <i>Dnmt1s</i> during preimplantation development.....	108
1.3.1.1.	Generation of mice that exogenously expressed <i>Dnmt1s</i> during oogenesis	108
1.3.1.2.	Generation of mice that contain a targeted replacement of exon 1s for exon 1o at the <i>Dnmt1</i> locus.....	108
1.3.1.3.	Generation of constructs and mice containing transgenes to exogenously express <i>Dnmt1s</i> during oogenesis.....	109
1.3.1.4.	Collection of oocytes and preimplantation embryos .....	110
1.3.1.5.	Immunoblot blot analysis .....	111
1.3.1.6.	Immunofluorescence analysis .....	112
1.3.1.7.	PCR genotyping.....	113
1.3.1.8.	DNA isolation.....	114
1.3.1.9.	Bisulfite genomic sequencing technique for DNA methylation analysis ...	114
1.3.1.10.	DNA sequence analysis.....	117
1.3.1.11.	Analysis of imprinted gene expression .....	118
1.3.1.12.	Methyltransferase activity assay .....	120
1.3.2.	Cloning and methylation.....	120
1.3.2.1.	Production of cloned embryos.....	120
1.3.2.2.	Production of tetraploid embryos .....	122
1.3.2.3.	Production of Parthenogenetic embryos .....	122
1.3.2.4.	Immunofluorescence analysis .....	123
1.3.2.5.	Quantitative analysis of <i>Dnmt1s</i> staining in nuclei of 8-cell embryos .....	123
1.4.	Discussion.....	124
1.4.1.	Functional significance of the <i>Dnmt1s</i> and <i>Dnmt1o</i> proteins during mouse preimplantation development .....	124

1.4.2.	The dynamics of Dnmt1s and Dnmt1o proteins in cloned mouse preimplantation embryos	128
2.	Role of Inpp4b and IP <sub>3</sub> R1 proteins in egg activation and formation of ovarian teratomas in mice	135
2.1.	Introduction	135
2.1.1.	Oocyte maturation and egg activation	135
2.1.1.1.	Cytostatic factor in oogenesis and egg activation	136
2.1.1.2.	The role of Ca <sup>++</sup> signaling at fertilization	137
2.1.2.	Ovarian teratomas	139
2.1.2.1.	Origin of ovarian teratoma	139
2.1.2.2.	Genetic analysis of ovarian teratomas	140
2.1.2.3.	Ovarian teratomas in genetically susceptible mouse strains	141
2.1.2.4.	Role of strain-specific modifier genes in ovarian teratoma formation	144
2.1.3.	Ovarian teratomas in the <i>Tgkd</i> line	145
2.1.3.1.	<i>Tgkd</i> allele as an insertional mutation	146
2.1.3.2.	Strain-specific effects on <i>Tgkd</i> ovarian teratomas	151
2.1.3.3.	Type of Meiotic error	153
2.1.4.	Specific Aims	155
2.1.4.1.	Specific Aim 1	155
2.1.4.2.	Specific Aim 2	156
2.2.	Results	157
2.2.1.	Role of Inpp4b in the formation of ovarian teratomas	157
2.2.1.1.	Measurement of Inpp4b protein levels in wildtype and <i>Tgkd</i> oocytes	157
2.2.1.2.	Measurement of <i>Inpp4b</i> mRNA levels in wildtype and <i>Tgkd</i> oocytes	158
2.2.1.3.	Measurement of Inpp4b activity in wildtype and <i>Tgkd</i> oocytes	161
2.2.1.4.	Inpp4b as a cytostatic factor	162
2.2.1.5.	Localization of Inpp4b protein in the MII oocyte	164
2.2.2.	Role of IP <sub>3</sub> R1 in the formation of ovarian teratomas	167
2.2.2.1.	Measurement of IP <sub>3</sub> R1 protein levels in the MII oocytes	170
2.2.2.2.	Analysis of sequence differences in the <i>Itpr1</i> gene among various strains of mice	170
2.3.	Materials and Methods	176
2.3.1.	Collection of oocytes and preimplantation embryos	176
2.3.2.	Role of Inpp4b in ovarian teratoma formation	177
2.3.2.1.	Immunoblot analysis	177
2.3.2.2.	Immunofluorescence analysis	178
2.3.2.3.	RT-PCR assay	178
2.3.2.4.	Inpp4b activity assay	179
2.3.3.	Role of IP <sub>3</sub> R1 in ovarian teratoma formation	180
2.3.3.1.	Immunoblot analysis	180
2.3.3.2.	Analysis of c-DNA for sequence differences in <i>Itpr1</i> gene	181

2.4. Discussion.....	184
2.4.1. Role of <i>Inpp4b</i> disruption on the formation of <i>Tgkd</i> ovarian teratomas .....	185
2.4.2. IP <sub>3</sub> R1 as a probable candidate for control of spontaneous egg activation.....	189
BIBLIOGRAPHY .....	195

## LIST OF TABLES

Table 1. Mapped parent-of-origin gene effects in humans .....	3
Table 2. Mouse imprinted regions and genes.....	6
Table 3. Percentage of CpG dinucleotide methylation in imprinted genes .....	80
Table 4. Paired Student T-test for analysis of methylation differences in imprinted genes .....	82
Table 5. Activity of Dnmt1 methyltransferase in mouse oocyte.....	86
Table 6. Types of errors that lead to formation of ovarian teratomas .....	142
Table 7. Measurement of Inpp4b activity in mouse ovary .....	162
Table 8. Single Nucleotide polymorphisms (SNPs) in <i>Itp1</i> cDNA between different strains of mice.....	174
Table 9. Primers to analyze <i>Itp1</i> c-DNA for SNPs .....	182

## LIST OF FIGURES

Figure 1. States of DNA methylation in the mammalian genome .....	12
Figure 2. Dynamics of DNA methylation patterns during mouse development.....	15
Figure 3. Structure of the known DNA Methyltransferases (Dnmt's).....	19
Figure 4. Sex-specific exons and oocyte-specific species of Dnmt1.....	25
Figure 5. <i>Dnmt1</i> <sup>1s/1o</sup> allele. ....	34
Figure 6. <i>Dnmt1s</i> transgene.....	36
Figure 7. Dnmt1s expression in oocytes from <i>Dnmt1s-TG1</i> and <i>Dnmt1</i> <sup>Δ1o</sup> mice .....	38
Figure 8. Expression and localization of Dnmt1 proteins during preimplantation development. 42	
Figure 9. Expression and localization of Dnmt1s protein, in the absence of Dnmt1o protein, during preimplantation development .....	44
Figure 10. Analysis of DNA methylation using bisulfite genomic sequencing.....	47
Figure 11. Analysis of imprinted gene methylation in <i>Dnmt1s-TG1</i> mice.....	49
Figure 12. Analysis of imprinted gene methylation in <i>Dnmt1</i> <sup>1s/1o</sup> mice.....	51
Figure 13. Analysis of imprinted gene methylation in survivors obtained from <i>Dnmt1s-TG1/Dnmt1</i> <sup>Δ1o</sup> females. ....	55
Figure 14. Analysis of <i>H19</i> methylation in day 13.5 embryos obtained from <i>Dnmt1s-TG1/Dnmt1</i> <sup>Δ1o</sup> females. ....	59
Figure 15. Analysis of <i>Snrpn</i> methylation in day 13.5 embryos obtained from <i>Dnmt1s-TG1/Dnmt1</i> <sup>Δ1o</sup> females.....	61
Figure 16. Analysis of <i>Peg3</i> methylation in day 13.5 embryo obtained from <i>Dnmt1s-TG1/Dnmt1</i> <sup>Δ1o</sup> females. ....	63
Figure 17 Analysis of imprinted gene expression using Single Nucleotide Primer Extension (SNuPE) .....	67
Figure 18. Expression analysis of imprinted genes. ....	69
Figure 19. Analysis of imprinted gene methylation in day 13.5 embryos obtained from homozygous <i>Dnmt1</i> <sup>Δ1o</sup> females on a FVB/N background.....	72
Figure 20. Analysis of imprinted gene methylation in day 13.5 embryo obtained from <i>Dnmt1s-TG2/Dnmt1</i> <sup>Δ1o</sup> females. ....	74
Figure 21. Analysis of imprinted gene methylation in day 13.5 embryo obtained from heterozygous <i>Dnmt1</i> <sup>Δ1o</sup> female on a FVB/N background. ....	76

Figure 22. Methylation analysis of imprinted genes. ....	78
Figure 23. Stability of the Dnmt1o protein. ....	90
Figure 24. Immunostaining of normal and cloned preimplantation mouse embryos with the UPT82 antibody. ....	94
Figure 25. UPT82 immunostaining of cloned eight-cell embryos derived by either a delayed- or an immediate-activation protocol. ....	96
Figure 26. Immunostaining of normal and cloned preimplantation mouse embryos with the PATH52 antibody, which recognizes both Dnmt1o and Dnmt1s. ....	98
Figure 27. Analysis of mosaic Dnmt1s and Dnmt1o protein expression in mutant and cloned embryos using simultaneous immunostaining with UPT82 and UPTC21 antibodies. ....	101
Figure 28. Quantitative analysis of nuclear staining for Dnmt1 proteins in cloned embryos, wildtype embryos and fertilized embryos from Dnmt1o-deficient oocytes. ....	105
Figure 29. Hypothesis to explain the dynamics of Dnmt1 proteins in cloned preimplantation development. ....	133
Figure 30. Schematics of <i>RSVlgmyc</i> transgene and its insertion in <i>Tgkd</i> mice. ....	149
Figure 31. Inpp4b expression in MII oocytes. ....	159
Figure 32. Expression of Inpp4b protein during oogenesis and fertilization. ....	165
Figure 33. Localization of Inpp4b protein in MII oocyte. ....	168
Figure 34. Measurement of IP <sub>3</sub> R1 protein levels in MII oocytes. ....	171
Figure 35. Hypothetical role of Inpp4b during MII stage of oogenesis. ....	193

## LIST OF ABBREVIATIONS

APC/C anaphase promoting complex/cyclosome

bp basepairs

BSA bovine serum albumin

CSF cytosstatic factor

CpG cytosine guanine dinucleotide

cpm counts per minute

DAG diacylglycerol

DMD differentially methylated domain

DNA deoxyribonucleic acid

Dnmt DNA methyltransferase enzyme

EC embryonic carcinoma cells

ES cells embryonic stem cells

GV germinal vescicle

*H19* gene encoding a fetal liver mRNA

hCG human chorionic gonadotrophin  
*Igf2* Insulin-like growth factor 2 gene  
*Igf2r* Insulin-like growth factor 2 receptor gene  
IP<sub>3</sub> 1,4,5 triphosphate  
IP<sub>3</sub>1 1,4,5 triphosphate receptor 1  
Inpp4b Inositol polyphosphate-4-phosphatase  
kb kilobases  
kD kilodalton  
LH leutinizing hormone  
MII metaphase II  
MAPK mitogen activated protein kinase  
MPF maturation promoting factor  
MBD methyl-binding domain  
mRNA messenger RNA  
nt nucleotides  
OT ovarian teratoma  
*Ots1* ovarian teratoma susceptibility gene 1  
*Ots2* ovarian teratoma susceptibility gene 2  
PCR polymerase chain reaction  
*Peg3* paternally expressed gene 3  
PGC primordial germ cell

PMSG pregnant mare's serum gonadotrophin

PtdIns(4,5)P<sub>2</sub> phosphatidylinositol (4,5) biphosphate

PWWP proline-tryptophan-tryptophan-proline domain

PWS Prader-Willi syndrome

RNA ribonucleic acid

RT-PCR reverse transcription-polymerase chain reaction

SAM S-adenosylmethionine

SDS-PAGE sodium dodecyl sulfate-polyacrylamide gel electrophoresis

SNP single nucleotide polymorphism

*Snrpn* small nuclear ribonucleoprotein polypeptide N gene

UPD uniparental disomy

*ZP3* zona pellucida 3 gene

# **1. Role of Dnmt1 cytosine methyltransferases in genomic imprinting during mouse preimplantation development**

## **1.1. Introduction**

In the classical Mendelian pattern of inheritance, each parent contributes a complete set of chromosomes to its offspring and in most cases the genetic contribution of each parent is equivalent. However, a subset of mammalian genes is controlled by genomic imprinting, a process that causes a gene to be expressed from only one chromosome homologue depending on whether it originally came from the egg or the sperm (Cattanach and Beechey 1997) and this subset of genes are called imprinted genes.

### **1.1.1. Genomic imprinting in humans**

The importance of genomic imprinting for mammalian development was first shown by the occurrence of a human tumor called the hydatidiform mole. These tumors are caused due to the fertilization of an egg, without a pronucleus, by a haploid sperm. The sperm chromosome content then replicates to form an androgenetic diploid genome (Kajii and Ohama 1977; Jacobs et al. 1980). Instead of proceeding with normal development, this egg develops into a mass of extra-embryonic tissue, suggesting that normal mammalian development cannot occur with genetic information solely derived from the male parent.

Normal mammalian development also does not occur with genetic information obtained only from the female parent. This has been shown by the formation of ovarian teratomas which develop from the activation of an egg in the absence of fertilization (parthenogenesis). These ovarian teratomas consist of differentiated tissues and include endoderm, mesoderm and ectoderm but there is no evidence of placental tissues in these tumors (Linder et al. 1975).

It has been shown that genomic imprinting is also involved in a number of genetic disorders in humans like the Prader-Willi syndrome and Angelman syndrome (Table 1). Prader-Willi syndrome is caused due to the lack of expression of paternally expressed imprinted genes in region q11-q13 of human chromosome 15 while Angelman syndrome is caused due to loss of expression of maternally expressed imprinted genes within the same region (Nicholls et al. 1989). Thus, understanding the inheritance of imprinted genes is critical to our understanding of the occurrence of various diseases and disorders in humans. But the extent of analysis possible through the study of families with imprinting disorders is very limited.

The mouse can be used as an excellent model system to study genomic imprinting. There are a number of reasons for this. Mice have a relatively short gestation period, a large litter size and are easy to handle and maintain. The process of genomic imprinting is conserved between humans and mice, and many human imprinted genes have mouse homologues that are also imprinted (Table 2; Morison and Reeve 1998). The genetics of inbred mouse strains has been well characterized and the large amount of sequence information available, including single nucleotide polymorphisms (SNPs), for various laboratory mouse strains helps us analyze the inheritance of imprinted genes. Also, the ability to generate transgenic or knockout mice using

**Table 1. Mapped parent-of-origin gene effects in humans**

The table describes the imprinted loci identified in humans and has been modified from Morison and Reeve 1998. Specific regions of chromosomes or uniparental disomy (UPD) of chromosomes that give rise to imprinting disorders in humans have been listed.

**Table 1. Mapped parent-of-origin gene effects in humans**

<b>Chromosome Location</b>	<b>Parent-of-origin effect</b>
1p36	<i>p73</i> is maternally expressed and located in the region showing preferential maternal loss of heterozygosity in neuroblastoma.
UPD of chromosome 1	One case of maternal heterodisomy including partial isodisomy of 1q has been reported.
2p24	N-Myc is amplified preferentially from the paternal allele in neuroblastoma.
UPD of chromosome 2	Maternal UPD is possibly associated with an abnormal phenotype.
4q21-q22	Anomalous imprinting has been hypothesized as the reason for the central nervous system overgrowth in the 4q21/4q23 syndrome.
5q22-q31	<i>U2AFBPL</i> the human homologue of <i>U2afbp-rs</i> is imprinted in mice but not in human placenta.
6q25.3-q26	<i>MASI</i> (a tyrosine kinase protooncogene) shows monoallelic expression in human breast
6q25.3	<i>IGF2R</i> (insulin-like growth factor II receptor; mannose 6-phosphate receptor, cation independent) is maternally expressed in mouse. It may be imprinted polymorphically in humans. Allele-specific methylation (methylation of the active maternal allele) is maintained in humans.
6q22-23	Neonatal diabetes mellitus. Two cases of neonatal diabetes had paternal UPD 6. Additionally, paternal UPD was associated with agenesis of pancreatic beta cells and neonatal diabetes although paternal UPD has also occurred in a normal child.
7q11.23	Williams syndrome was associated with significantly more severe growth retardation and microcephaly if the associated deletion of 7q11.23 was maternally derived.
7q32	<i>PEG1/MEST</i> (paternally expressed gene 1/mesoderm-specific transcript, member of the [alpha]/[beta]-hydroxylase fold family) is paternally expressed in human fetal tissues, but biallelically expressed in adult blood. <i>Peg1</i> is imprinted in mice.
UPD of chromosome 7	Several cases of maternal iso- and heterodisomy in Russell-Silver syndrome indicate the presence of imprinted growth gene(s).
UPD of chromosome 8	Paternal UPD is associated with normal development.
9q34	Loss of maternal ABO antigens has been reported in acute myeloid leukaemia cases.
11p15	The 11p15 region (involved in the Beckwith-Wiedemann syndrome) contains a number of imprinted genes, which are listed in order. <i>H19</i> is maternally expressed in mouse and humans. The gene product is an abundant untranslated RNA of unknown function. <i>IGF2</i> (insulin-like growth factor 2, a fetal growth factor) is paternally expressed in humans and rodents. Expression is not imprinted in the choroid plexus, leptomeninges, brain, adult human liver and chondrocytes. It is probably imprinted secondarily under the control of the H19 locus. <i>INS</i> (insulin) is paternally expressed in mouse yolk sac, but not imprinted in human or mouse pancreas. Insulin is suspected to be imprinted in humans since the susceptibility to type 1 diabetes is significantly influenced by the parent-of-origin of insulin alleles, but the mechanism of this effect is unclear. <i>ASCL2/HASH2</i> (achaete-scute complex like 2/human achaete-scute homologue 2, human homologue of murine <i>Mash2</i> , a helix-loop-helix transcription factor) is maternally expressed. It is expressed in human extravillous trophoblasts and in the spongiotrophoblast cells of mouse placenta. <i>KCNA9</i> ( <i>KvLQT1</i> , potassium channel involved in long QT syndrome) is maternally expressed. Its expression is imprinted in several tissues but not in the heart. <i>CDKN1C</i> ( <i>p57KIP2</i> , a cyclin-dependent kinase inhibitor) was maternally expressed in humans and mouse. It is completely imprinted in mouse but only partially in humans. <i>2G3-8</i> is under study, but may show allelic expression bias in some tissues. <i>IMPT1/BWR1A.ORCTL2</i> (imprinted multi-membrane-spanning polyspecific transporter-like gene-1) is relatively repressed on the paternal allele. <i>IPL/TSSC3/BWR1C</i> (imprinted in placenta and liver, tumor-suppressing STF cDNA 3) shows maternal expression with relative repression of the paternal allele. It is expressed in placenta and most fetal tissues and is homologous to mouse apoptosis-promoting gene TDAG51.
11p13	<i>WT1</i> ( <i>Wilms tumor 1</i> , a zinc finger protein): there are conflicting data. It was reported to be partially or completely imprinted and maternally expressed in some tissues (placenta and brain) but was paternally expressed in fibroblasts and lymphocytes from some individuals.

11q13	<i>FCER1B</i> ([beta] subunit of the high-affinity IgE receptor): in allergic asthmatics, the <i>Leu181</i> allele was always maternally inherited.
11q13.1, 11q22.3-q23.3	Familial glomus tumors (non-chromaffin paragangliomas): linkage studies suggest two distinct loci, but the tumor susceptibility is always inherited from carrier fathers.
13q14	<i>RB</i> locus: the retinoblastoma gene itself does not appear to be imprinted, but there may be parent-of-origin effects on the transmission of retinoblastoma susceptibility in humans and in mice (earlier onset of tumors when mutant <i>Rb</i> is paternally inherited).
13q14	<i>HTR2a</i> [ <i>serotonin (hydroxytryptamine) receptor type 2a</i> ] was expressed biallelically in normal tissues, but in fibroblasts of retinoblastoma patients with germline deletions or translocations it was only expressed in those with a paternally derived deletion or translocation, but not in those with a maternal deletion. Promoter region methylation (partial) corresponded positively with expression. It is imprinted in mouse.
14q24.3-q31	A case report of dup(14q24.3-31), inherited from a phenotypically normal father, suggests that this region may be imprinted.
UPD of chromosome 14	Both paternal and maternal UPD suggest parent-of-origin effects on this chromosome. Maternal uniparental heterodisomy and isodisomy is associated with a characteristic phenotype [hypotonia, motor developmental delay, mild dysmorphic facial features, low birth weight, growth abnormalities (precocious puberty)]. Paternal UPD is associated with a severe mental and musculoskeletal phenotype.
15q11-q13	The 15q11-q13 region contains a cluster of imprinted genes that may be involved in the pathogenesis of the Prader-Willi and Angelman syndromes; they are listed in order from the centromeric end: <i>ZNF127</i> and <i>FNZ127</i> are two overlapping paternally expressed transcripts. <i>ZNF127</i> putatively encodes a 505 amino acid polypeptide-containing zinc finger motif. <i>NDN (necdin)</i> is paternally expressed in brain (human and mouse) and fibroblasts. It is expressed in differentiated neurones. BD exons of <i>SNRPN</i> . This region may constitute the 15q imprinting centre and is comprised of alternate 5[prime] exons (the BD exons, BD1B, BD1B*, BD1A, BD2, BD3) of <i>SNRPN</i> . Mutations of these exons cause Angelman syndrome perhaps through failure to erase the imprint from the previous generation. <i>SNRPN (small nuclear ribonucleoprotein-associated polypeptide N)</i> is paternally expressed and may be involved in the pathogenesis of Prader-Willi syndrome. It may be imprinted secondarily, under the control of an imprinting centre. <i>PAR-SN</i> (an RNA transcript between <i>SNRPN</i> and <i>PAR5</i> ) is paternally expressed in lymphoblasts. <i>PAR5 (D15S226E)</i> (Prader-Willi/Angelman region) is paternally expressed but contains no open reading frames. <i>IPW</i> (imprinted in Prader-Willi) is paternally expressed but probably untranslated. <i>PAR1 (D15S227E)</i> (Prader-Willi/Angelman region) is paternally expressed but probably contains no open reading frames. <i>UBE3A/E6-AP</i> (ubiquitin protein ligase 3A) is maternally expressed in human and mouse brain, but is biallelically expressed in other tissues. This gene is mutated in some cases of Angelman syndrome, deleted in others (60-70%), and affected by paternal UPD in others. <i>GABAA receptor subunit</i> genes ( <i>GABRB3</i> , <i>GABRA5</i> , <i>GABRG3</i> ) are paternally expressed. There is paternal methylation of the 5' end of <i>GABRB3</i> .
15q11-q13	Autism in a family was associated with a 15q11-q13 duplication only when maternally transmitted
19q13.4	<i>PEG3</i> , the human homologue of imprinted mouse gene <i>Peg3</i> (see mouse 7) is located here, but its imprinting status has not been reported.
20q13.11	<i>GNAS (Gs alpha, a G protein)</i> is assumed to have specific paternal expression in some tissues based on in situ hybridization in mice with PatDp2 and MatDp2 and in humans because of the transmittance pattern of Albright hereditary osteodystrophy (33/36 transmitting parents were maternal). All 60 maternal offspring had full expression of the phenotype (pseudo-hypoparathyroidism type Ia) whereas all six paternal offspring had partial expression (pseudopseudo-hypoparathyroidism). However, transcription in human fetal tissues was not imprinted.
Xq13.2	<i>XIST</i> shows preferential paternal expression with associated silencing of the paternal X chromosome in the extraembryonic tissues of mouse and in trophoblastic cells in humans. <i>XIST</i> is an untranslated RNA. Most genes on the X chromosome could be described as secondarily imprinted, in response to <i>XIST</i> expression.
Xp11.23-Xqter	Turner syndrome patients with a maternally retained X (45,Xm) showed significantly poorer verbal and higher-order executive function skills than those with 45,Xp. A higher prevalence of cardiovascular abnormalities and neck webbing was noted when the retained X was maternal.
UPD of chromosome X	Maternal UPD had no obvious clinical stigmata. Paternal UPD was associated with impaired gonadal function and shortness of stature.

**Table 2. Mouse imprinted regions and genes**

The table describes the imprinted loci identified in mice and has been modified from Morison and Reeve 1998. Specific regions of chromosomes containing single or clusters of imprinted genes have been listed.

**Table 2. Mouse imprinted regions and genes**

Chromosome	Region	Comments
2	Proximal	Maternal disomy causes early embryonic lethality.
	Distal	There may be two imprinted regions. <i>Neuronatin</i> ( <i>Nnat</i> , <i>Peg5</i> ) is paternally expressed, maternally methylated, and expressed in pituitary, central and peripheral nervous systems. In a more distal region which contains <i>Gnas</i> (see human 20q13), both maternal and paternal disomy cause neonatal lethality.
6	Proximal	Maternal disomy of this region, which includes <i>Peg1/Mest</i> (see human 7q), is associated with early embryonic lethality.
7	Proximal	<i>Peg3/Apoc2</i> is a paternally expressed, zinc finger protein. <i>Asp3</i> ( <i>audiogenic seizure prone gene 3</i> ) is an as yet unidentified gene linked to proximal chromosome 7. The susceptibility of epilepsy-prone mice to audiogenic seizures was dependent on parental origin. Maternal disomy shows late fetal lethality with fetal and placental growth retardation.
	Central	This region is syntenic with human 15q11-q13 and includes <i>Ndn</i> , <i>Snrpn</i> , <i>Ipw</i> , <i>Ube3a</i> and <i>Znf127</i> .
	Distal	This region is syntenic with human 11p15.5 and includes <i>H19</i> , <i>Igf2</i> , <i>Ins2</i> , <i>Mash2</i> , <i>Tapa1</i> , <i>Kvlqt1</i> , <i>p57Kip2</i> , <i>Impt</i> and <i>Ipl</i> . Preliminary data indicate that <i>Tapa1</i> shows relative repression of the paternal allele in extra-embryonic tissues.
9		<i>Grf1</i> ( <i>Irlgs2/Cdc25Mm</i> , a guanine nucleotide exchange factor) is paternally expressed, but the maternal allele is expressed at low levels (<10% of paternal levels) in brain.
11	Proximal	<i>U2afbp-rs/U2af1-rs1/D11Ncvs75</i> ( <i>U2 small nuclear ribonucleoprotein auxiliary factor-binding protein-related sequence</i> ) is paternally expressed.
		<i>Grb10/Meg1</i> (growth factor receptor-bound protein 10/maternally expressed gene 1) is maternally expressed. The GRB10 protein binds to the insulin receptor and the IGF1 receptor, and is a candidate for the growth retardation of Russell-Silver syndrome in humans.
	UPD	Maternal disomy resulted in small size whereas paternal disomy resulted in large size. The mice were otherwise normal and fertile.
12		<i>Gtl2lacZ</i> : a dwarfism phenotype resulting from an insertional mutation of a LacZ-containing transgene. Although expression from the transgene was not affected by its parent-of-origin, the mutant dwarfism phenotype was expressed most strongly when paternally inherited.
	Distal	Early embryonic lethality occurs when both alleles are inherited paternally.
14	Band D3	<i>Htr2</i> ( <i>serotonin receptor 2a</i> ) shows maternal expression in mouse cerebrum, ovary and embryonic eye.
17	Proximal	This includes the <i>Tme</i> locus (T-maternal effect) which is related to the Hairpin tail mutation locus. This phenotype is attributable to disruption of the imprinted gene <i>Igf2r</i> ( <i>insulin-like growth factor 2 receptor</i> ). <i>Igf2r</i> is maternally expressed in mouse but there are conflicting data in humans.
	Distal	Paternal disomy causes small body size evident from day 7 after birth.
18	Proximal	Impact (imprinted and ancient, belongs to the YCR59c/yigZ protein family with unknown function) is paternally expressed.
	UPD	Maternal and paternal disomy are possibly associated with growth retardation.
19	Distal	<i>Ins1</i> ( <i>insulin 1</i> ) is paternally expressed. It was reported to be imprinted in yolk sac at day 16, but not in the pancreas. In contrast, others found no evidence of imprinting at days 12.5, 13.5 and 14.5. It has no human homologue.
X		Xist: there is preferential inactivation of the paternal X chromosome in extra-embryonic tissues, corresponding to preferential expression of the paternal Xist.
		<i>Mdx</i> (dystrophin) expression: parent-of-origin effects on the proportion of muscle cells expressing dystrophin in mice inheriting a heterozygous null mutation of dystrophin have been reported.
		Ovarian granulosa cell carcinoma: an X-linked imprinted gene modifies the predisposition to tumorigenesis in <i>SWR</i> and <i>SWRXJ</i> mice.

numerous techniques, is an added advantage to study the phenomenon of genomic imprinting.

### **1.1.2. Genomic imprinting in mice**

Maternal and paternal genome non-equivalence in the mouse was first demonstrated in 1984 by pronuclear transfer experiments (McGrath and Solter 1984; Surani et al. 1984). Zygotes in which both pronuclei were derived from the female parent were termed as gynogenotes, and those zygotes containing two paternal pronuclei were referred to as androgenotes. Neither diploid gynogenetic nor androgenetic embryos developed normally. Gynogenotes were characterized by fair embryonic tissue development and poor extraembryonic tissue development. In contrast, androgenotes were characterized by poor embryonic development and fair extraembryonic tissue development. These experiments clearly illustrated that an embryo must contain information from both parents in order to be viable.

Experiments later showed that inheriting two copies of certain subchromosomal regions from only one parent resulted in abnormal phenotypes in the embryo including embryonic lethality (Cattanach and Kirk 1985). This narrowed the focus from entire chromosomes to sub-chromosomal regions. These chromosomal regions were later shown to contain imprinted genes (Kaneko-Ishino 1995; Cattanach et al. 1992; Bartolomei et al. 1991). Approximately 50 mammalian imprinted genes have been identified which map to around 15 genomic locations in the mouse ([www.mgu.har.mrc.ac.uk/imprinting](http://www.mgu.har.mrc.ac.uk/imprinting)). Many are located in clusters containing maternally expressed genes alongside the paternally expressed genes. Imprinted domains can therefore contain closely linked but reciprocally imprinted genes. This organization is also seen in humans. For instance, the maternal uniparental disomic inheritance of human chromosome 15

leads to the Prader-Willi syndrome due to the absence of a number of paternally expressed imprinted genes found in a cluster in region q11-q13 (Nicholls and Knepper 2001).

#### 1.1.2.1. Imprinted gene loci in the mouse

The first imprinted locus identified in the mouse was the *RSV1gmyc* transgene (Swain et al. 1987, Chaillet et al. 1991; Chaillet et al. 1991). When the transgene was inherited from a female parent, it was not expressed in the mouse, but when the transgene was inherited from a male parent, it was expressed in the heart. The imprinting of the transgene was not dependant on its position of integration in the mouse genome.

The first endogenous imprinted gene that was identified was the *Insulin-like growth factor2 gene (Igf2)* (DeChiara et al. 1991). A targeted mutation of this gene resulted in a dwarfing phenotype when inherited paternally but not when inherited maternally. This phenotype was seen in both heterozygous and homozygous mice that inherited the mutation from their male parent.

#### 1.1.3. The imprinting mark

As has been observed, for normal mammalian development to occur certain information present exclusively in the male or female germlines is required. Therefore the male and female germlines must be marked or “imprinted” to distinguish each from the other. This mark is termed an “epigenetic mark” as it is distinct from the information contained in the sequence of the genome.

An epigenetic mark can include modifications like DNA cytosine methylation, and histone modifications such as phosphorylation, acetylation, methylation, ubiquitination, and ADP-ribosylation. At least four characteristics must be exhibited by an epigenetic mark capable of distinguishing the alleles of an imprinted gene. It must be associated with the DNA but does not alter the DNA sequence itself; it must be heritable through cell divisions; it must be removable during gametogenesis; and ultimately it must have an effect on gene expression. DNA methylation makes an excellent candidate for such a mark as it fulfils all of the above criteria (as will be described in detail in the following paragraphs).

#### **1.1.4. DNA Methylation**

DNA methylation is associated with transcriptional repression and occurs mainly at the cytosine in the dinucleotide CpG (Bird 2002). Over 70% CpGs are methylated in vertebrate DNA but distinct patterns can be observed between different somatic and germline tissues (Sanford et al. 1987). These inherited patterns of methylation were hypothesized early on to have functional consequences, and early studies indicated that there was a correlation between the methylation status of a gene and its expression status (Groudine et al. 1987; Weintrub H 1985).

DNA methylation occurs mainly by the enzymatic transfer of a methyl group from S-adenosylmethionine (SAM) to the fifth position of cytosine in a CpG (Bird, 2002; Bestor 2000). The mammalian genome contains  $\sim 3 \times 10^7$  residues of methylcytosine, most at the dinucleotide 5'-CpG-3' (Roy and Weissbach 1975). DNA cytosine methylation is established on both strands of the DNA duplex through a process called *de novo* methylation. There are three possible states

of DNA methylation in the mammalian genome (Figure 1). A DNA duplex containing methylation of the CpG dinucleotide on both strands of the DNA is referred to as fully methylated. Following semi-conservative DNA replication the parent strand of each duplex is methylated and the corresponding daughter strand is unmethylated. This state is referred to as hemimethylated. The pattern of methylation on the parent DNA strand is copied to the corresponding unmethylated daughter strand through a process termed maintenance methylation (Wigler 1981). The third state is the unmethylated state when both strands of DNA at the dinucleotide contain unmethylated cytosines.

DNA methylation can be erased by two possible mechanisms. Active DNA demethylation describes the removal of the methyl group from cytosine by the action of an enzyme termed a demethylase. However, there is currently no known DNA demethylase. Passive demethylation of DNA occurs by lack of maintenance methylation over successive cell divisions.

In mammals, DNA methylation is involved in a number of cellular processes like genomic imprinting (Chaillet et al. 1991; Chaillet et al. 1995), genome stabilization (Xu et al. 1997), X-chromosome inactivation (Lyon et al. 1992) and silencing of transposons and endogenous retroviruses (Yoder et al. 1997; Walsh et al. 1998). All of these processes are tightly regulated during development and this regulation involves the changes in DNA methylation states during development.

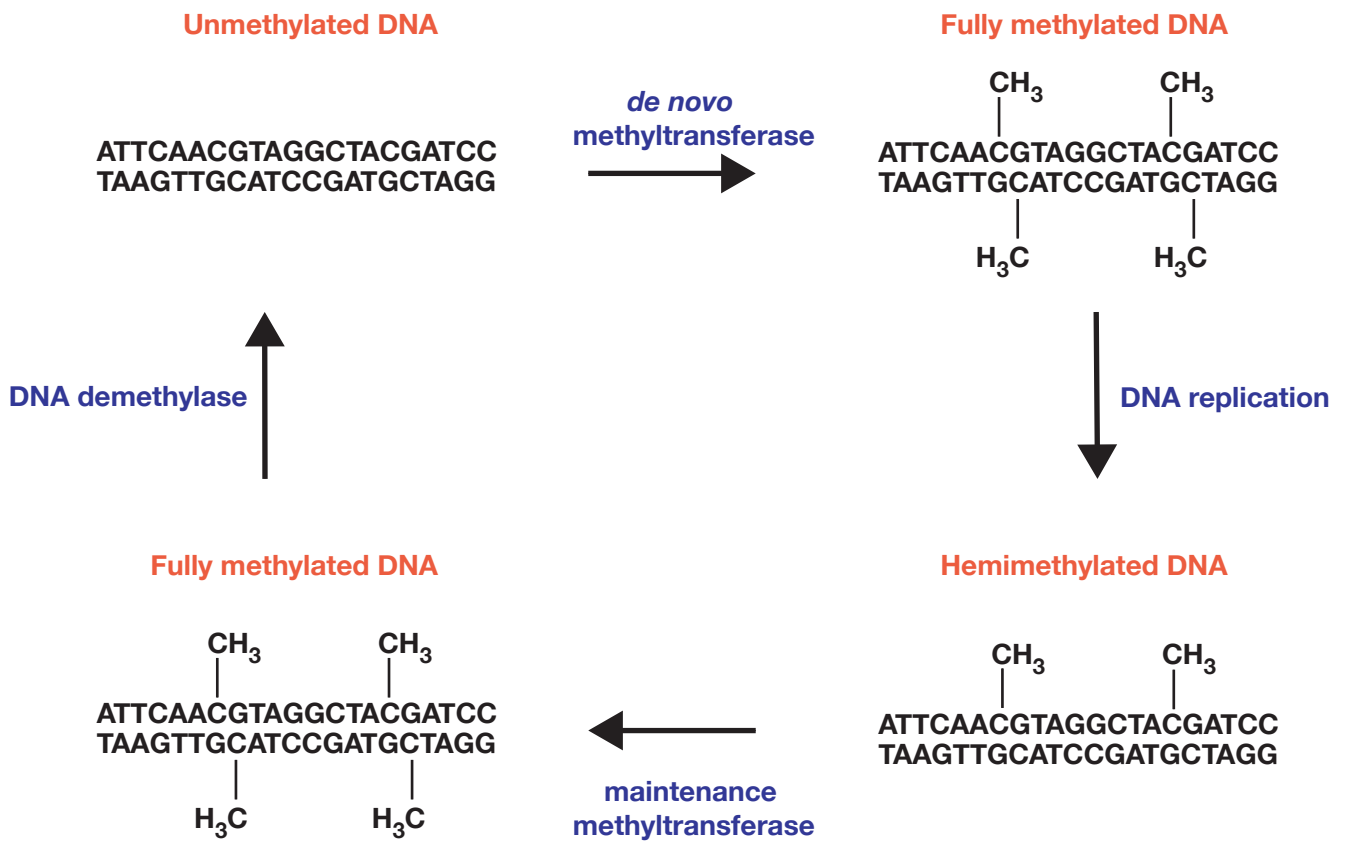


**Figure 1. States of DNA methylation in the mammalian genome**

### **Figure 1. States of DNA methylation in the mammalian genome**

In the mammalian genome, there are three possible states of DNA methylation. When both strands of DNA at the CpG dinucleotide contain unmethylated cytosines, it is called the unmethylated state. Due to *de novo* methyltransferases, CpG dinucleotides on both strands of the DNA get methylated and this state is referred to as fully methylated. Following semi-conservative DNA replication the parent strand of each duplex is methylated and the corresponding daughter strand is unmethylated. This state is referred to as hemimethylated state. The pattern of methylation on the parent DNA strand is copied to the corresponding unmethylated daughter strand through a process termed maintenance methylation by the action of maintenance methyltransferases (Wigler 1981). The DNA strands can lose their methylation either by active or passive demethylation.

#### 1.1.4.1. DNA methylation during mammalian development

DNA methylation patterns are dynamic during mammalian development. Mouse development is accomplished by two major waves of genome-wide demethylation and remethylation, one during germ cell development and another after fertilization (Meehan et al. 2003). Male primordial germ cells (PGCs) enter mitotic arrest and female PGCs enter meiotic arrest when genome-wide demethylation occurs. The *de novo* methylation takes place at the prospermatogonia stage in the male germ line, whereas in the female germ line it occurs after birth during the growth of the oocyte. Thus, remethylation during gametogenesis results in highly methylated genomes of mature sperm and oocyte with the establishment of differential methylation marks on paternal and maternal alleles of the imprinted genes that are essential for embryo growth (Sanford et al. 1987)

After fertilization, it has been observed that the male pronucleus is rapidly demethylated in a replication independent mechanism (Monk et al. 1987; Oswald et al. 2000). In contrast, the maternal genome initially maintains its methylation but this progressively drops until the 8-cell stage and the methylation content appears to be equivalent between the maternal and paternal genomes (Figure 2). The level of methylation drops to about 15% at the blastocyst stage. What determines the susceptibility of the maternal and paternal genomes to the replication-independent demethylase is unknown. Genome-wide *de novo* methylation occurs at the blastocyst stage after implantation resulting in higher levels and uniform pattern of methylation on the homologous chromosomes (Reik et al. 2001).

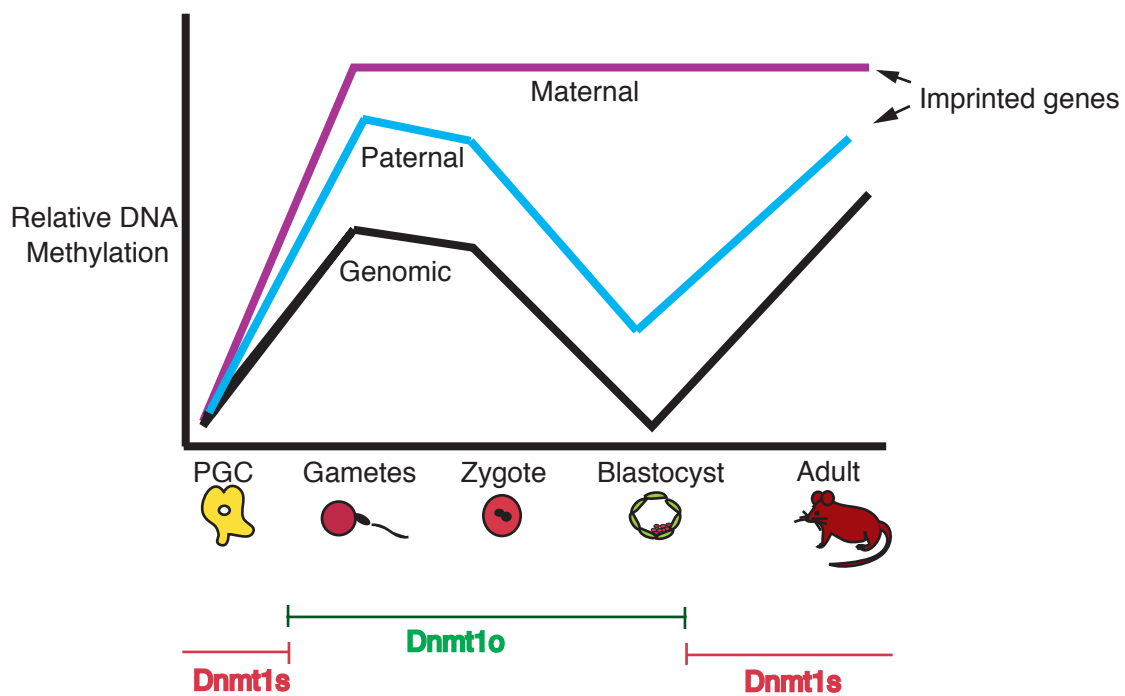


**Figure 2. Dynamics of DNA methylation patterns during mouse development.**

**Figure 2. Dynamics of DNA methylation patterns during mouse development.**

The black line represents the genomic methylation patterns where you see a loss of methylation during preimplantation development and then once again, an increase in methylation after the blastocyst stage. The blue line represents the methylation of the paternal allele of the imprinted gene, which shows a similar pattern to genomic methylation. The purple line represents the maternal allele, which maintains its methylation even during pre-implantation development. Dnmt1o protein is the only isoform that is expressed in the oocytes and during preimplantation development while Dnmt1s is expressed during postimplantation development and in the adult cells.

At imprinted genes, one of the alleles (either maternal or paternal) follows the similar pattern of demethylation and remethylation as the rest of the genome during early development. In contrast, the other (imprinted) allele maintains its methylation level during that critical period of preimplantation development when there is a decrease in the genome wide methylation level (Figure 2; Stoger et al. 1993; Tremblay et al. 1995). Genome-wide reprogramming of DNA methylation patterns has also been observed, although to differing extents with different timing, in bovine, pig and rat zygotes (Dean et al. 2001).

#### 1.1.4.2. DNA methylation and imprinting

The first gene shown to contain parental specific methylation imprints was the *RSVIgmyc* transgene (Chaillet et al. 1995). This transgene is heavily methylated on the maternal allele while showing lower levels of methylation on the paternal allele. This difference in methylation is maintained throughout embryogenesis and in adult cells.

Differential methylation patterns between parental alleles have also been seen in all the endogenous imprinted genes identified so far. These differences in methylation have been restricted to specific regions of these genes termed the differentially methylated domains (DMDs). This differential methylation on the two chromosome homologues affects the interactions between the genomic template and regulatory molecules, and causes some genes to be active on one parental allele and inactive on the other (Reik et al. 2002). DMD's of imprinted genes can act over both, short distances, influencing gene-specific regulatory elements such as promoters, and over long distances affecting the activity of several imprinted genes within a

cluster. As has been mentioned before, many imprinted genes in mouse are located in clusters containing maternally expressed genes alongside the paternally expressed genes. It now appears that this organization has implications for their control as can be seen from the ability of the DMD's of specific imprinted genes to act over long distances and affect the activity of other imprinted genes in their cluster.

### **1.1.5. DNA Methyltransferases**

The generation of genomic patterns of methylation is likely due to the interplay between DNA cytosine methyltransferases and chromatin remodelling machinery (Dennis et al. 2001; Meehan et al. 2001). To date, five mammalian cytosine DNA methyltransferases (Dnmt) have been identified, Dnmt1, Dnmt2, Dnmt3a, Dnmt3b and DnmtL (Figure 3). All of them contain a highly conserved C-terminal catalytic domain and a variable N-terminal extension (Bestor 2000). Splice sites and promoter specific variants have also been identified which generate functional diversity for the different DNA methyltransferases (Mertineit et al. 1998; Okano et al. 1998).

#### **1.1.5.1. Dnmt1 methyltransferase**

The predominant DNA (cytosine-5)-methyltransferase in mammals is the Dnmt1 protein, ( $M_r$  190,000) composed of an 1100 residue amino-terminal regulatory domain and a 500 residue, carboxy-terminal catalytic domain that is closely related to bacterial methyltransferases (Bestor 2000). Dnmt1 homologues have been identified in many species including sea-urchin, amphibians, fish, birds and mammals (Meehan 2003). Sequences within the N-terminal domain are required for the localization of Dnmt1 to the nucleus and to replication foci during S-phase

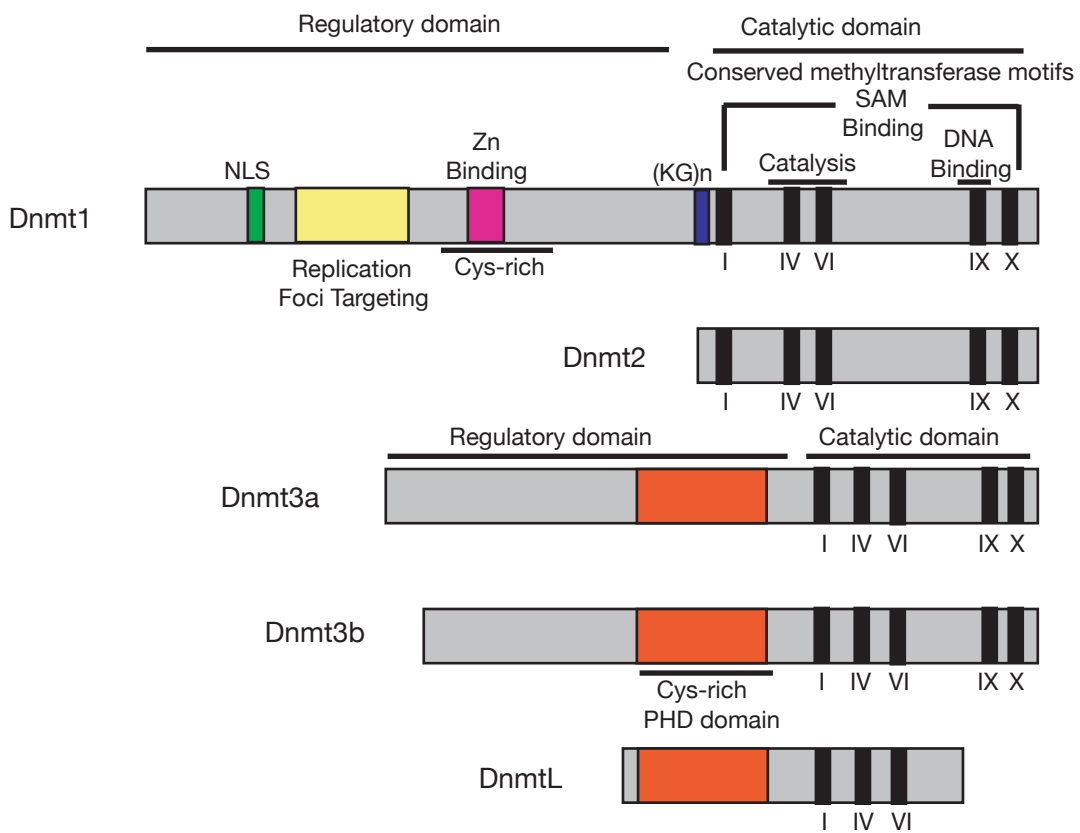


**Figure 3. Structure of the known DNA Methyltransferases (Dnmt's)**

**Figure 3. Structure of the known DNA Methyltransferases (Dnmt's)**

Dnmt1, Dnmt3a and Dnmt3b can be divided into two domains, the regulatory domain (the N-terminal domains) and the catalytic domain which contain five characteristic sequence motifs which show strong conservation (roman numerals) (As modified from Robertson et al., 2001)

(Leonhardt et al. 1992). Although Dnmt1 catalyzes both *de novo* and maintenance methylation *in vitro*, it has a 5-30 fold preference for hemimethylated DNA substrates over unmethylated substrates (Yoder et al. 1997). These data suggest that Dnmt1's main role, or only role, in mammalian organisms is to maintain DNA methylation patterns on hemimethylated DNA following DNA replication. Homozygous mutant embryonic stem (ES) cells and embryos derived from matings between parents heterozygous for *Dnmt1* null alleles have marked reductions in Dnmt1 and in the level of CpG methylation which results in the death of these embryos (Lei et al. 1996; Li et al. 1992). The residual methylation appears to be confined to repetitive DNA sequences, whose methylation may be due to other DNA (cytosine-5)-methyltransferases. Dnmt1 exists as three different isoforms, Dnmt1o, Dnmt1s and Dnmt1p, which are expressed at different periods of mouse development. The structure and significance of these isoforms will be discussed in detail in later paragraphs.

#### 1.1.5.2. Dnmt3 methyltransferases

Dnmt3a and Dnmt3b methyltransferases were identified *in silico* by screening mouse and human databases with sequences corresponding to the catalytic domain of Dnmt1 (Okano et al. 1998). In addition to the catalytic domain, they contain a proline-tryptophan-tryptophan-proline [PWWP] domain and a plant homeodomain [PHD]-like Zinc finger domain. The PWWP domain can bind DNA and may be involved in targeting these enzymes to specific loci. The Dnmt3a and Dnmt3b enzymes share about 80% homology over the catalytic domains and 60% homology over the PHD domains. *In vitro* and *in vivo*, Dnmt3a and Dnmt3b primarily possess *de novo* methyltransferase activities (Okano et al. 1998; Okano et al. 1999; Xu et al. 1999) and are required at different periods of mouse development. Dnmt3a-deficient mice survive to term

but die around 4 weeks of age while Dnmt3b-deficient mice develop normally up to embryonic day 9.5 (E9.5) but die before birth. Mice deficient in both Dnmt3a and Dnmt3b die during early embryogenesis, and have a more severe phenotype than mice deficient in either individual enzyme. Loss of maternal imprints have been observed in the embryos derived from the homozygous mutant Dnmt3a or mutant Dnmt3b oocytes (Hata et al. 2002).

In humans, mutations in DNMT3B are associated with ICF syndrome (immunodeficiency, centromeric region instability, and facial abnormalities) (Hansen et al. 1999). ICF syndrome is associated with hypomethylation of specific satellite repeats leading to chromosomal instability. This correlates well with the loss of minor satellite repeat methylation specific to Dnmt3b<sup>-/-</sup> embryos in mice. Null mutations in the human DNMT3B protein have never been observed in ICF patients, suggesting that DNMT3B is essential for viability in humans as well as in mice.

Dnmt3L was also identified by database screening and has the PWWP, PHD and catalytic domains related to those of Dnmt3a and Dnmt3b, however, it lacks the conserved PC and ENV residues in motifs IV and VI which are known to form the catalytic center of DNA cytosine methyltransferases (Hata et al. 2002). Dnmt3L is expressed in E7.5-E8.5 mouse embryos in the chorion and also in mouse oocytes and spermatocytes. Males deficient in Dnmt3L were infertile. Females deficient in Dnmt3L are fertile but their embryo die *in utero* around E9.5 with defects seen in the methylation of maternal imprints. Recombinant Dnmt3L cannot methylate DNA but interacts and co-localizes with Dnmt3a and Dnmt3b in the nuclei of transfected cells (Hata et al. 2002). These proteins probably co-operate to carry out *de novo* methylation of maternally imprinted genes during oogenesis and early mouse development.

#### 1.1.5.3. Dnmt2 methyltransferase

Like the Dnmt3 family of methyltransferases the Dnmt2 protein was identified due to its homology with the Dnmt1 methyltransferase (Yoder and Bestor 1998). Though Dnmt2 contains all 10 sequence motifs that are conserved among the methyltransferases it has no detectable methyltransferase activity towards DNA substrates and is not required for *de novo* and maintenance methylation of viral DNA in ES cells (Okano et al. 1998; Van den Wyngaert et al. 1998). Still, recent studies suggest that Dnmt2 may possess minimal methyltransferase activity (Tang et al. 2003; Hermann et al. 2003; Liu et al. 2003). Therefore, the involvement of Dnmt2 in the process of genomic methylation remains a possibility, and further investigation into this issue is required.

#### 1.1.5.4. The isoforms of Dnmt1 protein

The *Dnmt1* gene in mice contains three alternative 1<sup>st</sup> exons (exon 1s, exon 1o and exon 1p) driven by specific promoters that are differentially utilized in different cell types, thus, leading to the expression of three specific Dnmt1 isoforms at different periods of development. The promoter upstream of exon 1s drives the expression of a 5.2 kb mRNA species which is ubiquitously expressed in somatic cells (Figure 4). This mRNA contains an in frame ATG initiation codon in exon 1s and encodes for the Dnmt1s protein (*M<sub>r</sub>* 190,000) which is abundantly expressed in nuclei of somatic cells such as adult spleen cells and kidney cells, and it is readily detected in nuclei of all cells of the early post-implantation embryo (Trasler et al. 1996; Yoder et al. 1997). However, Dnmt1s has not been detected in oocytes and in cells of

preimplantation embryos (Carlson et al. 1992; Mertineit et al. 1998; Cardoso and Leonhart 1999). In these stages, there is an abundance of a variant Dnmt1 protein, Dnmt1o. Dnmt1o is found in the cytoplasm of the mature metaphase II (MII) oocyte, and in the cytoplasm of all preimplantation cleavage stages, but is found in the nuclei of the 8-cell embryo (Carlson et al. 1992; Mertineit et al. 1998; Cardoso and Leonhart, 1999; Howell et al. 2001). The promoter upstream of exon 1o (which, in turn, is located ~7 kb upstream of exon 1s) drives expression of an oocyte-specific 5.1 kb mRNA species which contains an open reading frame that does not begin until exon 4 (Figure 4; Mertineit et al. 1998). This open reading frame translates into a protein product that is the size of Dnmt1o ( $M_r$  175,000). Thus, The Dnmt1o form is identical to the Dnmt1s form except that it lacks a 118 amino acid extension that is present at the N-terminus of the Dnmt1s form (figure 3; Mertineit et al. 1998). What is interesting to note is that Dnmt1o is expressed at that critical period of development (preimplantation development) when the methylation on one of the alleles of an imprinted gene is maintained while there is a decrease in methylation levels in the rest of the genome (Figure 2). The mRNA encoding the somatic form of the protein, Dnmt1s, is expressed during the preimplantation period, but, as mentioned before, Dnmt1s protein does not appear in normal embryos until after implantation (Carlson et al. 1992; Mertineit et al. 1998; Ratnam et al. 2002). Thus, either the Dnmt1s mRNA is not translated or this protein cannot accumulate in the early embryo. The 6.0 kb transcript generated from the exon 1p promoter, specific to pachytene spermatocytes, is not translated into protein presumably due to multiple ATG initiation codons in the first exon (Mertineit et al. 1998)

Studies in mice homozygous for a targeted disruption of the Dnmt1 oocyte-specific promoter indicate that preimplantation Dnmt1o is derived from the oocyte's cytoplasmic store of

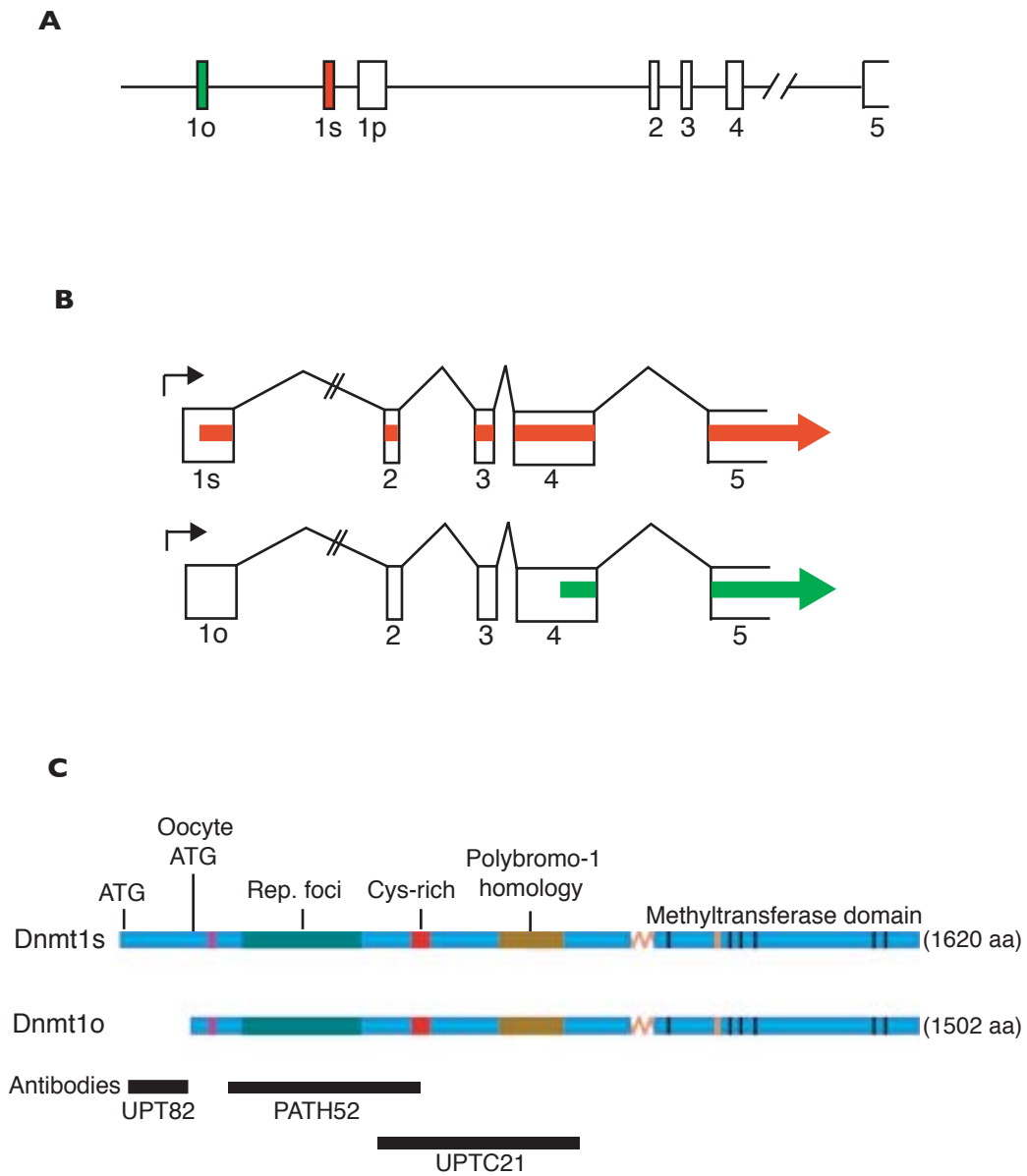


**Figure 4. Sex-specific exons and oocyte-specific species of Dnmt1.**

**Figure 4. Sex-specific exons and oocyte-specific species of Dnmt1.**

A. Organization of sex-specific exons in the 5' end of the Dnmt1 gene. B. The oocyte-specific Dnmt1<sub>o</sub> transcript initiates at exon 1<sub>o</sub> and is spliced to exon 2; Dnmt1<sub>o</sub> translation is initiated at the ATG in exon 4. The initiating ATG codon for Dnmt1<sub>s</sub> is located in exon 1<sub>s</sub> (also spliced to exon 2). C. Comparison of Dnmt1<sub>s</sub> and Dnmt1<sub>o</sub> proteins. The Dnmt1<sub>o</sub> protein is 118 amino acids shorter than the Dnmt1<sub>s</sub> form at the N-terminus and the difference between the two forms of Dnmt1 is not known to extend beyond this N-terminal truncation. The somatic and oocyte ATG codons are shown, as are, a sequence that mediates interaction of Dnmt1 with replication foci during S phase of somatic cells (Rep. foci), a zinc-binding cysteine-rich domain (Cys-rich) and a domain that is related to a domain in Polybromo-1 from chicken. The epitopes specific to the three antibodies UPT82, UTC21 and PATH52 are shown in the figure.

Dnmt1o (Howell et al. 2001). The *Dnmt1<sup>Δ1o</sup>* mutation results in loss of Dnmt1o expression from the mutant allele. Oocytes and preimplantation embryos from homozygous *Dnmt1<sup>Δ1o</sup>* female mice lack Dnmt1o protein. Embryos derived from Dnmt1o-deficient oocytes typically die during the last third of gestation with variable phenotypes. These embryos show a 50% reduction in methylated alleles of imprinted genes. This loss is most likely due to the loss of nuclear Dnmt1o at the 8-cell stage resulting in a loss of maintenance methylation in 8-cell blastomeres. The proteins that supply the maintenance methyltransferase activity for the other S phases of preimplantation development are unknown.

The reason for the use of two Dnmt1 isoforms at different periods of mouse development is not clear, particularly because they appear to have the same function in somatic cells (Ding et al. 2002). Dnmt1o when expressed in somatic cells, instead of Dnmt1s, maintained normal patterns of methylation. It is still to be determined if Dnmt1s can functionally replace Dnmt1o during oogenesis and preimplantation development, in terms of methyltransferase activity. Also, ES cell lines expressing both isoforms of Dnmt1 revealed that Dnmt1o is much more stable than Dnmt1s (Ding et al. 2002). It is still unknown if there is a difference in stability between the two isoforms during preimplantation development and if the reason for Dnmt1o being used as a maternal effect protein is its increased stability.

#### **1.1.6. Cloning and methylation**

Cloning is defined as the production of a group of individuals with the same genotype by asexual reproduction. This phenomenon occurs naturally in many plants and some lower forms of animals such as hydra, sea anemone and annelids. But the majority of the animal kingdom

solely uses bisexual reproduction for reproduction. The reason for this could be to avoid irreversible accumulation of detrimental mutations in the face of a constantly changing environment and to accelerate the rate of adaptation in evolution.

Artificial animal cloning was started towards the end of the 19<sup>th</sup> century when two or four smaller, but complete larvae were obtained from the separated blastomeres of a single 2-4-cell sea urchin embryo (Driesch, 1892; Yanagimachi 2002). The principle of this technique has been applied successfully to various animals including mammals like mice, rabbits, sheep and pigs (Willadsen 1979). Spemann in 1938 used another cloning technique where he ligated a recently fertilized newt egg so that cell division occurs in only one of two halves. When the nucleated portion cleaved to 8-16 cells, one of these nuclei was allowed to enter the enclaved portion of the egg before it was completely separated from the rest. This resulted in the development of two normal larvae, thus depicting the totipotency of the nuclei of an 8-16 cell embryo. In 1962, Gurdon obtained adult frogs by injecting enucleated oocytes with the nuclei of endothelial cells of swimming tadpoles.

The first successful animal cloning using adult somatic cells was achieved in mammals. In 1997, Campbell and his associates reported the birth of a sheep, Dolly, which was cloned by injecting the nucleus of a mammary gland cell derived from an adult sheep into an enucleated oocyte (Campbell et al. 1996; Wilmut et al. 1997). Later Wakayama et al. (1998) and Kato et al. (1999) confirmed that cloning using adult somatic cells was also possible in mice and cattle. Subsequently, pigs and goats were cloned with adult somatic cells (Polajeva et al. 2000; Behboodi et al. 2001).

The successful cloning of animals by transfer of embryonic or somatic nuclei into enucleated oocytes demonstrates that the genetic and epigenetic programs can be reversed and nuclear totipotency can be established. However, nuclear transfer using somatic cells is, so far, a very inefficient process. Cloned progeny often exhibit phenotypic anomalies (Eggan et al. 2001; Tamashiro et al. 2000; Tanaka et al. 2001; Renard et al. 1999). The reasons for these abnormalities have not been fully elucidated. Most cloned embryos arrest development before implantation, indicating defects in essential, early events (Eggan et al. 2001). A transplanted donor cell nucleus alters the physiology or metabolism of mouse embryos during preimplantation development, indicating that the normal activation of other genes associated with early embryonic development, or the inactivation of somatically expressed genes, may not occur readily in clones (Chung et al. 2002).

The frequent anomalies inherent in cloned animals in different species argue that epigenetic, rather than genetic, changes are responsible for many of the developmental failures. Increasing experimental evidence from diverse model organisms indicate that the abnormalities or fatalities of cloned animals are due, at least in part, to the faulty or incomplete establishment, maintenance, and resetting of epigenetic states during and after nuclear transfer (Young et al. 2001; Fairburn et al. 2002)

#### 1.1.6.1. Methylation reprogramming in cloned animals

The production of cloned animals by somatic nuclear transfer reveals at least some highly methylated and differentiated somatic nuclei can be reprogrammed to a large extent for

embryonic development. But the common gestational or neo-natal developmental failures resulting from cloning suggest a possible dysregulation of epigenetic control. There are indeed aberrant methylation patterns observed in cloned animals. Abnormalities in DNA methylation have been reported, including variable levels of methylation among embryos, incomplete DNA methylation at some tissue-specific sites, and hyper-methylation at other sites (Humpherys et al. 2001; Ohgane et al. 2001; Kang et al. 2001; Bourc'his et al. 2001; Reik et al. 2001; Dean et al. 2001). These observations indicate that incomplete or abnormal methylation occurs during reprogramming of the donor genome in cloned embryos.

#### 1.1.6.2. Dnmt1 methyltransferase in cloned animals

The reason for the aberrant methylation patterns found in cloned animals remains unclear. As mentioned earlier, in normal embryos, maintenance of a correct DNA methylation pattern requires both the expression and the correct, stage-specific post-translational regulation of Dnmt1 proteins (Ratnam et al. 2002; Howell et al. 2001; Li et al. 1992; Li et al. 1993). Since a somatic nucleus introduced into an enucleated oocyte contains the Dnmt1s isoform that is normally not present in early embryos, the incompatibility of the DNA methylation systems of somatic nuclei and early embryos might be partially responsible for the abnormal methylation reprogramming observed in clones. Also, as mentioned before, post-transcriptional gene regulatory mechanisms comprise some of the most critical mechanisms controlling early development during normal embryogenesis. These mechanisms require the temporally correct production of ooplasmic proteins, including the Dnmt1 protein, and efficient interaction of these proteins with the embryonic genome. Whether aberrant expression or localization of Dnmt1 proteins could contribute to methylation defects such as those reported previously for cloned

embryos, and possibly to developmental arrest at subsequent stages of development, has not been examined as yet.

### **1.1.7. Specific aims**

#### **1.1.7.1. Specific aim 1**

As mentioned before, the reason for two specific isoforms of Dnmt1, which only differ from each other by 118 amino acids at the N-terminus of one of the isoforms (Dnmt1s) and have a similar function of maintaining genomic DNA methylation, is still unknown. This study focuses on the efforts taken to determine if Dnmt1s protein can functionally replace Dnmt1o protein. Dnmt1s will be expressed during preimplantation development instead of Dnmt1o and the ability of Dnmt1s to maintain imprinted gene methylation and expression will be examined by analyzing the methylation and expression of certain imprinted genes like *H19* and *Snrpn*. The maintenance methyltransferase activity of the two isoforms in mature oocytes will be analyzed for functional equivalency. The relative stability of the two isoforms during preimplantation development will also be determined as previous studies have proven that the Dnmt1s protein is not as stable as the Dnmt1o protein in somatic cells. These experiments will thus address the functional significance of the Dnmt1 isoforms at various stages of development.

#### **1.1.7.2. Specific Aim 2**

It has already been noted that mammalian cloning by somatic cell nuclear transfer is very inefficient and the majority of cloned embryos arrest development before implantation. In normal embryos, maintenance of a correct DNA methylation pattern requires both the expression and the correct, stage-specific post-translational regulation of the Dnmt1 proteins. Whether

aberrant expression or localization of Dnmt1 proteins contributes to methylation defects in cloned embryos has not been examined. The second part of Chapter 1 discusses the studies undertaken to determine whether cloned preimplantation embryos exhibit a normal pattern of expression and cytoplasmic-nuclear trafficking of Dnmt1 proteins.

## 1.2. Results

To determine the functional significance of the Dnmt1s and Dnmt1o isoforms, Dnmt1s was forced to express during oogenesis and preimplantation development in mouse. Two approaches were used by Carina Howell and Richard Chaillet to generate mice that expressed Dnmt1s during oogenesis. The first approach was to produce mice that contained a targeted mutation of the *Dnmt1* locus whereby the coding region of exon1s was substituted in place of exon1o. These mice were designated *Dnmt1<sup>1s/1o</sup>*, and encoded for an oocyte-specific *Dnmt1s* transcript. Homozygous *Dnmt1<sup>1s/1o</sup>* males and females were phenotypically normal and fertile. This line was maintained on a C57/BL6/J background.

The second approach was to generate mice that contained a transgene that drove the expression of Dnmt1s during oogenesis. Two different lines were obtained with this transgene, the *Dnmt1s-TG1* and *Dnmt1s-TG2*. Females and males from both lines were phenotypically normal and fertile. This line was maintained on a FVB/N background.

### 1.2.1. Functional analysis of Dnmt1s protein in the presence of Dnmt1o protein

To determine if the expression of Dnmt1s protein during preimplantation development lead to abnormal methylation patterns, we analyzed the *Dnmt1<sup>1s/1o</sup>* mice, which expressed both forms of the protein (as will be discussed in the following paragraph), and the *Dnmt1s-TG1* and *Dnmt1s-TG2* mice, carrying the *Dnmt1s* transgene, which overexpressed the Dnmt1s protein in their oocytes.

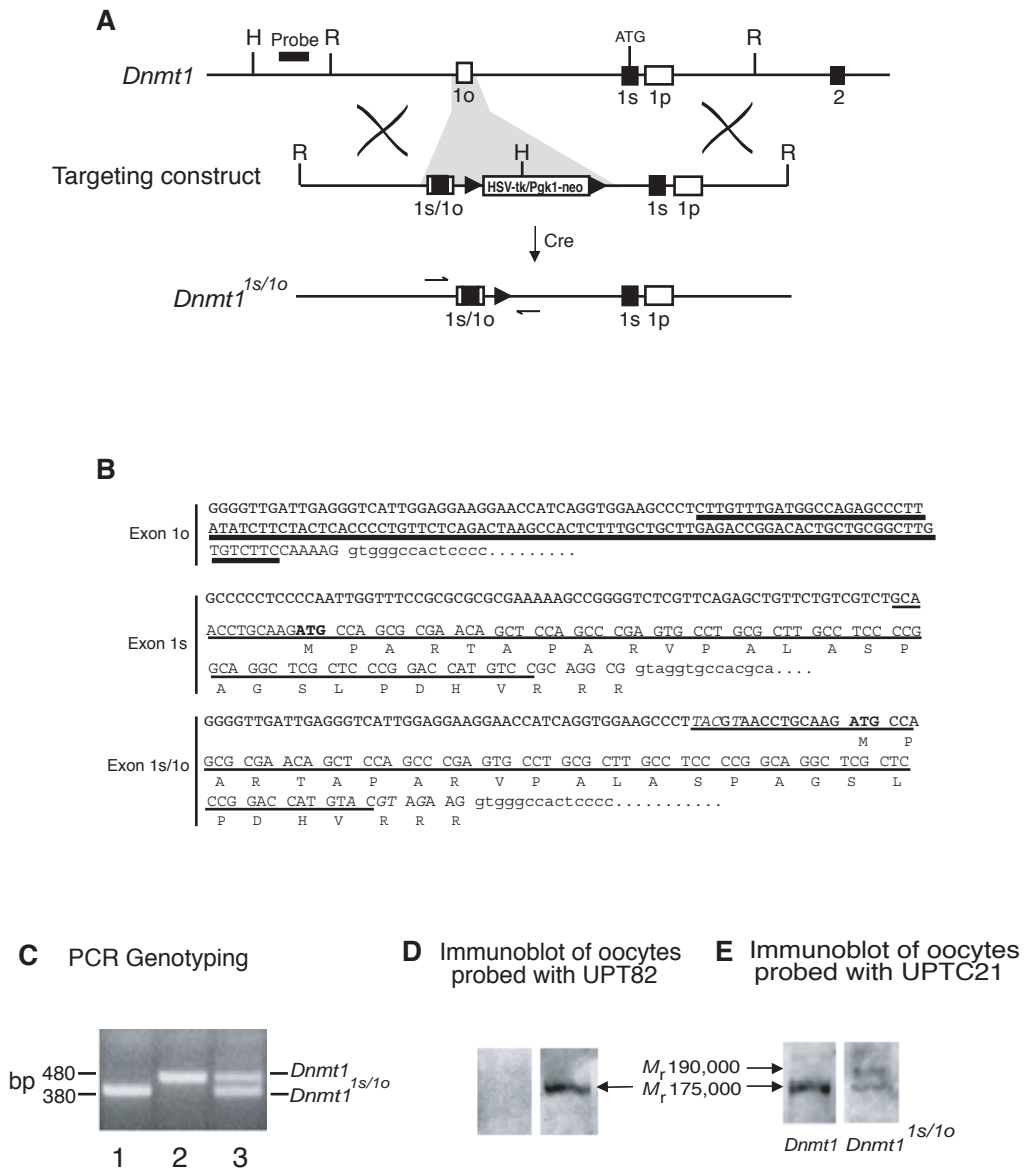


**Figure 5. *Dnmt1*<sup>1s/1o</sup> allele.**

**Figure 5. *Dnmt1*<sup>1s/1o</sup> allele.**

Targeted modification of the *Dnmt1* locus by insertion of *Dnmt1* exon 1s sequences into exon 1o and Cre-mediated excision of resistance cassette placed approximately 100 bp 3' of the modified exon 1o. H, *HindIII*; R, *EcoRI*; X, *XbaI*. B. Sequences of exon 1o, exon 1s, and hybrid exon 1s/1o. The overlined sequences in exon 1s replace the underlined sequences in exon 1o to give rise to the mutant exon 1s/1o. The amino acid codons for exon 1s and exon 1s/1o are shown. The nucleotides represented in italics are the changes made in exon 1s to create *SnaBI* restriction sites (TACGTA). These sites were used to replace a portion of exon 1o with exon 1s sequences. C. PCR primers flanking exon 1o and exon 1s/1o (shown in panel A) distinguish wildtype *Dnmt1* and mutant *Dnmt1*<sup>1s/1o</sup> alleles following Cre-mediated excision of the resistance cassette. D. Immunoblot probed with the UPT82 antibody shows the  $M_r$  190,000 *Dnmt1* somatic isoform in oocytes obtained from homozygous *Dnmt1*<sup>1s/1o</sup> females. E. Immunoblot probed with the UPTC21 antibody reveals the  $M_r$  175,000 *Dnmt1o* variant in addition to the  $M_r$  190,000 *Dnmt1* isoform in oocytes obtained from homozygous *Dnmt1*<sup>1s/1o</sup> females.

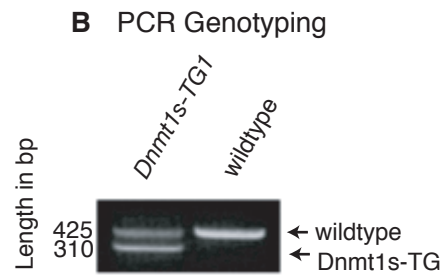
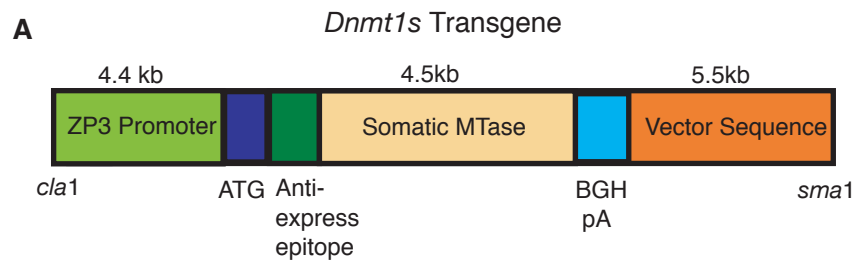


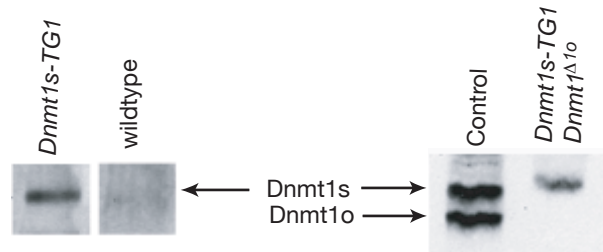
**Figure 6. *Dnmt1s* transgene**

### **Figure 6. *Dnmt1s* transgene**

A. The coding region for *Dnmt1s* (4.5 kb) was inserted into the multiple cloning site of pcDNA3.1/His at a unique *EcoRV* site. An epitope containing an ATG initiation codon, polyhistidine region, Anti-Xpress antibody epitope, an enterokinase recognition site are contained on the N-terminus of *Dnmt1s* expressed from this vector. The bovine growth hormone polyadenylation signal is located 3' of the *Dnmt1s* sequence inserted. The pcDNA3.1'His vector sequence remains (5.5 kb) 3' of the *Dnmt1s* insertion. The promoter region is from the *ZP3 zona pellucida 3* gene in mice. B. PCR analysis with the *Mtase44* and *Mtase 45* primers show the presence of a 310 bp band, in addition to a 425 bp band, in the *Dnmt1s-TG1* mice while the wildtype mice show the presence of only the 425 bp band.

**A** Immunoblot with UPT82

**B** Immunoblot with PATH52



**C** Immunoblot with UPT82

**D** Immunoblot with UPTC21

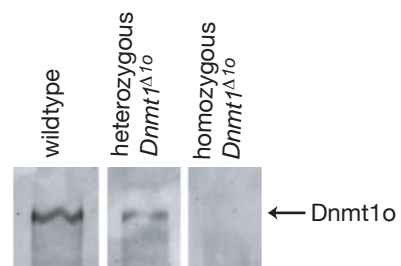
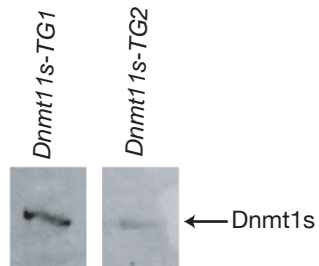


**Figure 7. Dnmt1s expression in oocytes from *Dnmt1s-TG1* and *Dnmt1 $\Delta$ 1o* mice**

**Figure 7. Dnmt1s expression in oocytes from *Dnmt1s-TG1* and *Dnmt1<sup>Δ1o</sup>* mice**

A. Immunoblot probed with the UPT82 antibody shows the  $M_r$  190,000 (Dnmt1s) isoform in oocytes obtained from *Dnmt1s-TG1* females. B. Immunoblot probed with the PATH52 antibody reveals the presence of only the Dnmt1s isoform in oocytes obtained from *Dnmt1s-TG1/Dnmt1<sup>Δ1o</sup>* females. C. Immunoblot probed with the UPT82 antibody reveals the difference in the amount of Dnmt1s protein expressed between the *Dnmt1s-TG1* and *Dnmt1s TG2* oocytes. D. Immunoblot probed with the UPTC21 antibody shows the decrease in the Dnmt1o protein to half its level in the oocytes obtained from heterozygous *Dnmt1<sup>Δ1o</sup>* females when compared to the wildtype oocytes, and absence of the Dnmt1o protein in the oocytes obtained from homozygous *Dnmt1<sup>Δ1o</sup>* females.

#### 1.2.1.1. Expression of Dnmt1s protein in the *Dnmt1<sup>1s/1o</sup>* females during oogenesis

The homozygous mutant female mice produced MII oocytes containing both the  $M_r$  190,000 and the  $M_r$  175,000 form of Dnmt1, as shown on immunoblots stained with UPT82 and UPTC21 (Figure 5). Both forms of Dnmt1 are probably expressed because of the short 5'UTR in the *Dnmt1<sup>1s/1o</sup>* transcript and thus frequent translation initiation from the methionine codon in exon 4. This codon is normally the initiation codon for Dnmt1o produced from wildtype Dnmt1o transcripts. Preimplantation embryos derived from these mutant oocytes also expressed both isoforms of the Dnmt1 protein (Figures 8B and 8C).

#### 1.2.1.2. Expression of the Dnmt1s protein in the *Dnmt1s-TG1* and *Dnmt1s-TG2* females during oogenesis

The *Dnmt1-TG1* and *Dnmt-TG2* mice also produced Dnmt1s protein in the oocytes. The MII oocytes from both the lines produced full-length tagged Dnmt1s protein that was detected on immunoblots of MII oocyte extract stained with UPT82 antibody, an antibody specific to the Dnmt1s protein (Figure 7A). The concentration of the Dnmt1s protein in the *Dnmt1s-TG1* oocytes was comparable to the concentration of the endogenous Dnmt1o protein. The *Dnmt1s-TG2* mice produced lesser amounts of Dnmt1s protein in their oocytes than the *Dnmt1s-TG1* mice. This was determined by staining immunoblots of extracts of *Dnmt1s-TG1* or *Dnmt1s-TG2* oocytes with the UPT82 antibody (Figure 7C).

### 1.2.1.3. Localization and trafficking of the Dnmt1s protein during oogenesis and preimplantation development

Using the UPT82 and UPTC21 antibodies we analyzed the localization of the Dnmt1s protein in preimplantation embryos obtained from either the homozygous *Dnmt1<sup>1s/1o</sup>* females or the *Dnmt1s-TG1* females. The time course of nuclear localization of Dnmt1s in the embryos obtained from *Dnmt1<sup>1s/1o</sup>* females parallels that of Dnmt1o in wild type embryos, with nuclear localization evident only at the 8-cell stage. However, cytoplasmic localization of Dnmt1s evident in 2-cell, 4-cell and 8-cell embryos stained with UPT82 was different than the pattern of cytoplasmic localization of Dnmt1o seen in wild type embryos (Carlson et al. 1992; Howell et al. 2001). Cytoplasmic Dnmt1s from homozygous *Dnmt1<sup>1s/1o</sup>* oocytes was aggregated, whereas wild-type cytoplasmic Dnmt1o is more evenly distributed (Figure 8). The distribution of both forms was seen after staining with the UPTC21 antibody (Figure 8). The difference in intracytoplasmic distribution of the two Dnmt1 forms is likely to be due to differences in the way the two proteins are stored in the oocyte's cytoplasm and the way they traffic after fertilization.

The *Dnmt1s-TG1* mice also showed a similar cytoplasmic-nuclear localization of the Dnmt1s protein as the wild type Dnmt1o isoform. Using the UPT82 antibody it was seen that the Dnmt1s protein localized to the cytoplasm of the MII oocytes, 2-cell embryos, 4-cell embryos and morulae. In 8-cell embryos Dnmt1s was found in both the nucleus and cytoplasm (Figure 8D). What was also confirmed by this analysis is that the epitope-tagged Dnmt1s expressed from the Dnmt1s transgene localized in a similar way to the untagged Dnmt1s protein from the

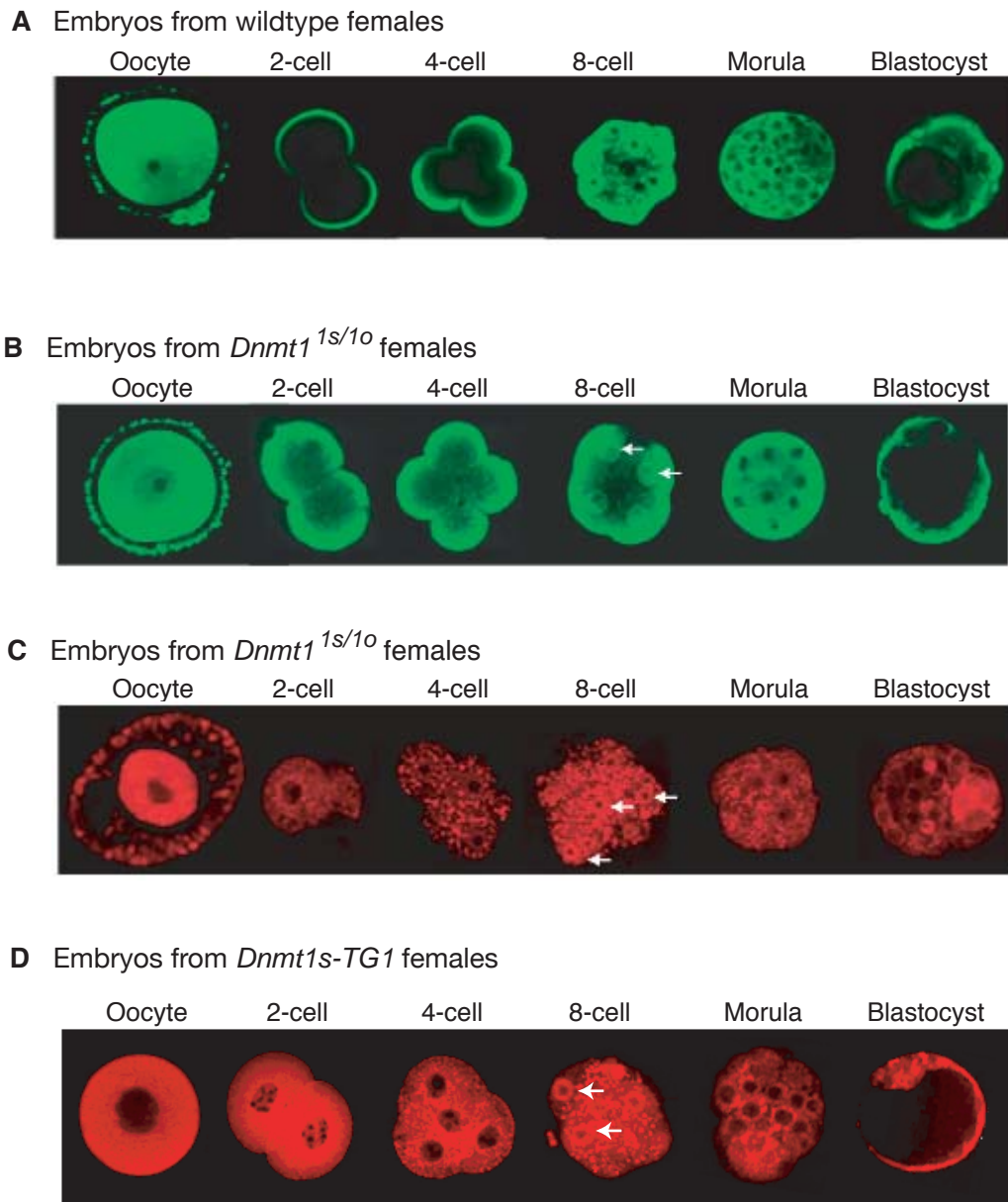


**Figure 8. Expression and localization of Dnmt1 proteins during preimplantation development.**

**Figure 8. Expression and localization of Dnmt1 proteins during preimplantation development.**

Immunostaining with UPTC21 to show A. Dnmt1o localization in wildtype preimplantation embryos and B. Dnmt1s and Dnmt1o proteins in *Dnmt1<sup>1s/1o</sup>* embryos. Immunostaining with UPT82 to localize Dnmt1s in the embryos from C. *Dnmt1<sup>1s/1o</sup>* females and D. *Dnmt1s TGI* females. Arrows indicate the nuclear localization of Dnmt1s protein.

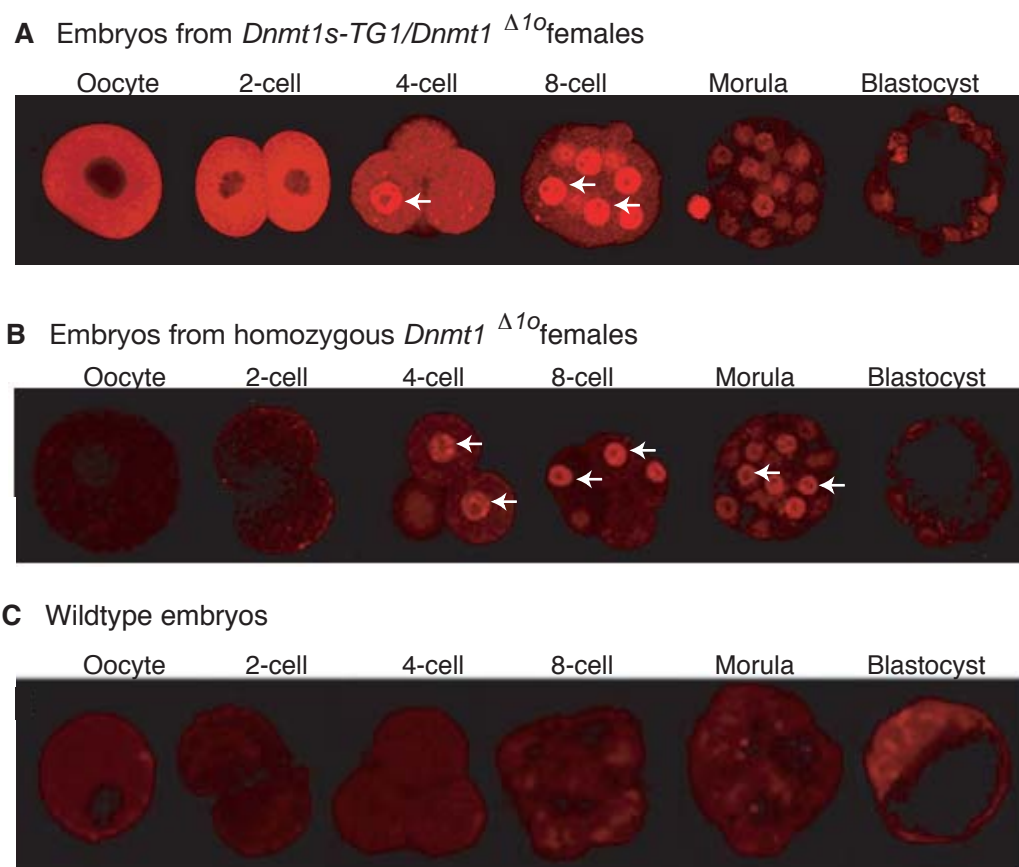


**Figure 9. Expression and localization of Dnmt1s protein, in the absence of Dnmt1o protein, during preimplantation development**

**Figure 9. Expression and localization of Dnmt1s protein, in the absence of Dnmt1o protein, during preimplantation development**

Immunostaining with UPT82 to show Dnmt1s nuclear localization in 4-cell, 8-cell and 16-cell stages of preimplantation development in A. embryos from *Dnmt1s-TG1/Dnmt1<sup>Δ1o</sup>* females and B. embryos from homozygous *Dnmt1<sup>Δ1o</sup>* females C. Immunostaining with UPT82 to show absence of Dnmt1s expression in wildtype preimplantation embryos. Arrows indicate the nuclear localization of Dnmt1s protein.

*Dnmt1*<sup>1s/1o</sup> allele. But in the transgenic mice, the cytoplasmic Dnmt1s was not as aggregated as was seen in the *Dnmt1*<sup>1s/1o</sup> mice (Figure 8D).

#### 1.2.1.4. Methylation of imprinted genes with forced expression of Dnmt1s protein

The oocytes obtained from either the homozygous *Dnmt1*<sup>1s/1o</sup> females or the *Dnmt1s-TG1* females, expressed both the Dnmt1s and Dnmt1o proteins. Offspring obtained from these mice were fertile and phenotypically normal. But there was the possibility of abnormal imprinted gene methylation due to the presence of the Dnmt1s protein in the nuclei of 8-cell stage embryos. To rule out this possibility, the methylation of imprinted genes *H19* and *Snrpn* were analyzed in offspring obtained from the mice misexpressing the Dnmt1s protein during oogenesis. This was done by using the bisulfite genomic sequencing technique to determine parental-allele specific methylation patterns on these imprinted gene sequences (Figure 10).

The methylation of *H19* and *Snrpn* genes in the E13.5 embryos obtained from *Dnmt1*<sup>1s/1o</sup> mice and *Dnmt1s-TG1* mice was found to be similar as in the wildtype embryos (Figures 11 and 12; Tables 3 and 4). The paternal alleles of the *H19* gene showed extensive methylated CpG dinucleotides while the maternal alleles showed very few methylated CpG dinucleotides, just like it is seen in wildtype mice. Similarly, the maternal *Snrpn* alleles showed extensive methylation while the paternal alleles showed insignificant amount of methylation. Thus, it appears that the forced expression of the Dnmt1s protein during oogenesis and preimplantation development does not cause aberrant methylation of imprinted genes.

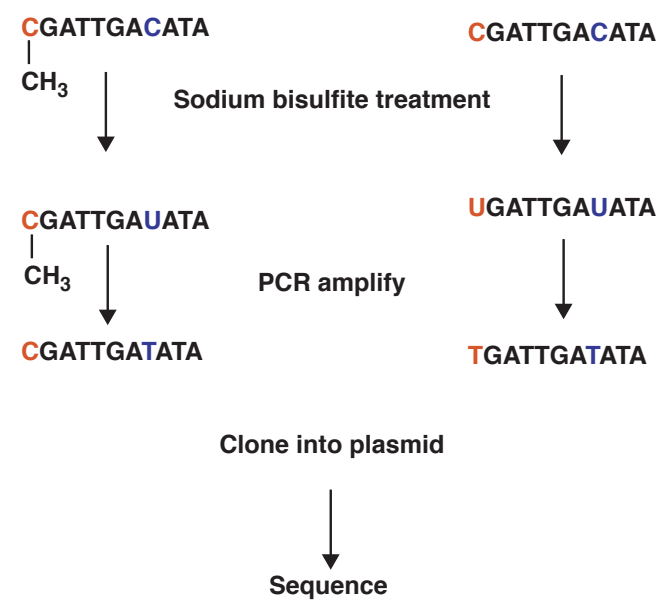
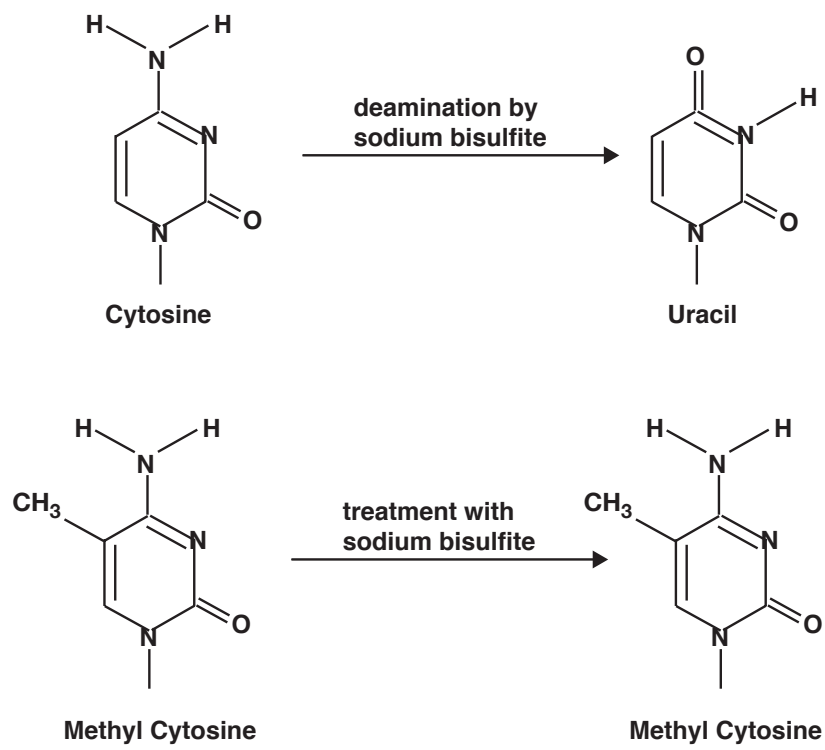


**Figure10. Analysis of DNA methylation using bisulfite genomic sequencing.**

**Figure 10. Analysis of DNA methylation using bisulfite genomic sequencing.**

Methylated CpG dinucleotides in a specific DNA sequence of interest can be detected using the bisulfite genomic sequencing technique. When treated with Sodium bisulfite, cytosines are converted to uracils while the methylcytosines are not converted. The specific regions to be analyzed are PCR amplified, the PCR products are cloned and sequenced. The presence of CpGs in the sequence indicate that they were originally methylated in the genomic sequence, while the replacement of CpGs by CpAs indicate that they were not methylated.

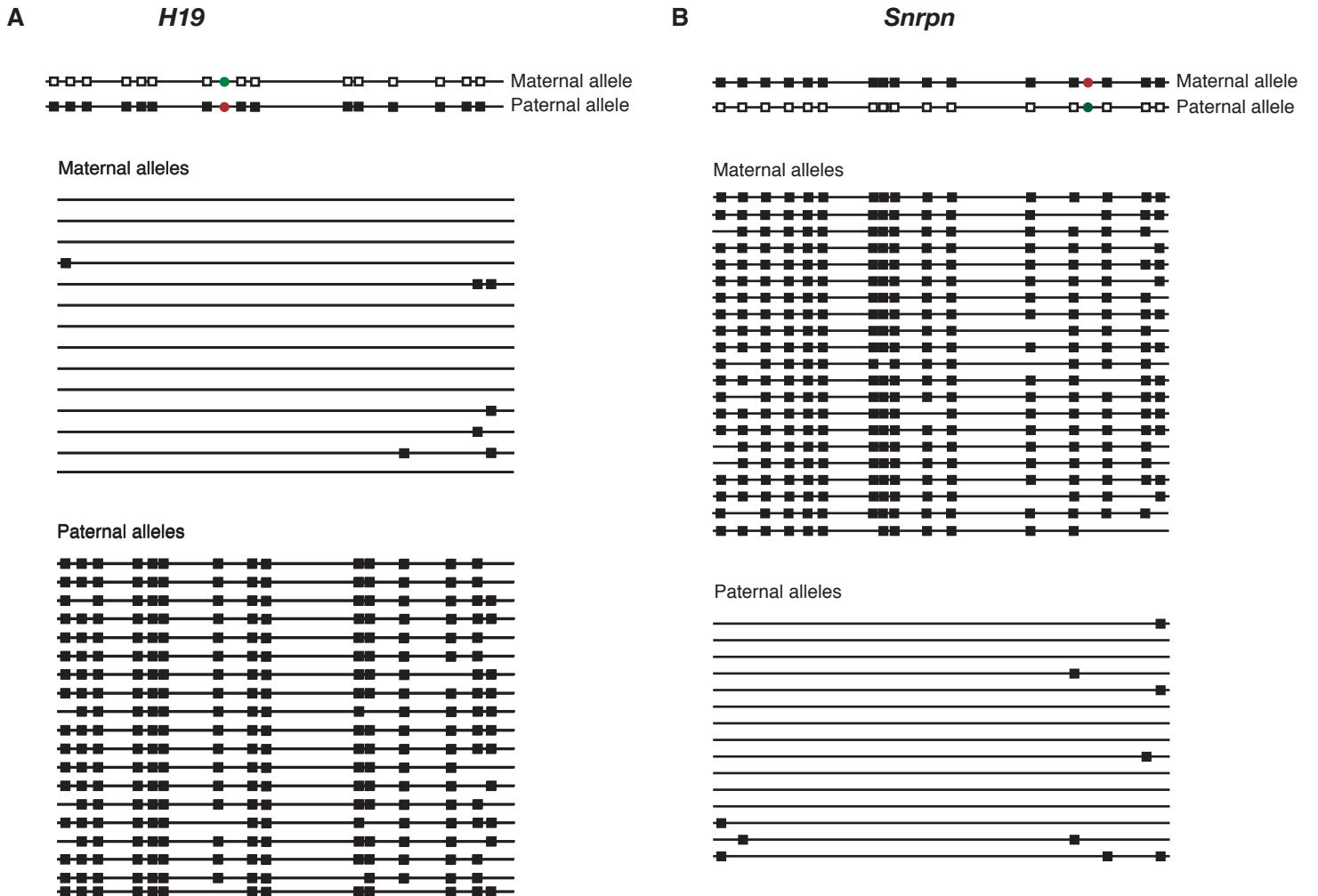
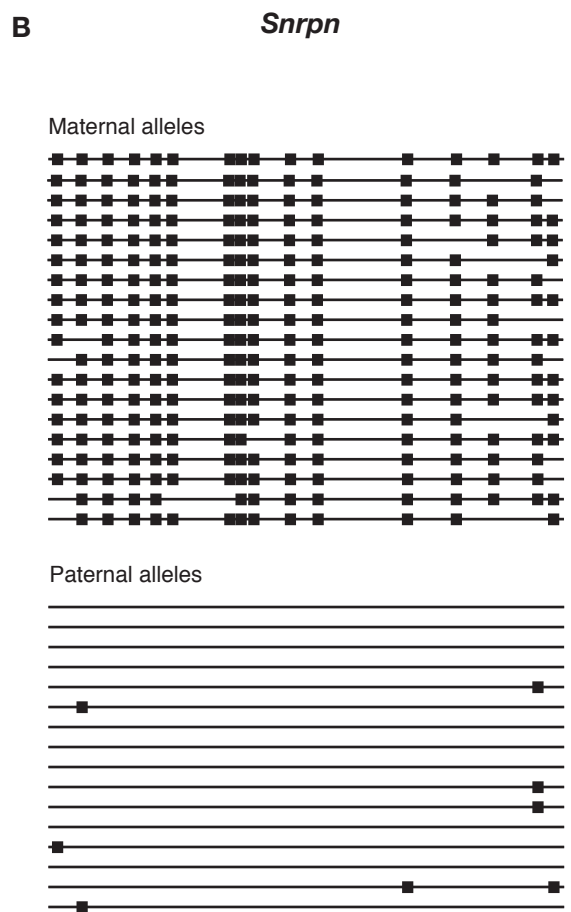
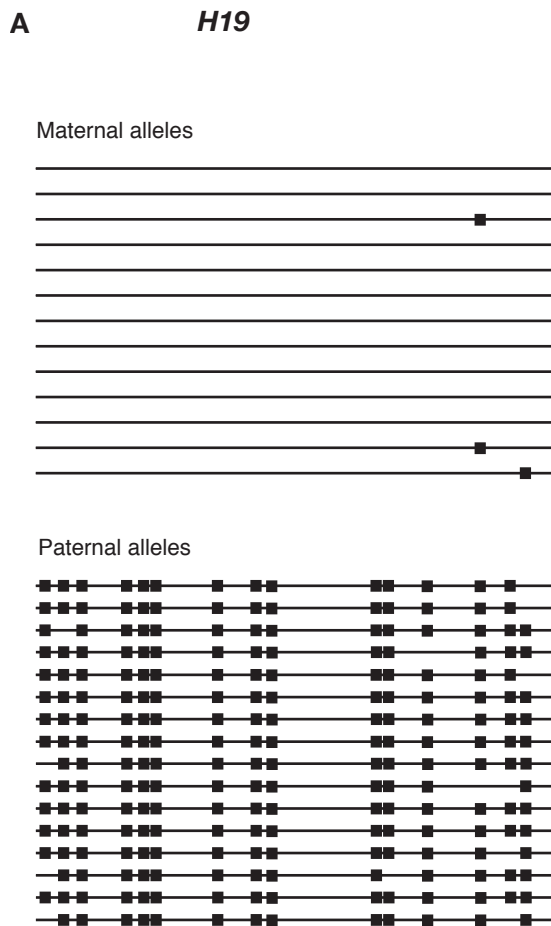


Figure 11. Analysis of imprinted gene methylation in *Dnmt1s-TG1* mice

### Figure 11. Analysis of imprinted gene methylation in *Dnmt1s-TG1* mice

To determine if *Dnmt1s* expression during preimplantation development causes abnormal imprinted gene methylation, tail DNA from *Dnmt1s-TG1* mice (hybrids for C57B6/J and CAST7 strains) were subjected to sodium bisulfite treatment and specific regions of imprinted genes were PCR amplified. The PCR products were cloned and sequenced to detect the methylated CpG dinucleotides. Each horizontal line represents an allele of the imprinted gene being analyzed. Each square represents a methylated CpG dinucleotide in the analyzed sequence. Lack of methylation at a CpG dinucleotide is depicted by the absence of a square. The paternal alleles were distinguished from the maternal alleles by a specific single nucleotide polymorphism (SNPs) between the C57B6/J and CAST7 strains of mice in the region being analyzed. A. Analysis of ~400 bp region of *H19* gene in *Dnmt1s-TG1* mice. As is depicted at the top of panel, the wildtype paternal alleles (the blue circle represents the paternal SNP) show methylation of almost all the CpG dinucleotides in the *H19* region while the wildtype maternal alleles (the red circle represents the maternal SNP) show absence of CpG methylation in the same region. In the *Dnmt1s-TG1* mice a wildtype pattern of methylation is seen in the *H19* region where the paternal alleles show methylation of almost all their CpG dinucleotides while the maternal alleles show nearly complete absence of methylated CpG dinucleotides. B. Analysis of ~400 bp region of *Snrpn* gene in *Dnmt1s-TG1* mice. As is depicted at the top of figure, the wildtype paternal alleles show absence of methylation of almost all the CpG dinucleotides in the *Snrpn* region while the wildtype maternal alleles methylation of almost all the CpG dinucleotides in the same region. In the *Dnmt1s-TG1* mice a wildtype pattern of methylation is seen in the *Snrpn* region where the maternal alleles show methylation of almost all their CpG dinucleotides while the paternal alleles show nearly complete absence of methylated CpG dinucleotides.



**Figure 12. Analysis of imprinted gene methylation in *Dnmt1<sup>1s/1o</sup>* mice**

**Figure 12. Analysis of imprinted gene methylation in *Dnmt1*<sup>1s/1o</sup> mice**

In the *Dnmt1*<sup>1s/1o</sup> mice, wildtype patterns of methylation are observed in the *H19* and *Snrpn* genes. A. Analysis of *H19* region in *Dnmt1*<sup>1s/1o</sup> mice. The paternal alleles show methylation of almost all their CpG dinucleotides in the *H19* region while the maternal alleles show nearly complete absence of methylated CpG dinucleotides. B. Analysis of *Snrpn* region in *Dnmt1*<sup>1s/1o</sup> mice. The maternal alleles show methylation of almost all their CpG dinucleotides while the paternal alleles show nearly complete absence of methylated CpG dinucleotides.

### 1.2.2. Functional analysis of Dnmt1s protein in Dnmt1o-deficient mice

As mentioned before, homozygous *Dnmt1<sup>Δ1o</sup>* females, when mated to wildtype males very rarely gave rise to live births due to lack of maintenance methylation in certain imprinted genes of the embryos. There was loss of one half of methylation in the imprinted genes studied. To determine if Dnmt1s can functionally replace Dnmt1o during preimplantation development and maintain normal methylation on imprinted genes, the *Dnmt1s-TG1* mice and the *Dnmt1s-TG2* were mated onto the *Dnmt1<sup>Δ1o</sup>* background to get mice that produce the Dnmt1s protein in their oocytes instead of the Dnmt1o form. These mice were called the *Dnmt1s-TG1/Dnmt1<sup>Δ1o</sup>* and the *Dnmt1s-TG2/Dnmt1<sup>Δ1o</sup>* mice respectively.

#### 1.2.2.1. Expression of the Dnmt1s protein in the *Dnmt1s-TG1/Dnmt1<sup>Δ1o</sup>* females during oogenesis

The mature oocytes from *Dnmt1s-TG1/Dnmt1<sup>Δ1o</sup>* females expressed only the Dnmt1s protein. This was determined by staining immunoblots of extracts of *Dnmt1s-TG1/Dnmt1<sup>Δ1o</sup>* oocytes with the PATH52 antibody which recognizes both the Dnmt1s and Dnmt1o proteins (Figure 7B). Only the  $M_r$  190,000 form of the Dnmt1 protein was picked up by the antibody on the immunoblot.

### 1.2.2.2. Localization and trafficking of the Dnmt1s protein in Dnmt1o-deficient mice during oogenesis and preimplantation development

In the embryos derived from the *Dnmt1s-TG1/Dnmt1<sup>Δ1o</sup>* females there is a somewhat different pattern of nuclear localization of the Dnmt1s protein when compared to the endogenous Dnmt1o protein. The Dnmt1s protein was observed, using the UPT82 antibody, in the nuclei of the 4-cell, 8-cell and 16-cell embryos, as opposed to the endogenous Dnmt1o protein which only shows nuclear localization at the 8-cell stage (Figure 9A). Similar expression and nuclear localization of the Dnmt1s protein was observed in the preimplantation embryos derived from the homozygous *Dnmt1<sup>Δ1o</sup>* females (Figure 9B) without the Dnmt1s transgene. This ectopic Dnmt1s protein is not seen in the embryos derived from the homozygous *Dnmt1<sup>1s/1o</sup>* females which produce both the Dnmt1s and Dnmt1o proteins. Therefore, the absence of the maternal Dnmt1o protein and subsequent aberrant embryonic synthesis of the Dnmt1s protein might be the cause of the aberrant nuclear localization of the Dnmt1s protein seen in the 4-cell and 16-cell embryos derived from *Dnmt1s-TG1/Dnmt1<sup>Δ1o</sup>* and homozygous *Dnmt1<sup>Δ1o</sup>* females.

### 1.2.2.3. Restoration of genomic imprinting in offspring derived from *Dnmt1s-TG1/Dnmt1<sup>Δ1o</sup>* mice

To study the ability of Dnmt1s protein to functionally rescue the Dnmt1o-deficient oocytes, we mated the *Dnmt1s-TG1/Dnmt1<sup>Δ1o</sup>* females to wild type males and recorded the number of live births obtained from these matings. The number of live births (survivors) obtained was significantly higher (6 litters out of 9 matings) than in the mutant homozygous *Dnmt1<sup>Δ1o</sup>* females. But the number of mice in a litter was still lesser than in a wildtype litter.

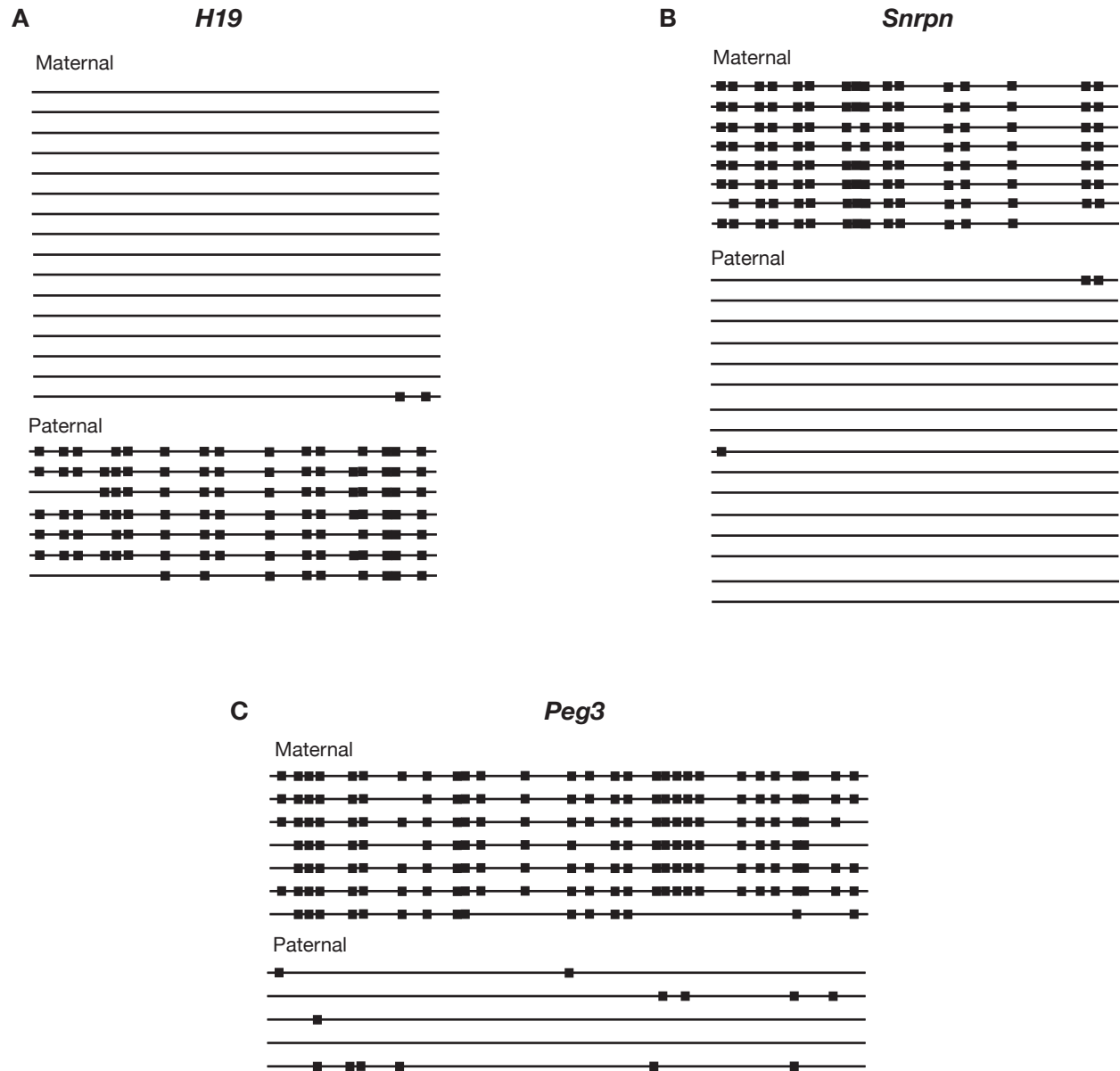


**Figure 13. Analysis of imprinted gene methylation in survivors obtained from *Dnmt1s-TG1/Dnmt1<sup>Al0</sup>* females.**

**Figure 13. Analysis of imprinted gene methylation in survivors obtained from *Dnmt1s-TG1/Dnmt1<sup>Δ10</sup>* females.**

Tail DNA from survivors obtained from *Dnmt1s-TG1/Dnmt1<sup>Δ10</sup>* females were subjected to sodium bisulfite treatment and specific regions of imprinted genes were analyzed for CpG dinucleotide methylation. A. Analysis of *H19* region in survivor 1 from *Dnmt1s-TG1/Dnmt1<sup>Δ10</sup>* female. Wildtype patterns of methylation are observed in the *H19* region in survivor 1 where the paternal alleles show methylation of almost all their CpG dinucleotides while the maternal alleles show nearly complete absence of methylation of all their CpGs. B. Analysis of *Snrpn* region in survivor 1 from *Dnmt1s-TG1/Dnmt1<sup>Δ10</sup>* female. The maternal alleles show primarily methylated CpG dinucleotides while the paternal alleles show mostly unmethylated CpG dinucleotides. C. Analysis of *Peg3* region in survivor 1 from *Dnmt1s-TG1/Dnmt1<sup>Δ10</sup>* female. Just like in the *Snrpn* gene, the maternal alleles contain predominantly methylated CpG dinucleotides and the paternal alleles contain mostly unmethylated CpG dinucleotides. Thus, it appears that survivor 1 from *Dnmt1s-TG1/Dnmt1<sup>Δ10</sup>* female shows a wildtype pattern of methylation on the imprinted genes, *H19*, *Snrpn* and *Peg*. The other three survivors analyzed also showed similar patterns of imprinted gene methylation as survivor 1.

To determine if there were normal methylation patterns established in these survivors obtained from the *Dnmt1s-TG1/Dnmt1<sup>Δ10</sup>* females, we studied the maintenance of methylation in the three imprinted genes: *H19*, *Snrpn* and *Peg3* using the bisulfite genomic sequencing technique.

In all 4 survivors analyzed in a litter, there was complete restoration of methylation in all three genes (Figures 13 and 22; Table 13). Specifically, all the paternal alleles of the *H19* gene showed extensive methylation of CpG dinucleotides, unlike in the embryos derived from the homozygous *Dnmt1<sup>Δ10</sup>* females where the paternal alleles of the *H19* gene showed a 50% reduction in methylation. The maternal alleles showed an insignificant level of CpG dinucleotide methylation, as is normally seen in wildtype alleles. The *Snrpn* and *Peg3* genes also showed normal methylation patterns. The maternal alleles of these genes showed a high level of methylation at CpG dinucleotides, comparable to wildtype alleles while the paternal alleles showed virtually no methylation. It seemed like *Dnmt1s* had a similar function to *Dnmt10* during preimplantation development and could thus functionally rescue the *Dnmt10*-deficient phenotype.

But as mentioned before, the number of mice in a litter was significantly lower than in a wildtype litter. We therefore looked at E13.5 embryos from *Dnmt1s-TG1/Dnmt1<sup>Δ10</sup>* females and found that the number of E13.5 embryos obtained was similar to that from a wildtype litter. We then analyzed the methylation of imprinted genes in these embryos obtained from *Dnmt1s-TG1/Dnmt1<sup>Δ10</sup>* females to look for differences in the maintenance of methylation on imprinted genes (namely *H19*, *Snrpn* and *Peg3* genes) between the embryos. Among the 4 embryos studied, one of them (embryo 1 and embryo 3) showed normal methylation patterns for the *H19*

gene. The other two embryos (embryo 2 and embryo 4) exhibited patterns of maternal and paternal methylation that were more consistent with a partial or incomplete restoration of *H19* methylation (Figures 14 and 22; Table 3). The maternal alleles in these two embryos showed no evidence of aberrant methylation yet there was a distinct deficit of methylation on the paternal alleles when compared to the methylation on the paternal alleles from wildtype embryos. But this loss was not as high as a 50% loss that was seen in the embryos from *Dnmt1<sup>Δ10</sup>* homozygous females (Figure 17; Howell et al. 2001).

Similar patterns of methylation were seen for the *Snrpn* and *Peg3* genes. Embryo 1 showed the normal pattern of methylation as seen in wildtype embryos. But the other three embryos showed less than complete methylation on the maternal alleles that would normally have been completely methylated (Figures 15 and 16; Tables 3 and 4). But the loss of methylation was significantly lower than a 50% loss that was seen in embryos derived from *Dnmt1<sup>Δ10</sup>* homozygous females. Thus, a partial or nearly complete restoration of imprinted methylation was once again evident for the *Snrpn* and *Peg3* genes, just like in the *H19* gene. Taken together, the methylation analysis on these four embryos was consistent with oocyte-derived Dnmt1s protein maintaining imprinted methylation patterns, either wholly or partially, during preimplantation development.

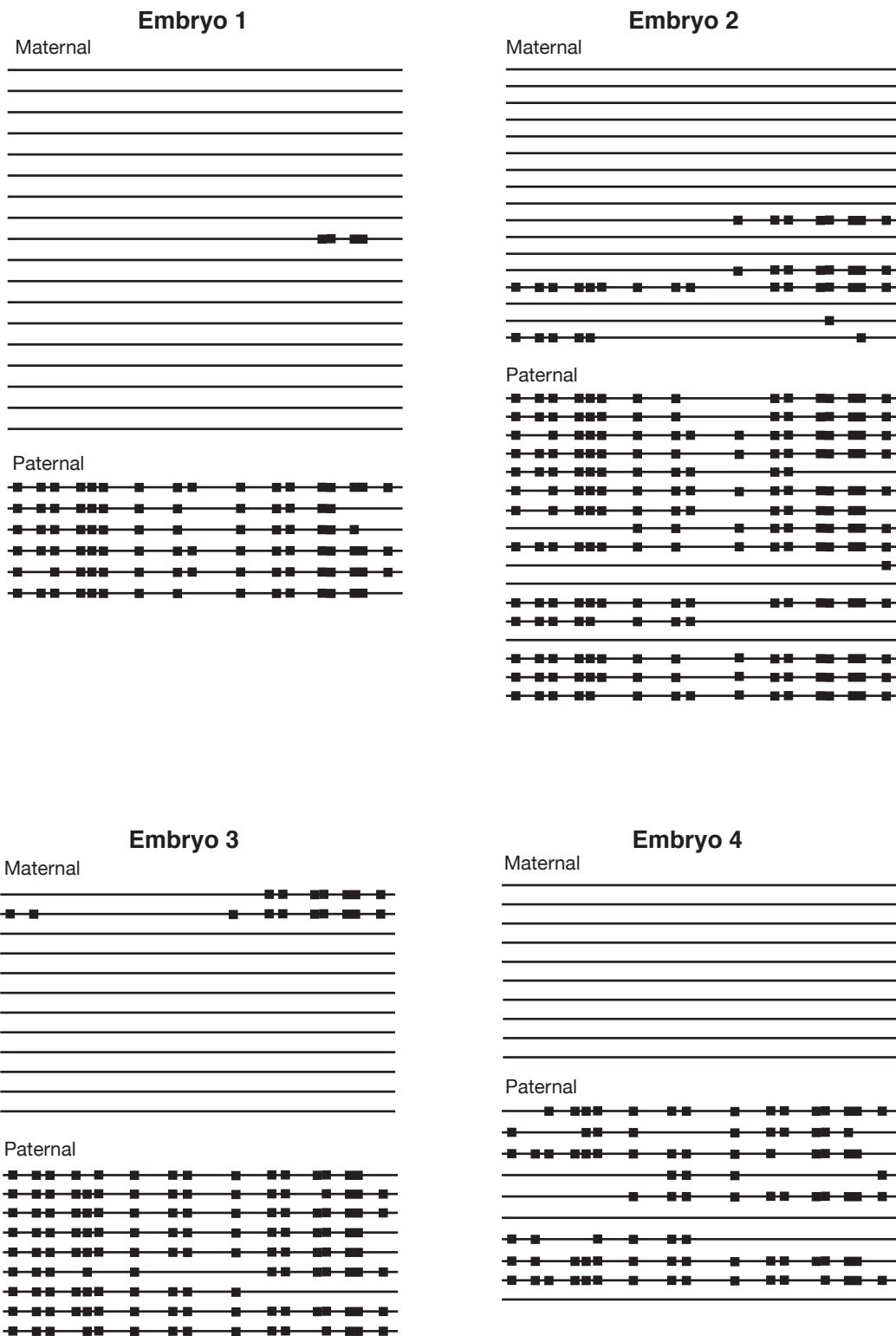


Figure 14. Analysis of *H19* methylation in day 13.5 embryos obtained from *Dnmt1s-TG1/Dnmt1<sup>Δ10</sup>* females

**Figure 14. Analysis of *H19* methylation in day 13.5 embryos obtained from *Dnmt1s-TG1/Dnmt1<sup>Δ10</sup>* females.**

Day 13.5 embryos were obtained from *Dnmt1s-TG1/Dnmt1<sup>Δ10</sup>* females, ground in liquid nitrogen, subjected to sodium bisulfite treatment and specific regions of imprinted genes were analyzed for CpG dinucleotide methylation. A variation in *H19* methylation is observed in the four embryos (embryo1, embryo 2, embryo 3 and embryo 4) obtained from *Dnmt1s-TG1/Dnmt1<sup>Δ10</sup>* females. Embryo 1 and embryo 3 show a pattern of methylation that is similar to the wildtype pattern of methylation where almost all the paternal alleles have their CpG dinucleotides methylated while the maternal alleles have near or complete absence of methylated CpG dinucleotides. On the other hand, some of the paternal alleles from embryo 2 and embryo 4 show a loss of methylation on a significant number of their CpG dinucleotides.

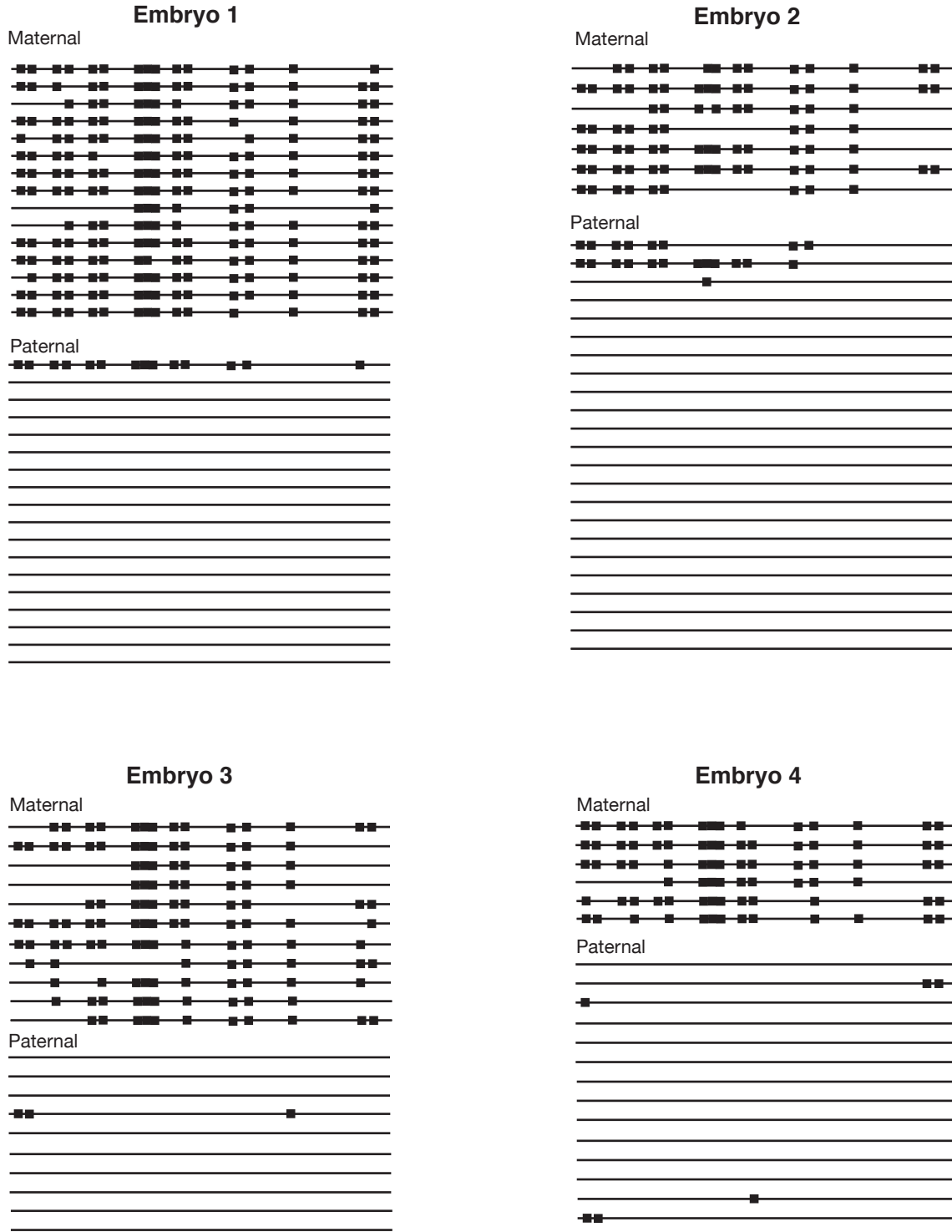


Figure 15. Analysis of *Snrpn* methylation in day 13.5 embryos obtained from *Dnmt1s-TG1/Dnmt1<sup>Δ10</sup>* females

**Figure 15. Analysis of *Snrpn* methylation in day 13.5 embryos obtained from *Dnmt1s-TG1/Dnmt1<sup>Δ10</sup>* females**

Just like in figure 14, a variation in *Snrpn* methylation is also observed in the four embryos (embryo 1, embryo 2, embryo 3 and embryo 4) obtained from *Dnmt1s-TG1/Dnmt1<sup>Δ10</sup>* females. Embryo 1 shows the normal pattern of methylation as seen in wildtype embryos. But the other three embryos show less than complete methylation on the maternal alleles that would normally have been completely methylated.

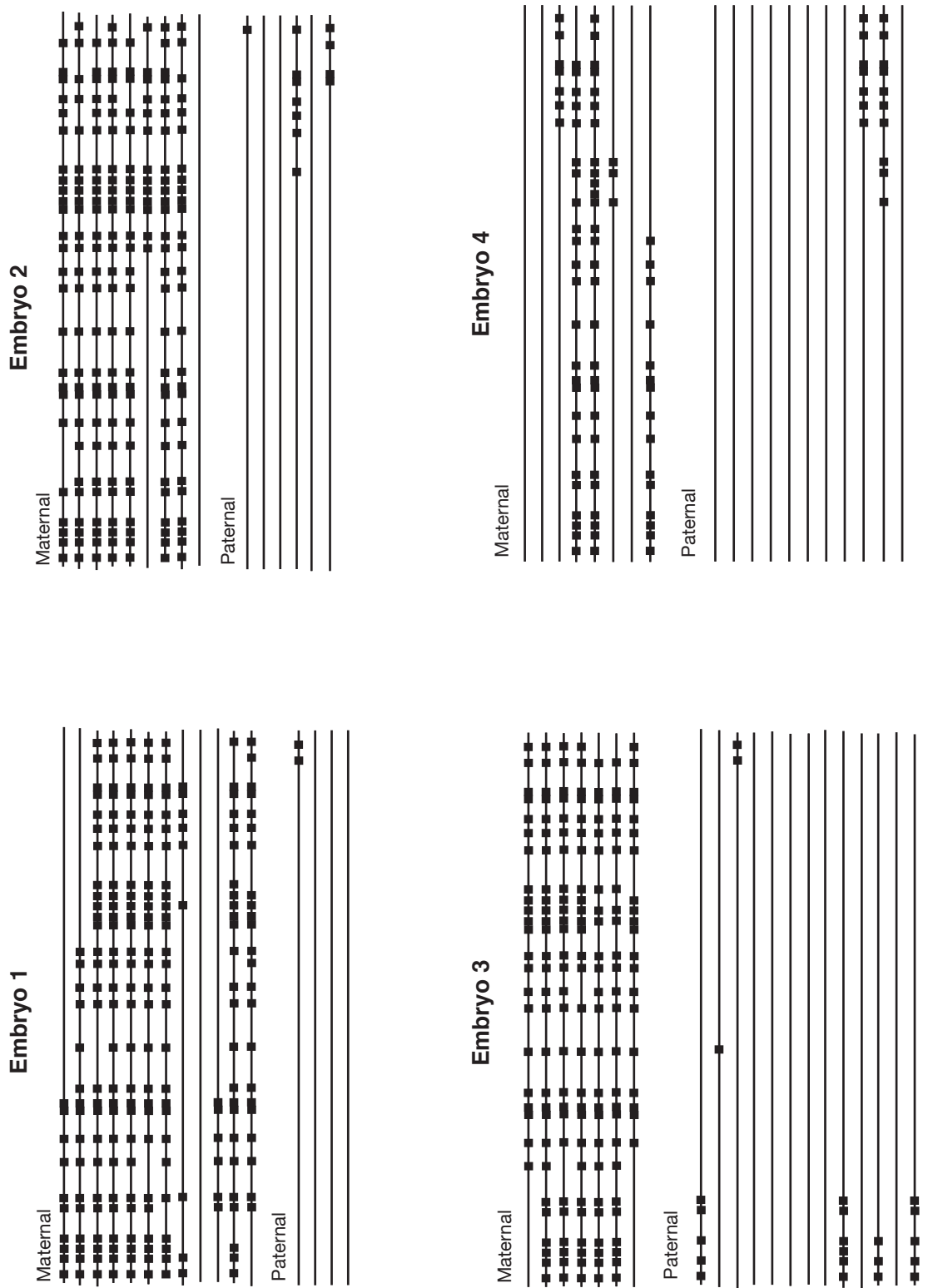


Figure 16. Analysis of *Peg3* methylation in day 13.5 embryo obtained from *Dnmt1s-TG1/Dnmt1<sup>Δ10</sup>* females

**Figure 16. Analysis of *Peg3* methylation in day 13.5 embryo obtained from *Dnmt1s-TG1/Dnmt1<sup>Δ10</sup>* females.**

As in figures 14 and 15, a variation in *Peg3* methylation is also observed in the four embryos (embryo 1, embryo 2, embryo 3 and embryo 4) obtained from *Dnmt1s-TG1/Dnmt1<sup>Δ10</sup>* females. Embryo 1 shows a wildtype pattern of methylation. But the other three embryos show less than complete methylation on the maternal alleles that would normally have been completely methylated. Thus, a partial or nearly complete restoration of imprinted methylation is evident for the *H19*, *Snrpn* and *Peg3* genes in these embryos.

#### 1.2.2.4. Expression of imprinted genes in offspring derived from *Dnmt1s-TG1/Dnmt1<sup>Δ1o</sup>* females

As mentioned before, there is a strict correlation between the parental allele-specific methylation of imprinted genes and their expression (Groudine et al. 1987; Weintrub H 1985). This would lead to the expectation that the restoration of imprinted gene methylation in the offspring obtained from *Dnmt1s-TG1/Dnmt1<sup>Δ1o</sup>* females is also reflected in the parental allele-specific expression of these imprinted genes. To confirm this, we analyzed the expression of maternal and paternal alleles of *H19* and *Snrpn* genes in both the survivors and the E13.5 embryos derived from the *Dnmt1s-TG1/Dnmt1<sup>Δ1o</sup>* female mice. As shown in Figure 18, the expression analysis of the *H19* and *Snrpn* genes showed that there was monoallelic expression of these genes (maternal allele expression in *H19* and paternal allele expression in *Snrpn*) in all the survivors, correlating with their methylation pattern and confirming the restoration of gene imprinting in the survivors.

We also looked at the expression of these imprinted genes in the E13.5 embryos. Two of the embryos (embryo 1 and embryo 3) showed monoallelic expression of *H19* and *Snrpn* genes that was consistent with the restoration of methylation in these embryos (Figure 18). The other two embryos showed biallelic expression of the *H19* and *Snrpn* genes and this correlated with the reduced levels of methylation observed in the paternal *H19* alleles and the maternal *Snrpn* alleles in these embryos.

Thus, it appears that Dnmt1s can either completely or partially restore the function of Dnmt1o during preimplantation development. Only some of the embryos in the litter appeared to show complete maintenance methylation of imprinted genes and their corresponding monoallelic expression and presumably it is these embryos which give rise to live births. The other embryos that showed reduced levels of methylation in the imprinted genes analyzed are probably the ones that do not survive to term.

#### 1.2.2.5. Analysis of genomic imprinting in embryos obtained from *Dnmt1s-TG2/Dnmt1<sup>Δ1o</sup>* females

To determine if it is important to have high levels of Dnmt1s protein in the mature oocyte to restore genomic imprinting in the Dnmt1o-deficient mice, the *Dnmt1s-TG2/Dnmt1<sup>Δ1o</sup>* line of mice was analyzed. As shown in Figure 7C, the MII oocytes from the *Dnmt1s-TG2* females expressed lesser amounts of Dnmt1s protein when compared to the oocytes from the *Dnmt1s-TG1* females. So this line of mice would be suitable to study the differences in restoration of genomic imprinting in Dnmt1o-deficient mice due to differences in the level of oocyte-derived Dnmt1s protein.

*Dnmt1s-TG2/Dnmt1<sup>Δ1o</sup>* females were mated to wildtype CAST7 males to obtain embryos and survivor offspring. Not unexpectedly, no survivors were obtained from *Dnmt1s-TG2/Dnmt1<sup>Δ1o</sup>* females. We then looked for E13.5 embryos in the *Dnmt1s-TG2/Dnmt1<sup>Δ1o</sup>* females. The number of embryos obtained from a single litter was lesser than that normally derived from a wildtype female but corresponded to the number of embryos typically obtained from a homozygous *Dnmt1<sup>Δ1o</sup>* female (Howell et al. 2000).

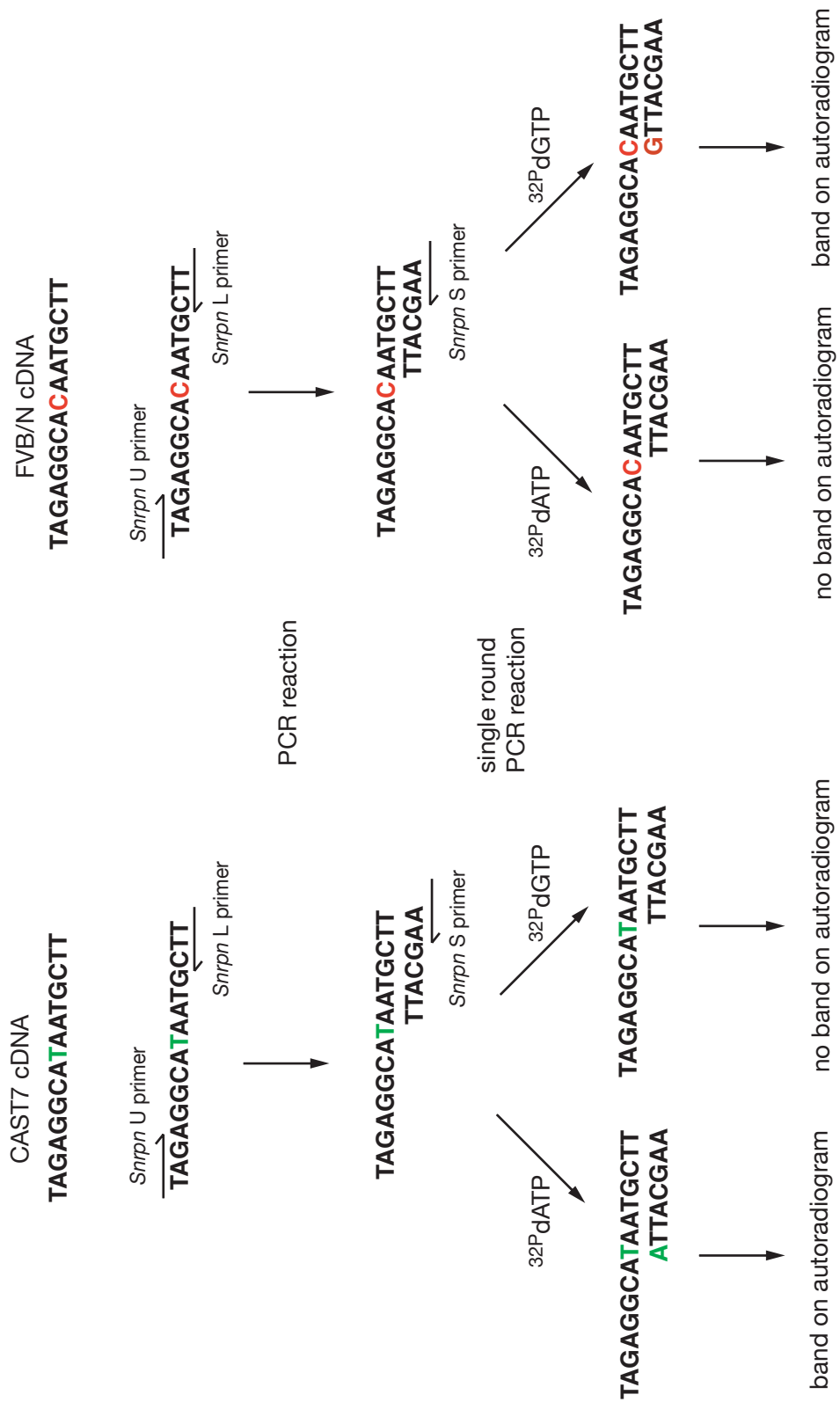


**Figure 17 Analysis of imprinted gene expression using Single Nucleotide Primer Extension (SNUPE)**

**Figure 17 Analysis of imprinted gene expression using Single Nucleotide Primer Extension (SNUPE)**

The SNUPE method (Szabo and Mann 1995) uses the single nucleotide polymorphisms (SNPs) found between the C57B6/J and CAST7 strains of mice. RNA from a hybrid mouse tissue is obtained and subjected to RT-PCR. The cDNA is mixed with a radiolabeled nucleotide specific to the allele of the parent to be tested for expression and one round of amplification is performed without the addition of other nucleotides. The PCR product is run on an acrylamide gel and exposed to film.

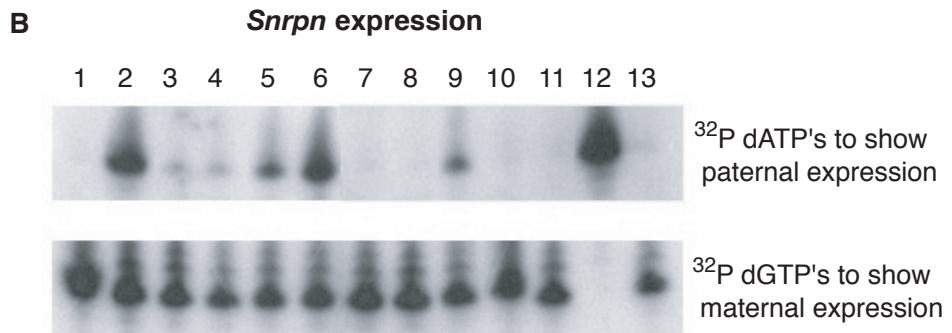
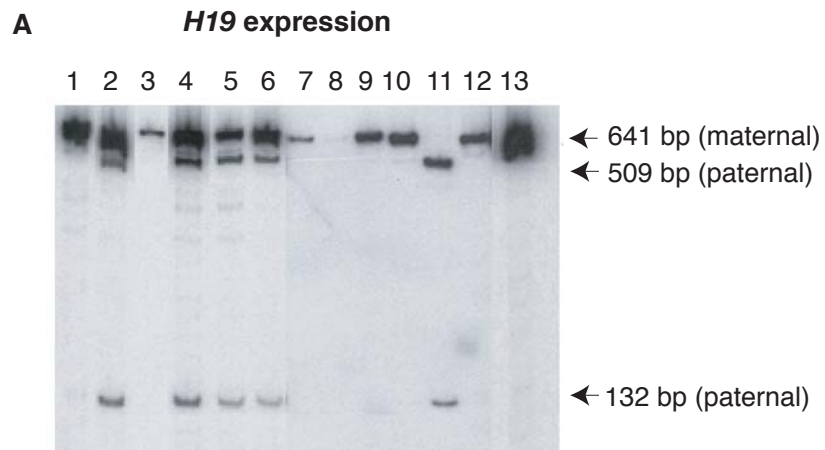


**Figure 18. Expression analysis of imprinted genes.**

**Figure 18. Expression analysis of imprinted genes.**

A. Analysis of *H19* expression. cDNA was obtained from the various samples and the H19 region was PCR amplified. The PCR product was digested by *Cac81*. The presence of a 641 bp band indicated maternal expression and the presence of a 509 bp band indicated paternal expression. B. Analysis of *Snrpn* expression using SNUPE. cDNA was obtained from the various samples and the *Snrpn* region was PCR amplified, followed by the SNUPE assay. Presence of a band with only  $^{32}\text{P}$  dGTPs indicated monoallelic expression while presence of bands with both  $^{32}\text{P}$  dATPs and  $^{32}\text{P}$  dGTPs indicated biallelic expression. 1-4 > D13.5 embryos from *Dnmt1-TG1* female on a *Dnmt1<sup>Δ1o</sup>* background, 5-6 > D13.5 embryos from homozygous *Dnmt1<sup>Δ1o</sup>* female, 7-10 > tissue samples from survivors obtained from *Dnmt1-TG1* female on a *Dnmt1<sup>Δ1o</sup>* background, 11 > tissue sample from a CAST7 female, 12 > tissue sample from a FVB/N female, 13 > tissue sample from a wildtype female.

We then analyzed the methylation of imprinted genes, specifically *H19*, *Snrpn* and *Peg3* in one of these E13.5 embryos obtained from *Dnmt1s-TG2/Dnmt1<sup>Δ1o</sup>* females. As expected, *H19* and *Snrpn* showed an almost 50% loss of methylation in their paternal and maternal alleles respectively when compared to the alleles in wildtype embryos (Figure 20; Tables 3 and 4). *Peg3* showed a 30% loss of methylation from the maternal alleles. The maternal alleles in *H19* and paternal alleles in *Snrpn* and *Peg3* showed no aberrant methylation in their CpG dinucleotides. The methylation pattern seen in the embryos from *Dnmt1s-TG2/Dnmt1<sup>Δ1o</sup>* oocytes is very similar to that seen in embryos derived from *Dnmt1o*-deficient oocytes (Howell et al. 2000; Figure 19; Tables 3 and 4). Thus, it appears that the *Dnmt1s-TG2/Dnmt1<sup>Δ1o</sup>* line cannot rescue the *Dnmt1<sup>Δ1o</sup>* phenotype. As seen before, the only difference between the *Dnmt1s-TG1/Dnmt1<sup>Δ1o</sup>* oocytes and *Dnmt1s-TG2/Dnmt1<sup>Δ1o</sup>* oocytes is the amount of *Dnmt1s* protein expressed in the mature oocyte. This leads to the conclusion that the *Dnmt1s* protein needs to be present in high levels in the MII oocyte for the maintenance of methylation in imprinted genes during the 8-cell preimplantation stage of development.

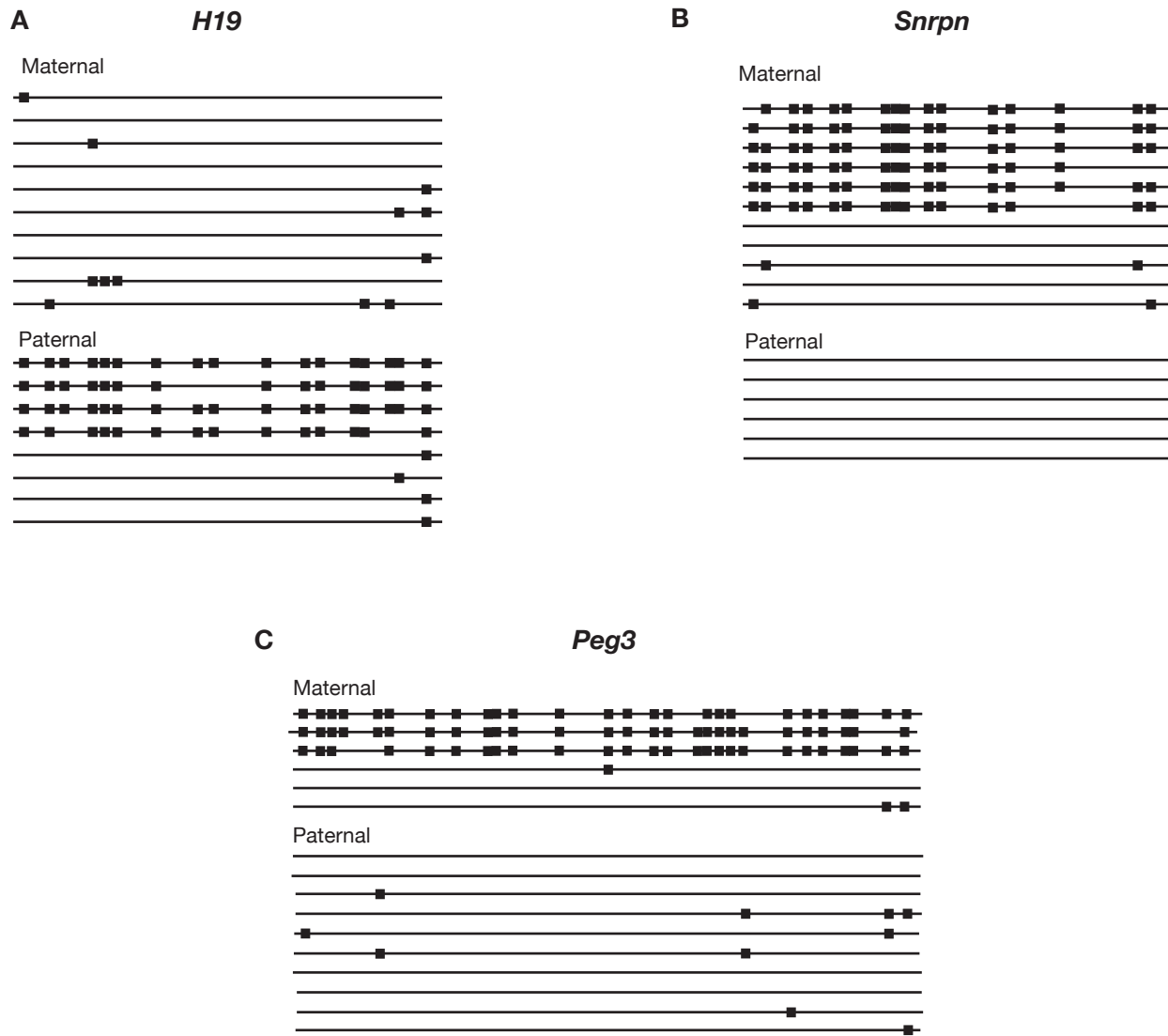


**Figure 19.** Analysis of imprinted gene methylation in day 13.5 embryos obtained from homozygous *Dnmt1*<sup>Δ10</sup> females on a FVB/N background.

**Figure 19. Analysis of imprinted gene methylation in day 13.5 embryos obtained from homozygous *Dnmt1*<sup>Δ10</sup> females on a FVB/N background.**

Day 13.5 embryo was obtained from homozygous *Dnmt1*<sup>Δ10</sup> females, ground in liquid nitrogen, subjected to sodium bisulfite treatment and specific regions of imprinted genes were analyzed for CpG dinucleotide methylation. The *H19* region show a marked loss of methylation on its CpG dinucleotides as can be seen in panel A. Specifically, about half the paternal alleles show a complete absence of methylated CpG dinucleotides. The maternally methylated imprinted genes *Snrpn* and *Peg3* also show a similar 50% loss of methylation as can be seen in panels B and C respectively.

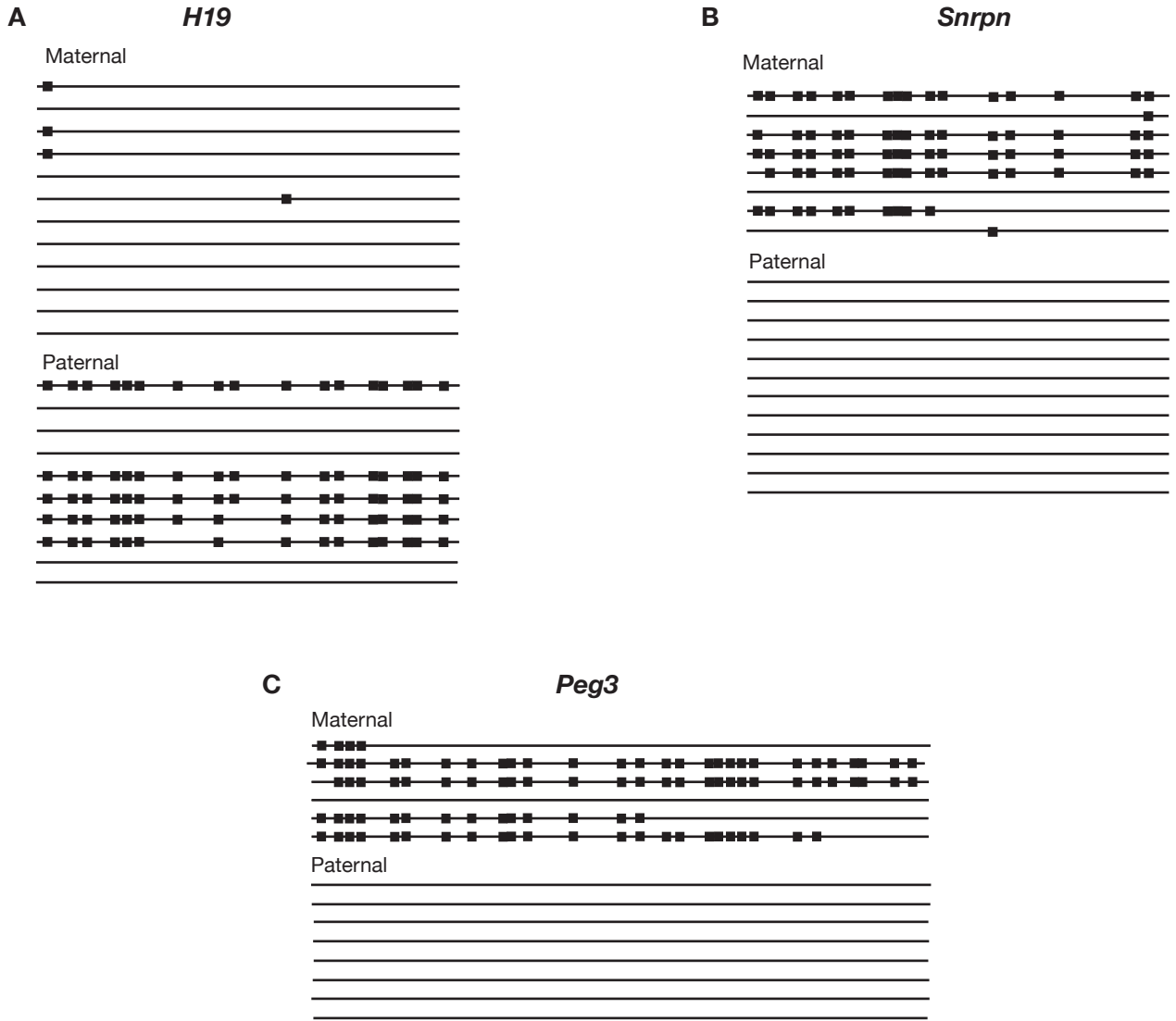


**Figure 20.** Analysis of imprinted gene methylation in day 13.5 embryo obtained from *Dnmt1s-TG2/Dnmt1<sup>Δ10</sup>* females.

**Figure 20. Analysis of imprinted gene methylation in day 13.5 embryo obtained from *Dnmt1s-TG2/Dnmt1<sup>Δ1o</sup>* females.**

Panel A demonstrates that in the embryo obtained from *Dnmt1s-TG2/Dnmt1<sup>Δ1o</sup>* female, the *H19* region did not show a restoration of methylation as seen in the embryos obtained from *Dnmt1s-TG1/Dnmt1<sup>Δ1o</sup>* females. Instead, the paternal alleles still showed a 50% loss of methylation on its CpG dinucleotides as seen in the embryos obtained from homozygous *Dnmt1<sup>Δ1o</sup>* females. The maternally methylated imprinted genes *Snrpn* and *Peg3* also show a similar 50% loss of methylation as can be seen in panels B and C respectively.

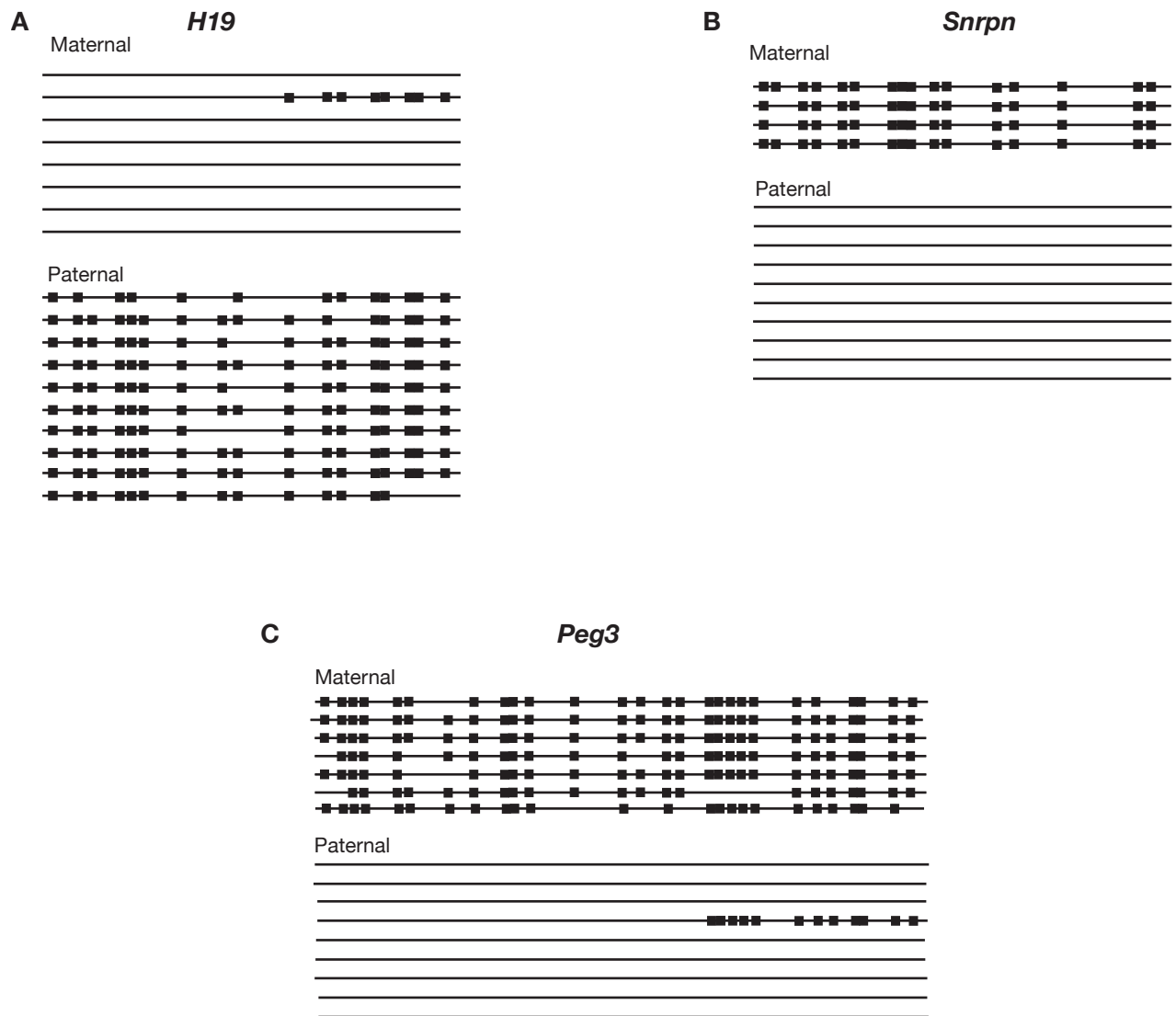


**Figure 21. Analysis of imprinted gene methylation in day 13.5 embryo obtained from heterozygous *Dnmt1*<sup>Δ10</sup> female on a FVB/N background.**

**Figure 21. Analysis of imprinted gene methylation in day 13.5 embryo obtained from heterozygous *Dnmt1*<sup>Δ10</sup> female on a FVB/N background.**

In spite of lower levels of Dnmt1o protein in the oocytes compared to wildtype oocytes, day 13.5 embryo obtained from heterozygous *Dnmt1*<sup>Δ10</sup> female shows wildtype patterns of imprinted gene methylation. Specifically, all the paternal alleles of *H19* gene show complete CpG dinucleotide methylation (A) while all the maternal alleles of *Snrpn* and *Peg3* genes contain predominantly methylated CpG dinucleotides (B and C respectively).

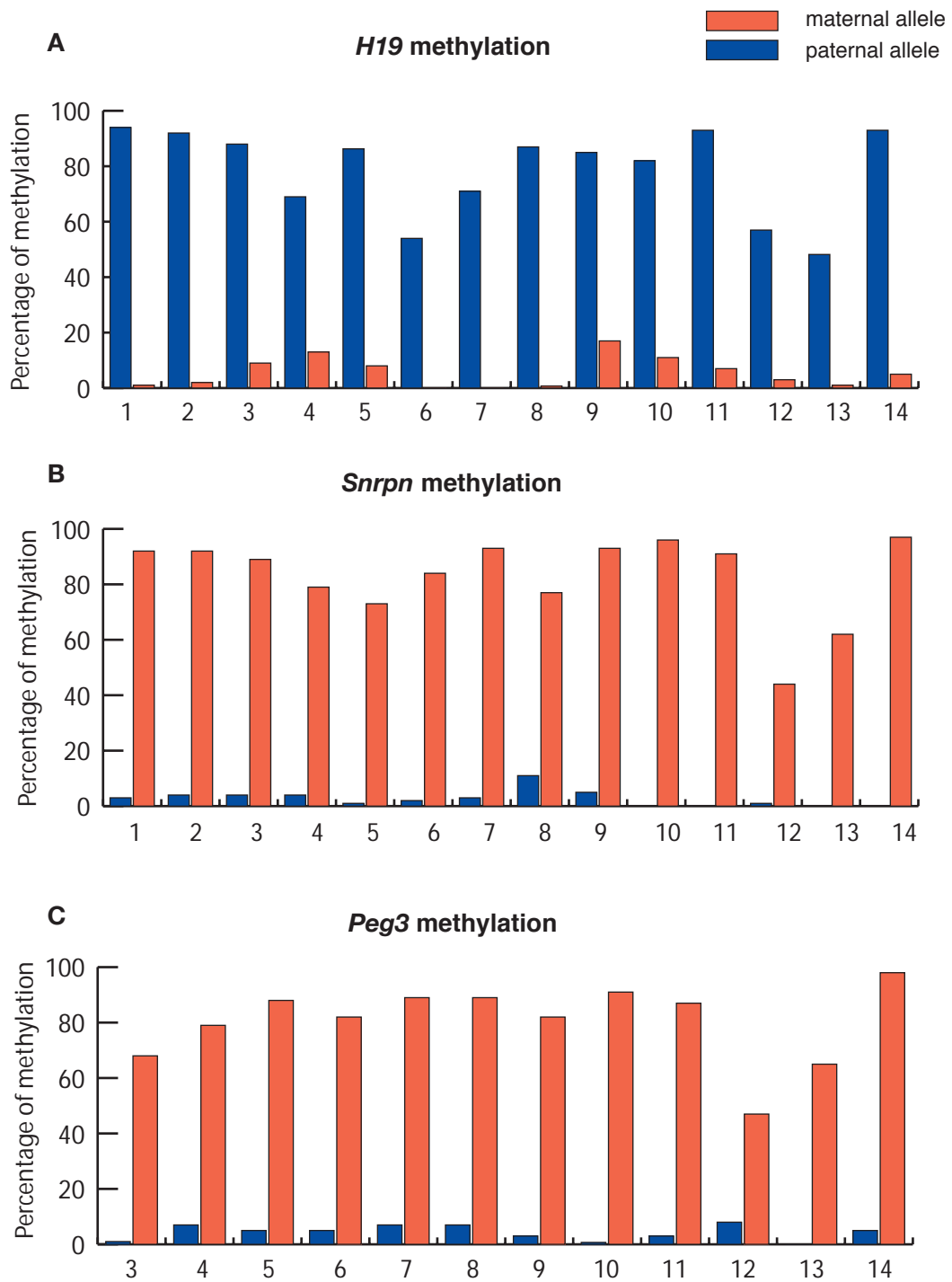


**Figure 22. Methylation analysis of imprinted genes.**

**Figure 22. Methylation analysis of imprinted genes.**

A. Graph depicting the methylation of the *H19* gene. Blue bars depict the paternal allele and red bars depict the maternal alleles. B. Graph representing the methylation of the *Snrpn* gene. C. Graph showing the methylation of the *Peg3* gene. 1 > D13.5 embryo from *Dnmt1<sup>ls/lo</sup>* female, 2 > D13.5 embryo from *Dnmt1s-TG1* female, 3-6 > D13.5 embryos from *Dnmt1s-TG1/Dnmt1<sup>Δlo</sup>* female, 7-10 > survivors from *Dnmt1-TG1* female on a *Dnmt1<sup>Δlo</sup>* background, 11 > D13.5 embryos from a wildtype female, 12 > D13.5 embryo from a homozygous *Dnmt1<sup>Δlo</sup>* female, 13 > D13.5 embryo from *Dnmt1s-TG2/Dnmt1<sup>Δlo</sup>* female, 14 > D13.5 embryo from *Dnmt1<sup>Δlo/+</sup>* female.

### **Table 3. Percentage of CpG dinucleotide methylation in imprinted genes**

Using the bisulfite genomic sequencing analysis, the number of methylated CpG dinucleotides per allele (paternal or maternal) was calculated for each gene (*H19*, *Snrpn* and *Peg3*). The total number of methylated CpG dinucleotides from all the paternal or maternal alleles of *H19* was then compared to the total number of CpG dinucleotides (methylated and unmethylated) present in the paternal or maternal alleles of *H19* and thus, the percentage of methylated CpG dinucleotides was calculated. Similarly the percentage of methylated CpG dinucleotides was calculated for *Snrpn* and *Peg3*.

**Table 3. Percentage of CpG dinucleotide methylation in imprinted genes**

	Embryo or Survivor #	<i>H19</i>		<i>Snrpn</i>		<i>Peg3</i>	
		Paternal alleles	Maternal alleles	Paternal alleles	Maternal alleles	Paternal alleles	Maternal alleles
<b>Wildtype</b>	Embryo1	93	3	0	91	3	87
<i>Dnmt1s-TG1</i>	Embryo 1	92	2	4	92	NA	NA
<i>Dnmt1<sup>1s/1o</sup></i>	Embryo 1	94	1	3	92	NA	NA
<i>Dnmt1s-TG1/Dnmt1<sup>Δ1o</sup></i>	Embryo 1	88	9	4	89	1	68
	Embryo 2	69	13	4	79	7	79
	Embryo 3	87	8	1	73	5	88
	Embryo 4	54	0	2	84	5	82
	Survivor1	71	0	3	93	7	89
	Survivor2	87	0.7	11	77	7	89
	Survivor3	85	17	5	93	3	82
	Survivor4	82	11	0	96	0.7	91
<i>Dnmt1s-TG2/Dnmt1<sup>Δ1o</sup></i>	Embryo 1	48.2	1	0	62	0	65
<b>Homozygous <i>Dnmt1<sup>Δ1o</sup></i></b>	Embryo 1	57	3	1	44	8	47
<b>Heterozygous <i>Dnmt1<sup>Δ1o</sup></i></b>	Embryo 1	93	5	0	97	98	5

**Table 4. Paired Student T-test for analysis of methylation differences in imprinted genes**

Using the bisulfite genomic sequencing analysis, the methylated CpG dinucleotides per allele (paternal or maternal) were identified for each gene (*H19*, *Snrpn* and *Peg3*). The average number of methylated CpGs per allele and their standard deviation was calculated for all the paternal alleles of *H19* from a specific strain of mice. The significance in difference in CpG dinucleotide methylation in the paternal alleles of *H19* between two different strains of mice was then calculated using the standard formula for paired student T-test:  $t = \frac{\bar{x}_1 - \bar{x}_2}{\sqrt{A * B}}$

where  $A = (n_1 + n_2) \div n_1 n_2$

and  $B = [(n_1 - 1) s_1^2 + (n_2 - 1) s_2^2] \div [n_1 + n_2 - 2]$

$\bar{x}_1$  and  $\bar{x}_2$  = sample mean from the two strains

$s_1$  and  $s_2$  = standard deviation from the two strains

$n_1$  and  $n_2$  = total number of methylated CpGs in each of the two strains

Similarly the significance in difference in methylated CpG dinucleotides was calculated for the maternal alleles of *Snrpn* and *Peg3* between different strains of mice.

**Table 4. Paired Student T-test for analysis of methylation differences in imprinted genes**

Mouse strain	Embryo or Survivor #	Test for significant difference with wildtype CpG methylation			Test for significant difference with homozygous <i>Dnmt1<sup>Δ1o</sup></i> CpG methylation		
		<i>H19</i> paternal alleles	<i>Snrpn</i> maternal alleles	<i>Peg3</i> maternal alleles	<i>H19</i> paternal alleles	<i>Snrpn</i> maternal alleles	<i>Peg3</i> maternal alleles
<b>Wildtype</b>	Embryo 1	-	-	-	p < 0.025	p < 0.025	p < 0.025
<b><i>Dnmt1s-TG1</i></b>	Embryo 1	No SD	No SD	NA	p < 0.025	p < 0.025	p < 0.025
<b><i>Dnmt1<sup>1s/1o</sup></i></b>	Embryo 1	No SD	No SD	NA	p < 0.025	p < 0.025	p < 0.025
<b><i>Dnmt1s-TG1/Dnmt1<sup>Δ1o</sup></i></b>	Embryo 1	No SD	p < 0.05	p < 0.05	p < 0.025	P < 0.05	p < 0.05
	Embryo 2	p < 0.05	No SD	No SD	p < 0.05	p < 0.025	p < 0.025
	Embryo 3	No SD	No SD	No SD	p < 0.025	p < 0.025	p < 0.025
	Embryo 4	p < 0.05	No SD	p < 0.025	No SD	p < 0.025	p < 0.025
	Survivor1	No SD	No SD	No SD	p < 0.05	p < 0.025	p < 0.05
	Survivor2	No SD	No SD	No SD	p < 0.025	p < 0.025	p < 0.025
	Survivor3	No SD	No SD	No SD	p < 0.025	p < 0.05	p < 0.025
	Survivor4	No SD	No SD	No SD	p < 0.025	p < 0.025	p < 0.025
<b><i>Dnmt1s-TG2/Dnmt1<sup>Δ1o</sup></i></b>	Embryo 1	p < 0.025	p < 0.05	p < 0.05	No SD	No SD	No SD
<b>Heterozygous <i>Dnmt1<sup>Δ1o</sup></i></b>	Embryo 1	No SD	No SD	No SD	p < 0.025	p < 0.025	p < 0.025
<b>Homozygous <i>Dnmt1<sup>Δ1o</sup></i></b>	Embryo 1	p < 0.025	p < 0.025	p < 0.025	-	-	-

#### 1.2.2.6. Dnmt1o versus Dnmt1s protein during preimplantation development

From our earlier analyses, it appears that the concentration of oocyte-derived Dnmt1s is critical for its function. In the *Dnmt1s-TG1/Dnmt1<sup>Δ1o</sup>* females, we observed a restoration of imprinting to a number of Dnmt1o-deficient embryos. In contrast, there was complete lack of restoration of imprinting in Dnmt1o-deficient embryos obtained from *Dnmt1s-TG2/Dnmt1<sup>Δ1o</sup>* females that produced lesser amounts of Dnmt1s protein in their oocytes. This confirmed the importance of the levels of Dnmt1s protein in the oocytes to maintain genomic imprinting.

Another important observation is that, even though the *Dnmt1s-TG1/Dnmt1<sup>Δ1o</sup>* females produced levels of oocyte-derived Dnmt1s protein that were consistent with the levels of endogenous Dnmt1o proteins in wildtype oocytes, imprinting abnormalities were consistently observed in E13.5 embryos from the *Dnmt1s-TG1/Dnmt1<sup>Δ1o</sup>* females. Only some of the embryos showed complete restoration of imprinting and went on to survive after birth. This suggests that the oocyte-derived Dnmt1s protein is not as effective as the stored Dnmt1o protein in maintaining imprinted DNA methylation patterns during preimplantation development.

There are two possible explanations as to why the stored Dnmt1s protein is less effective than the Dnmt1o protein. The first reason is that the maintenance methyltransferase activity of oocyte-derived Dnmt1s protein is less than that of the oocyte-derived Dnmt1o protein. The second reason is that the oocyte-derived Dnmt1s protein is less stable than the Dnmt1o protein. We examined both possibilities using the various mouse lines that had been created.

#### 1.2.2.7. Maintenance methyltransferase activity of oocyte-derived Dnmt1s and Dnmt1o proteins

To compare the maintenance methyltransferase activity of the Dnmt1s and Dnmt1o proteins, we employed an *in vitro* enzymatic assay that measures the transfer of methyl groups from S-Adenosyl Methyltransferase to poly (dIdC) templates in extracts of MII oocytes. As shown in Table 5, an oocyte from homozygous *Dnmt1<sup>Δ1o</sup>* female showed only a slight increase in activity level from the background level of activity whereas a wildtype oocyte showed a 50-fold increase in activity when compared to the background level. This confirms that the Dnmt1o protein is responsible for the majority of maintenance methyltransferase activity in the oocyte. Therefore, any increase in activity seen in the *Dnmt1s-TG1* or *Dnmt1s-TG2* oocytes should be due to the transgene-derived Dnmt1s protein. The residual activity seen in the homozygous *Dnmt1<sup>Δ1o</sup>* oocytes may be attributed to the maintenance methyltransferase activity of the Dnmt3a and Dnmt3b proteins.

A *Dnmt1s-TG1* oocyte, which has equal levels of Dnmt1s and Dnmt1o proteins, showed twice the activity seen in a wildtype oocyte (Table 5). A *TG1/Dnmt1<sup>Δ1o</sup>* oocyte, which expressed levels of Dnmt1s protein alone that was comparable to the levels of Dnmt1o protein seen in the wildtype oocyte, showed equal maintenance methyltransferase activity as that found in wildtype oocytes (Table 5). These results lead us to the conclusion that Dnmt1s and Dnmt1o have equal maintenance methyltransferase activities.

**Table 5. Activity of Dnmt1 methyltransferase in mouse oocyte**

The assay was adapted from Issa et al. 1993. The MII stage oocytes were lysed and the oocyte protein was incubated with 5ug of poly (dIdC) and 3uCi of <sup>3</sup>H-S-Adenosyl methyltransferase (SAM) at 37°C for 2 hours. The radiolabeled methyl group was transferred from SAM to the poly (dIdC) by the activity of the DNA methyltransferase in the oocyte. Thus, by measuring the radioactivity in the poly (dIdC) sample, using a liquid scintillation counter, the DNA methyltransferase activity was measured. The values shown in the table are values obtained after subtracting them from the background (poly (dIdC) + SAM) activity value which was 7.1

**Table 5. Activity of Dnmt1 methyltransferase in mouse oocyte**

<b>Strain of origin of the oocyte</b>	<b>Maintenance methyltransferase activity per oocyte</b>
Wildtype	13416.4
Dnmt1s-TG1	26391
<i>Dnmt1s-TG1/Dnmt1<sup>Δ1o</sup></i>	12457.6
<i>Dnmt1s-TG2/Dnmt1<sup>Δ1o</sup></i>	5178.8
Homozygous <i>Dnmt1<sup>Δ1o</sup></i>	19.7
Heterozygous <i>Dnmt1<sup>Δ1o</sup></i>	6722.9

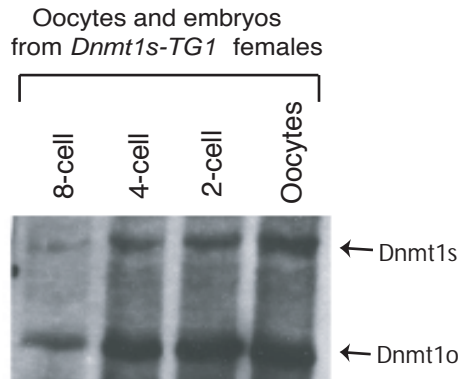
As observed earlier, heterozygous *Dnmt1<sup>Δ1o</sup>* females are able to maintain normal methylation patterns on imprinted genes inspite of lower levels of Dnmt1o protein in their oocytes. To confirm that the level of protein correlates with its enzymatic activity, the maintenance methylation activity was measured in oocytes from heterozygous *Dnmt1<sup>Δ1o</sup>* female. As seen from Table 5, an oocyte from a heterozygous *Dnmt1<sup>Δ1o</sup>* female has only half the activity seen in a wildtype oocyte. This confirms that, inspite of lower levels of Dnmt1o activity, oocytes from heterozygous *Dnmt1<sup>Δ1o</sup>* females still maintain imprinted gene methylation during preimplantation development.

When the enzymatic activity in a *Dnmt1-TG2/Dnmt1<sup>Δ1o</sup>* oocyte was measured, it was found to be lesser than the activity in a *Dnmt1-TG2/Dnmt1<sup>Δ1o</sup>* oocyte. This was expected as the amount of Dnmt1s protein is lesser in a *Dnmt1-TG2/Dnmt1<sup>Δ1o</sup>* oocyte. Surprisingly, the activity was similar to the activity found in a heterozygous *Dnmt1<sup>Δ1o</sup>* oocyte. But when imprinted genes, *H19*, *Snrpn* and *Peg3* were analyzed in embryos derived from heterozygous *Dnmt1<sup>Δ1o</sup>* females, they showed normal patterns of methylation as seen in wildtype embryos (Figure 21). Thus, inspite of similar levels of maintenance methyltransferase activity, oocytes from heterozygous *Dnmt1<sup>Δ1o</sup>* females are able to maintain genomic imprinting while oocytes from *Dnmt1-TG2/Dnmt1<sup>Δ1o</sup>* fail to do so. This suggests that the Dnmt1o protein is more effective than the Dnmt1s protein inspite of similar maintenance methyltransferase activity. This leads us to the second explanation that there may be differences in their stability during preimplantation development.

#### 1.2.2.8. Stability of oocyte-derived Dnmt1s and Dnmt1o proteins during preimplantation development

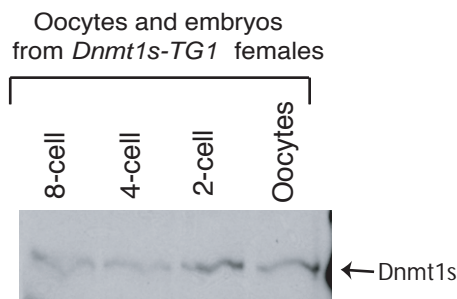
It has already been shown that Dnmt1o protein that is misexpressed in somatic cells of the mouse is much more stable than the normally expressed Dnmt1s protein (Ding and Chaillet 2002). To determine if oocyte-derived Dnmt1s protein is less stable than oocyte-derived Dnmt1o protein, we compared the level of Dnmt1o protein to the level of Dnmt1s protein during preimplantation development in embryos expressing both proteins, specifically the *Dnmt1s-TG1* and the *Dnmt1<sup>1s/1o</sup>* embryos. The *ZP3* promoter that has been used for the *Dnmt1s-TG1* transgene is only active during the growth phase of oogenesis (Philpott 1987). Similarly the Dnmt1o promoter is also inactive after fertilization, as measured by the absence of Dnmt1o transcripts (Ratnam et al. 2001). Thus, the Dnmt1s and Dnmt1o proteins measured during preimplantation development are both derived from oocyte stores and so the time course of protein levels during preimplantation development reflects the *in vivo* decay of the protein. Equal number of oocytes, 2-cell, 4-cell and 8-cell embryos were collected from *Dnmt1s-TG1* females that had been mated to wildtype males and these lysed samples were run on a 5% acrylamide gel, transferred to a PVDF membrane and probed with PATH52 antibody which recognizes both proteins. As shown in Figure 23, the ratio between the Dnmt1s and Dnmt1o proteins steadily increased through preimplantation development leading us to the conclusion that Dnmt1s protein is less stable than the Dnmt1o protein. To confirm this result, the UPT82 antibody, which only recognizes the Dnmt1s protein, was used to probe a blot containing the oocyte and preimplantation embryo samples derived from the *Dnmt1s-TG1* females. A definite decrease was observed in the level of Dnmt1s protein from the oocyte stage to the 8-cell stage of development (Figure 23).

**A** Immunoblot probed with UPTC21



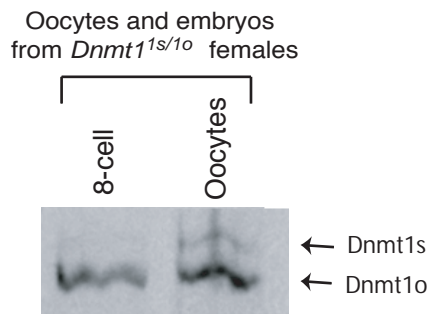
Protein	Stages of preimplantation development			
	8-cell	4-cell	2-cell	Oocyte
Dnmt1o	2	4.5	4.6	5.3
Dnmt1s	1	4.3	4.3	5
Ratio	2	1.05	1.06	1.06

**B** Immunoblot probed with UPT82



Protein	Stages of preimplantation development			
	8-cell	4-cell	2-cell	Oocyte
Dnmt1s	0.5	0.52	3.1	3

**C** Immunoblot probed with UPTC21



Protein	Stages of preimplantation development	
	8-cell	Oocyte
Dnmt1o	4.7	5
Dnmt1s	0.2	1
Ratio	23.5	5

**Figure 23. Stability of the Dnmt1o protein.**

**Figure 23. Stability of the Dnmt1o protein.**

A. Immunoblot of protein extracts from oocytes, 2-cell, 4-cell and 8-cell embryos obtained from *Dnmt1s-TG1* females and probed with the PATH52 antibody that detects both Dnmt1o and Dnmt1. The Dnmt1o protein is seen to be relatively constant from the oocyte stage to the 8-cell stage of preimplantation development. In contrast, the Dnmt1s protein shows a significant decrease in levels at the 8-cell stage when compared to the oocyte stage. B. Immunoblot of protein extracts from oocytes 2-cell, 4-cell and 8-cell embryos obtained from *Dnmt1s-TG1* females and probed with the UPT82 antibody that detects only Dnmt1s protein. There is a rapid decline in the levels of Dnmt1s protein from the oocyte stage to the 8-cell stage confirming the results from panel B. C. Immunoblot of protein extracts from oocytes and 8-cell embryos obtained from *Dnmt1<sup>ls/1o</sup>* females and probed with the PATH52 antibody. The results obtained are similar to those shown in panels A and B where the Dnmt1s protein shows a decrease in its level at the 8-cell stage while the Dnmt1o protein level stays constant. The intensity of the bands on the immunoblots was measured using the National Institutes of Health Image program (<http://rsb.info.nih.gov/niimage/>). The values obtained for the bands on each immunoblot is tabulated beside the specific immunoblot.

In the *Dnmt1s-TG1* embryos, the Dnmt1s protein is expressed with an epitope tag that was incorporated at the N-terminus during the construction of the *Dnmt1s-TG1* transgene (Materials and Methods). To confirm that the decrease in stability of the Dnmt1s protein is not due to the additional epitope tag, we analyzed the *Dnmt1<sup>1s/1o</sup>* strain of mice as well. The *Dnmt1<sup>1s/1o</sup>* females, as mentioned before, express roughly equal amounts of Dnmt1s and Dnmt1o proteins from their *Dnmt1<sup>1s/1o</sup>* allele (Figure 5) during oogenesis. Equal number of oocytes and 8-cell embryos were collected from heterozygous *Dnmt1<sup>1s/1o</sup>* females and analyzed by immunoblots using the PATH52 antibody. There was a distinct fall in the level of Dnmt1s protein at the 8-cell stage, when compared to the Dnmt1o protein, indicating that Dnmt1s protein is not as stable as Dnmt1o protein to last till the 8-cell stage where it is required for maintaining methylation on imprinted genes.

Thus, our observations support the notion that, during preimplantation development, the Dnmt1s and the epitope-tagged Dnmt1s proteins are intrinsically much less stable than the Dnmt1o protein.

### **1.2.3. Dnmt1 expression in cloned preimplantation embryos**

To analyze the expression and localization of Dnmt1 proteins during cloned mouse preimplantation development, cloned preimplantation embryos were obtained from Dr. Keith Latham (Temple University, Philadelphia, PA) and analyzed by immunofluorescence techniques using antibodies specific to Dnmt1 proteins.

#### 1.2.3.1. Aberrant expression of Dnmt1s protein in cloned preimplantation embryos

The cloned preimplantation embryos were fixed and stained with the UPT82 antibody, which specifically recognizes epitopes present in Dnmt1s, but not in Dnmt1o (Ratnam et al. 2002). Aberrant Dnmt1s protein expression was observed in blastomeres of 8-cell stage cloned embryos (Figure 24B). Dnmt1s was present in the cytoplasm of all blastomeres, but Dnmt1s was detected in only some blastomere nuclei (Figure 25). Of 35 cloned embryos examined, all displayed staining for the somatic form of the protein. No nuclear staining for Dnmt1s was observed for cloned embryos at the 1-cell, 2-cell or 4-cell stages indicating that the staining seen at later stages was not likely the result of carryover of protein from the donor nucleus. Some cytoplasmic staining persisted at the morula and blastocyst stages, but no nuclear staining was seen. In contrast, no nuclear staining for Dnmt1s was ever observed in any of the 21 control embryos examined, all of which were derived from normally fertilized eggs (Figure 24A and Ratnam et al. 2002), thus indicating a significant difference between cloned and fertilized embryos ( $p < 1 \times 10^{-6}$ ). When analyzed with PATH52 antibody, which recognizes both Dnmt1s and Dnmt1o proteins, similar mosaic nuclear expression of Dnmt1 was observed at the 8-cell stage (Figure 26). Thus, it was obvious that at the 8-cell stage, certain nuclei lacked both the Dnmt1s and Dnmt1o proteins.

To confirm that the aberrant expression of Dnmt1s protein was only seen in cloned embryos, 8-cell stage tetraploid embryos and parthenogenetic embryos were also fixed and stained with UPT82. None of the eight 8-cell stage tetraploid embryos examined displayed nuclear staining for Dnmt1s (Figure 24C), which thus differed significantly from diploid cloned embryos ( $p < 1 \times 10^{-6}$ ), indicating that endogenous oocyte-derived chromosomes (which

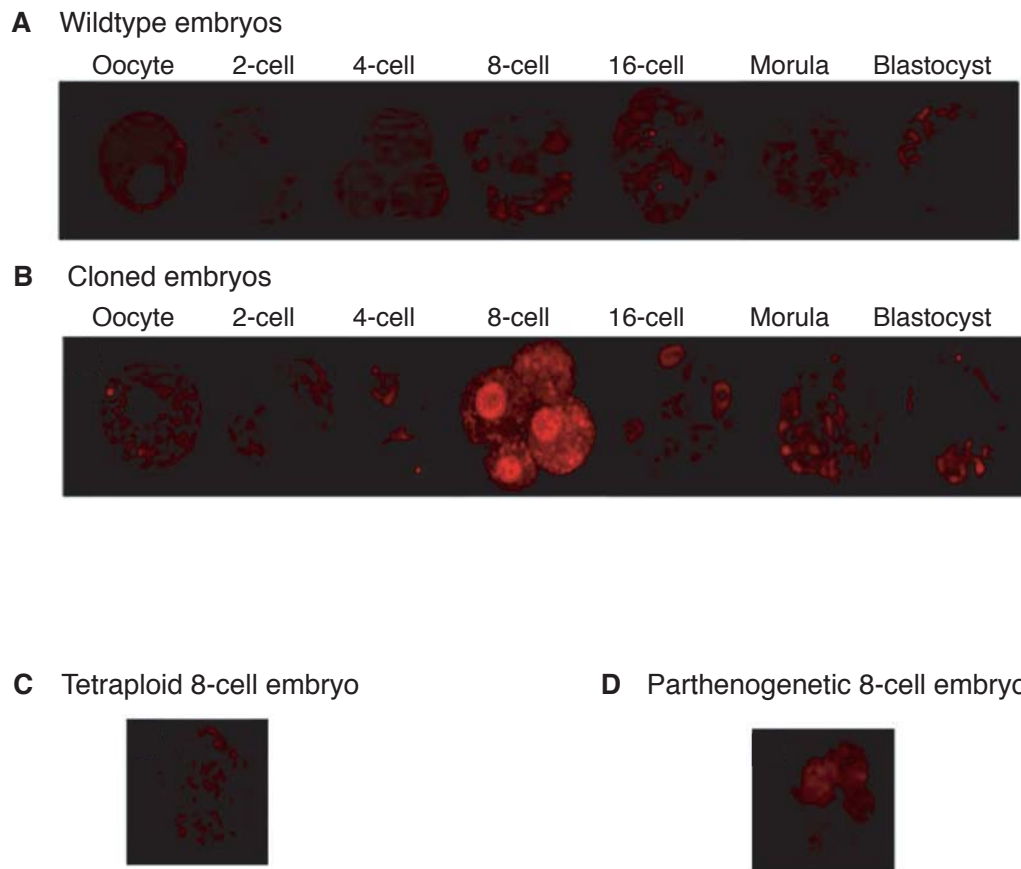
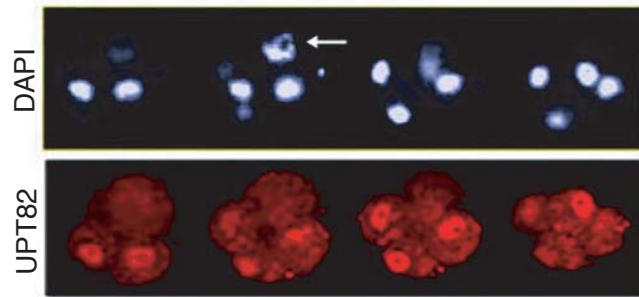


**Figure 24. Immunostaining of normal and cloned preimplantation mouse embryos with the UPT82 antibody**

**Figure 24. Immunostaining of normal and cloned preimplantation mouse embryos with the UPT82 antibody.**

A. Dnmt1s protein expression in an eight cell-stage clone. UPT82 staining was absent in other cleavage stages. B. Absence of Dnmt1s expression in preimplantation stage embryos derived from normal, fertilized eggs. C. Absence of Dnmt1s expression in an eight-cell-stage tetraploid cloned embryo. D. Absence of Dnmt1s expression in an eight-cell-stage parthenogenetic embryo.

**A** Cloned 8-cell embryo after delayed activation



**B** Cloned 8-cell embryo after immediate activation

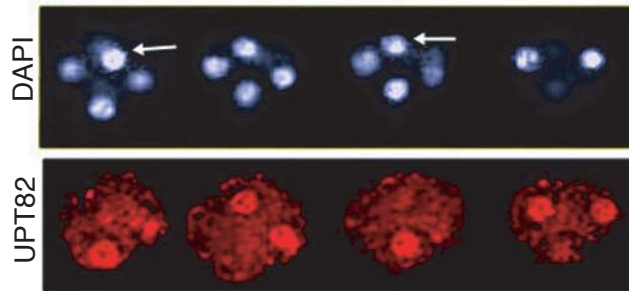


**Figure 25. UPT82 immunostaining of cloned eight-cell embryos derived by either a delayed- or an immediate-activation protocol.**

**Figure 25. UPT82 immunostaining of cloned eight-cell embryos derived by either a delayed- or an immediate-activation protocol.**

A. Confocal sections through a cloned eight-cell embryo (delayed activation), stained with DAPI (upper panel) and UPT82 (lower panel). B. Confocal sections through a cloned eight-cell embryo (immediate activation), stained with DAPI (upper panel) and UPT82 (lower panel). The arrows in panels A and B mark the nuclei that did not stain with UPT82, thus indicating the mosaic nuclear staining pattern seen with the UPT82 antibody.

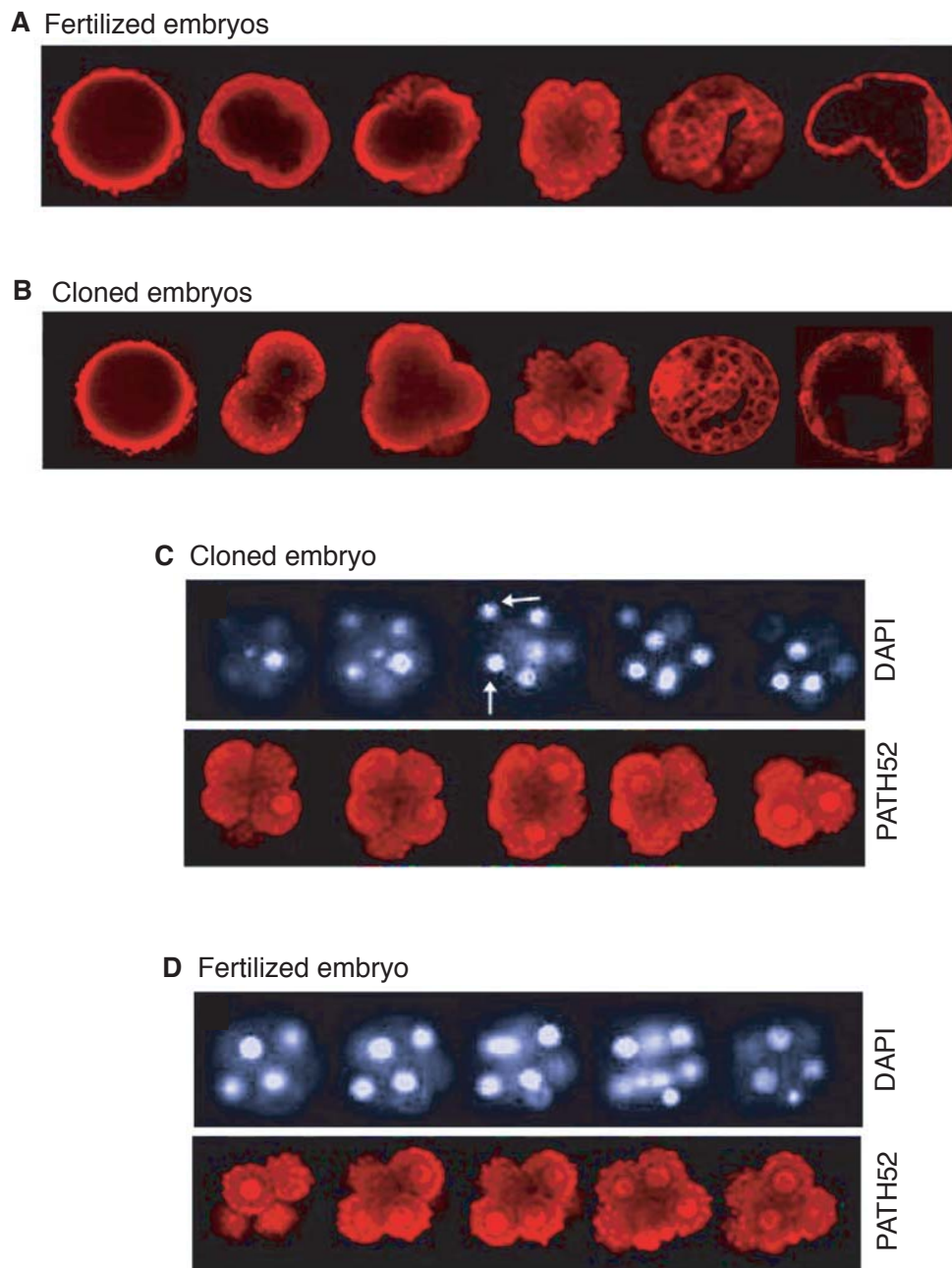


**Figure 26. Immunostaining of normal and cloned preimplantation mouse embryos with the PATH52 antibody, which recognizes both Dnmt1o and Dnmt1s.**

**Figure 26. Immunostaining of normal and cloned preimplantation mouse embryos with the PATH52 antibody, which recognizes both Dnmt1o and Dnmt1s.**

A. Stage-specific nuclear staining for Dnmt1 protein in cloned embryos. B. Stage-specific nuclear staining for Dnmt1 protein in control (wildtype) embryos. C. Confocal sections through an eight-cell cloned embryo (lower panel) and corresponding DAPI images (upper panel). The arrows mark the nuclei that did not stain with PATH52, thus indicating the mosaic pattern of nuclear staining seen with PATH52. D. Confocal sections through normal fertilized eight-cell embryo (lower panel) and corresponding DAPI images (upper panel), revealing positive staining in all nuclei.

comprise part of an authentic embryonic genome) prevented the aberrant nuclear expression of the Dnmt1s protein that was observed in diploid cloned embryos. As expected, none of the seven diploid parthenogenetic embryos examined showed Dnmt1s nuclear staining (Figure 24D). The absence of Dnmt1s protein in the nuclei of tetraploid embryos also indicated that the nuclear expression of Dnmt1s seen in cloned embryos was neither a result of protein carryover from the donor cell, nor an artifact of the injection procedure or the culture system, as the tetraploid embryos experienced the identical series of treatments as cloned embryos except for removal of the oocyte spindle-chromosome complex. The aspect of the maternal chromosomes that confers the embryonic type of Dnmt1s regulation in the tetraploid cloned embryos is not known. The maternal chromosomes may express regulatory factors that are lacking in cloned embryos containing only somatic nuclei from differentiated cells.

#### 1.2.3.2. Lack of Dnmt1o expression in the nuclei of 8-cell cloned embryos

There are different explanations for the mosaic patterns of UPT82 and PATH52 (Figures 25 and 26) staining in 8-cell clones. PATH52-stained nuclei may contain only Dnmt1s, only Dnmt1o, or a mixture of Dnmt1o and Dnmt1s. To distinguish among these possibilities, single 8-cell cloned embryos were stained simultaneously with both the UPT82 rabbit antibody which only detects Dnmt1s, and the UPTC21 chicken antibody, which detects both Dnmt1s and Dnmt1o. They were then simultaneously incubated in their corresponding secondary antibodies. Because no antibody that is specific for Dnmt1o can be generated, dual immunofluorescent labeling combined with confocal microscopic image analysis constitutes the best method for determining which Dnmt1 proteins reside in the blastomere nuclei. As shown in Figure 27B,

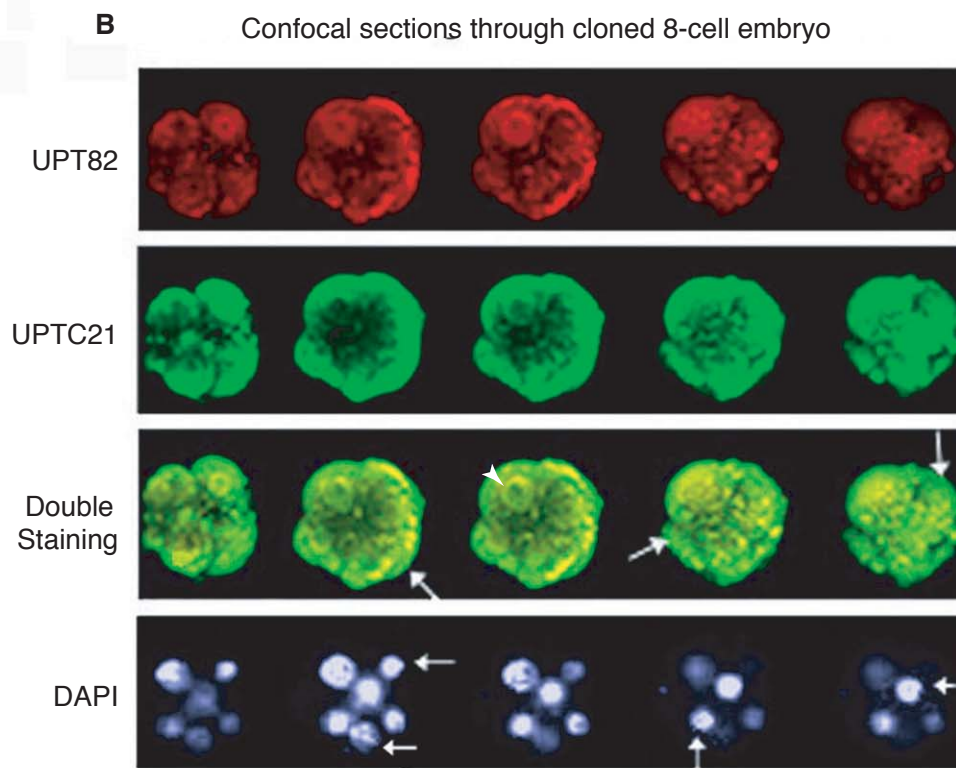
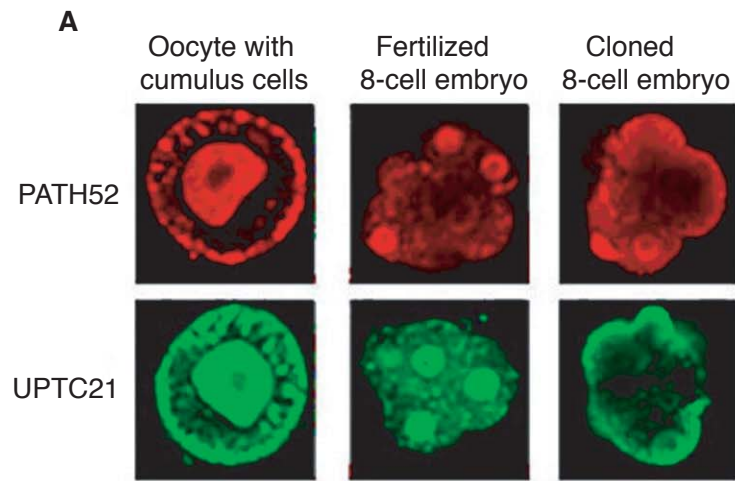


**Figure 27. Analysis of mosaic Dnmt1s and Dnmt1o protein expression in mutant and cloned embryos using simultaneous immunostaining with UPT82 and UPTC21 antibodies.**

**Figure 27. Analysis of mosaic Dnmt1s and Dnmt1o protein expression in mutant and cloned embryos using simultaneous immunostaining with UPT82 and UPTC21 antibodies.**

A. Comparison between confocal fluorescent images of PATH52 and UPTC21 staining in oocyte-cumulus cell complex, eight-cell fertilized embryos, and eight-cell cloned embryos. Note the highly similar staining patterns. B. Confocal fluorescent images of an eight-cell cloned embryo by simultaneous immunostaining with UPT82 and UPTC21 antibodies and their secondary antibodies. In the merged UPT82/UPTC21 images, green-stained cytoplasm (indicated by arrows) indicates the presence of Dnmt1o and the absence of Dnmt1s. The arrowheads mark the nuclei that stained with both UPT82 and UPTC21, indicating the expression of the Dnmt1s protein in those nuclei. No nucleus was observed that stained with UPTC21 but not with UPT82 thus indicating the lack of Dnmt1o protein in any of the 8-cell stage nuclei in cloned embryos. In the corresponding DAPI images, the arrows mark the nucleus that did not stain with either UPT82 or UPTC21, thus indicating the mosaic pattern of staining seen with both UPT82 and UPTC21.

there were areas of cytoplasm that stained with UPTC21, but did not stain with UPT82, indicating that both Dnmt1o and Dnmt1s are in the cytoplasm. All of the nuclei that stained with UPTC21 also stained with UPT82. This observation is consistent with the presence of only Dnmt1s or a mixture of Dnmt1o and Dnmt1s in stained nuclei of cloned 8-cell embryos. It is not consistent with the presence of only Dnmt1o in any of the stained nuclei. Because the intensity of nuclear staining with UPTC21 or PATH52 was lesser in cloned embryos than in control (fertilized) embryos (Figure 27A), if any Dnmt1o enters the nuclei of cloned embryos, the amount is probably diminished compared to normal embryos. We conclude from this analysis that none of the blastomeres examined in cloned embryos exhibited the appropriate embryonic pattern of nuclear Dnmt1 staining.

Because trafficking of the Dnmt1o protein from the cytoplasm to the nucleus in 8-cell-stage blastomeres is greatly reduced, Dnmt1s expression in these nuclei may be a consequence of the reduced nuclear abundance of Dnmt1o. As seen from earlier data, 4-cell, 8-cell, and 16-cell embryos derived from homozygous mutant *Dnmt1<sup>Δ1o</sup>* females, lacking Dnmt1o in their oocytes, showed intense UPT82 staining for Dnmt1s in all their nuclei (Figure 9). This is consistent with the hypothesis that the absence of Dnmt1o in the nucleus leads to aberrant expression of Dnmt1. Despite the expression of the Dnmt1s protein in these embryos, they remain non-viable and show a loss of methylation on imprinted genes, indicating a lack of functional compensation for the missing Dnmt1o protein (Howell et al. 2001). Based on this observation, the Dnmt1s protein in nuclei of 8-cell cloned embryos may also be unable to maintain methylation patterns on alleles of imprinted genes.

### 1.2.3.3. Quantitative analysis of aberrant Dnmt1s expression in nuclei of eight-cell stage embryos

The mosaic pattern of nuclear UPT82 staining in the 8-cell cloned embryos was analyzed further. The intensity of staining of each nucleus was measured using the National Institutes of Health Image program (<http://rsb.info.nih.gov/nihimage/>). There was a wide range of staining intensities among nuclei of individual clones (Figure 28A). The average number of nuclei per cloned embryo showing moderate-to-intense levels of UPT82 staining was  $4.4 \pm 1.03$  (mode 4, median 4.0). Similar degrees of mosaic protein expression were seen in cloned embryos stained with PATH52 (Figure 28B), with  $5.4 \pm 0.70$  nuclei stained per embryo (mode 6, median 5.5). We also made clones using an immediate oocyte activation protocol, which avoids the possibility of chromosome loss (Wakayama et al. 2001). Embryos from this immediate-activation protocol also showed a mosaic pattern of Dnmt1 expression with a wide range of nuclear staining intensities (Figures 25B and 28A). Mosaicism appeared to be reduced slightly, with  $5.3 \pm 0.82$  nuclei showing moderate-intense staining (mode 6, median 5.5), but this reduction was not statistically significant. Thus, the mosaic Dnmt1s nuclear staining cannot be explained by the loss of chromosomes, consistent with the expression of Dnmt1 protein in the cytoplasm of all blastomeres of cloned embryos. Also, mosaic Dnmt1s nuclear staining in cloned embryos contrasted significantly ( $p < 1 \times 10^{-6}$ ) with the Dnmt1s staining of embryos from Dnmt1o-deficient mothers ( $n = 5$  examined), in which all of the nuclei were within approximately 80% of the intensity of the most heavily stained nucleus (Figure 28A).

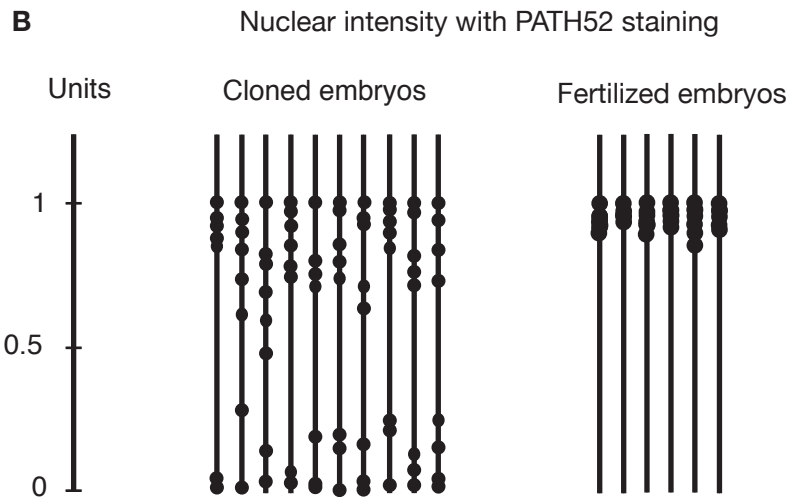
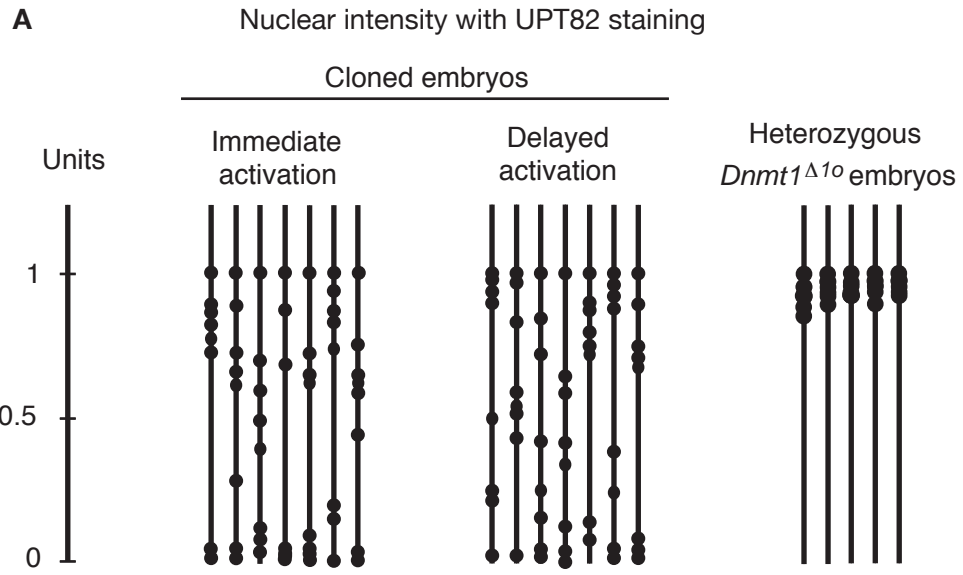


**Figure 28. Quantitative analysis of nuclear staining for Dnmt1 proteins in cloned embryos, wildtype embryos and fertilized embryos from Dnmt1o-deficient oocytes.**

**Figure 28. Quantitative analysis of nuclear staining for Dnmt1 proteins in cloned embryos, wildtype embryos and fertilized embryos from Dnmt1o-deficient oocytes.**

A. Quantitative analysis of nuclear staining with UPT82 for Dnmt1s in 8-cell stage cloned embryos (both immediate and delayed activation) and fertilized embryos from Dnmt1o-deficient oocytes. For each embryo, confocal images through the middle of each nucleus were obtained. The intensity of staining of each nucleus was measured in these confocal sections using the NIH *Image* program (<http://rsb.info.nih.gov/nih-image/>). The eight intensity values for each embryo were then plotted as a fraction of the maximum nuclear intensity value. Each filled circle represents a nucleus and each line represents an embryo. Note the variable nuclear intensities among cloned embryos, but not among nuclei in embryos derived from *Dnmt1<sup>Δ1o</sup>* homozygous mutant females. B Quantitative analysis of nuclear staining with PATH52 for Dnmt1 proteins in 8-cell stage cloned embryos and 8-cell stage fertilized embryos. The nuclear intensity values for the embryos were calculated as in A.

Thus, the results reported here indicate that there is a highly consistent, early disruption in regulation of Dnmt1 protein expression in cloned embryos. Cloned embryos thus lack the ability to regulate post-transcriptionally the expression and cytoplasmic-nuclear trafficking of Dnmt1 proteins, and possibly other proteins. The apparent uniformity of these defects among cloned embryos indicates that these defects are likely to affect all cloned embryos and thus are likely to be a general feature of early clonal development.

### 1.3. Materials and Methods

#### 1.3.1. Functional significance of Dnmt1s during preimplantation development

##### 1.3.1.1. Generation of mice that exogenously expressed Dnmt1s during oogenesis

Two different approaches were used by Carina Howell and Richard Chaillet to generate mice that expressed Dnmt1s during oogenesis. The first approach was to produce mice that contained a targeted mutation of the *Dnmt1* locus in an attempt to express Dnmt1s instead of Dnmt1o and this was done by substituting the coding region of exon1s in place of exon1o. The second approach was to generate mice which contained a transgene that drove the expression of Dnmt1s during this specific time period.

##### 1.3.1.2. Generation of mice that contain a targeted replacement of exon 1s for exon 1o at the Dnmt1 locus

A targeting construct was designed which contained the coding region for exon 1s instead of exon 1o, the LTNL selectable marker and surrounding genomic DNA (Figure 5). The 1s exon contains an ATG start codon and the coding sequence for part of the N-terminal extension found in exon 1s. This exon was placed in exon 1o, leaving both the 5' and 3' splice sites intact. An LTNL selectable marker cassette was placed 3' of the 1o exon, leaving room for accurate splicing to occur. This construct was electroporated into W9.5 embryonic stem (ES) cells and clones were selected. Southern blot analysis of DNA isolated from ES cells revealed lines which contained a homologous recombination event at the *Dnmt1* locus. Homologous recombination

events at this locus were high, approximately 40% of ES lines obtained contained homologously recombined DNA. *Cre*-mediated recombination allowed removal of the selectable marker cassette in ES cells. ES clones containing the 1s substitution were injected into blastocysts obtained from C57BL6/J females. Chimeric mice were obtained and bred to C57BL6/J mice. After germ line transmission, mice were bred to obtain homozygotes for this modified allele which is designated *Dnmt1<sup>1s/1o</sup>*, and encodes for an oocyte-specific *Dnmt1s* transcript. Homozygous *Dnmt1<sup>1s/1o</sup>* males and females are phenotypically normal and fertile. This line is being maintained on a C57/BL6/J background.

#### 1.3.1.3. Generation of constructs and mice containing transgenes to exogenously express Dnmt1s during oogenesis

Three constructs were generated to express Dnmt1s in oocytes. In this paragraph only the design of the functional construct has been described. The construct was assembled in the pcDNA3.1/His expression vector (Invitrogen, San Diego, CA). The coding region for Dnmt1s (4.5 kb) was inserted into the multiple cloning site of pcDNA3.1/His vector at a unique *EcoRV* site. An epitope tag containing an ATG initiation codon, polyhistidine region, Anti-Xpress antibody epitope and an enterokinase recognition site were contained on the N-terminus of Dnmt1s expressed from this vector. In addition, the bovine growth hormone polyadenylation signal was located 3' of the Dnmt1s inserted sequence. The pcDNA3.1'His vector sequence (5.5 kb) remains 3' of the Dnmt1s insertion. The construct was linearized using a unique *MfeI* site. The 3' vector sequence was mostly removed by a *SmaI* digestion. The promoter region was from the mouse *ZP3*, *zona pellucida 3* gene. The *ZP3* is specifically expressed in mouse oocytes (Philpott et al. 1987), and the region that directs this expression was used in this study (Lira et al.

1990; Lira et al. 1993). *ZP3* promoter has been shown to express in growing oocyte prior to completion of first meiotic division (Wassermann and Kinloch, 1993). The transgene was injected into the oocytes from FVB/N females and reimplanted into the oviducts of pseudopregnant Swiss Webster female mice. Two different lines were obtained with this transgene, the *Dnmt1s-TG1* and *Dnmt1s-TG2*. Females and males from both lines were phenotypically normal and fertile.

#### 1.3.1.4. Collection of oocytes and preimplantation embryos

Oocytes of all stages were obtained by puncture of ovarian follicles of 7-12 week-old females in MII medium (Specialty Media, Phillipsburg, NJ), as previously described (Clarke et al. 1992). Metaphase II (MII) oocytes were collected from 7-24 week-old females that were superovulated by injection of 5 IU of pregnant mares' serum gonadotropin, PMSG (CalBioChem, La Jolla, CA), followed 44 to 48 hours later by 5 IU of human chorionic gonadotropin, hCG (CalBioChem, La Jolle, CA). These oocytes were recovered from the oviducts 20 hours post-hCG and the cumulus cells were dispersed with 1 mg/ml hyaluronidase (Roche Diagnostics, Mannheim, Germany), as described (Hogan et al. 1986).

Preimplantation embryos were obtained as previously described (Clarke et al. 1992). Superovulated females were caged individually with stud males overnight, and examined for the presence of a vaginal plug the next morning. One-cell embryos were recovered from the oviducts at E0.5 in HEPES-buffered CZB medium (Erbach et al. 1994) and the cumulus mass dispersed as described above. Two-cell, four-cell embryos, eight-cell embryos, morulae and

blastocysts were obtained by culturing one-cell embryos in 5  $\mu$ l drops of bicarbonate-buffered CZB media under oil at 37°C in an atmosphere of 5% CO<sub>2</sub> in air. Postimplantation embryos were dissected out of the uterine horns at E13.5.

For all isolation procedures, healthy-looking oocytes and preimplantation embryos were collected in a 35 mm petri dish using a mouth-controlled micropipette and washed free of any adhering somatic cells by transfer through two dishes of culture medium. Oocytes and embryos were either processed immediately for immunofluorescence; or stored at –80°C in lysis buffer for immunoblotting; or stored at –80°C in culture medium for DNA and RNA isolation.

#### 1.3.1.5. Immunoblot blot analysis

To look for the expression of the Dnmt1s isoform in the oocytes collected from *Dnmt1<sup>1s/1o</sup>*, *Dnmt1s-TG1* and *Dnmt1s-TG2* females, we used the immunoblot technique. The antibodies used for this technique were the UPT82, UPTC21 and PATH52 antibodies. UPT82 was generated by immunizing a rabbit with a fusion protein that contained the full-length bacterial GST protein and the amino terminal 118 amino acids of Dnmt1s (Ratnam et al. 2002). These 118 amino acids are not found in Dnmt1o. UPT82 was affinity purified on a column containing a 6-histidine-118 amino acid fusion protein. UPTC21 was generated by immunizing a chicken with a fusion protein of 6-histidine plus a segment of Dnmt1 from amino acid 636 to amino acid 1108. These amino acids are present in both Dnmt1 and Dnmt1o. PATH52 was a kind gift from Dr. Tim Bestor (Columbia University, NY) and was generated against epitopes between amino acids 255 and 753 of Dnmt1 (Carlson et al. 1992).

Oocytes were collected manually from washings of oviducts or uteri and pooled and lysed in 5% SDS, 2.5% glycerol, 2.5%  $\beta$ -mercaptoethanol, 0.01% bromophenol blue, 0.025M Tris-HCl, pH 6.8 (1X sample buffer). All samples were denatured by heating at 95°C for 5 minutes, and then separated by electrophoresis on SDS-5% polyacrylamide gels. Afterwards they were transferred to PVDF membranes (Millipore Corporation, Bellerica, MA). The gels were stained with Coomassie Blue to examine the efficiency of protein transfer. Membranes were blocked in 5% Carnation dry skim milk in 10 mM Tris-HCl (pH 8.0), 140 mM NaCl, for a least one hour and probed with UPT82 (diluted 1:3,000 in blocking buffer) or UPTC21 (diluted 1: 1000 in blocking buffer) or PATH52 (diluted 1:15,000 in blocking buffer) for 3 hours. Following three washes of 5 minutes each in 0.1% Tween-20 TBS, the membrane were incubated for one hour at room temperature in biotinylated donkey anti-rabbit IgG (Amersham, Piscataway, NJ) diluted 1:5,000 in blocking buffer or in rabbit anti-chicken IgG (Jackson ImmunoResearch Laboratories, Inc., West Grove, PA) diluted 1:50,000 in blocking buffer and washed as above. Bound antibody was detected by chemiluminescence (ECL Plus, Amersham, Piscataway, NJ).

#### 1.3.1.6. Immunofluorescence analysis

To study the expression and localization of the Dnmt1s protein in the oocytes and preimplantation embryos from *Dnmt1<sup>1s/1o</sup>*, *Dnmt1s-TG1* and *Dnmt1s-TG2* mice, and *Dnmt1s-TG1/Dnmt1<sup>Δ1o</sup>* mice, we used the UPT82 and UPTC21 antibodies that have been described in the previous paragraph.

Denuded oocytes and preimplantation embryos were freed of the zona pellucida using acidified (pH 2.5) Tyrode's medium (Hogan et al. 1986), and fixed for 10 to 15 minutes at room

temperature in 3.7% formaldehyde in PBS. Alternatively, small ovarian follicles were fixed intact. All solutions for immunofluorescence of Dnmt1 were prepared in PBS and procedures carried out at room temperature. The fixed cells were blocked for at least one hour in blocking buffer (3% BSA, 0.1% Triton X-100) and then incubated in either 1:100 preimmune serum, 1:100 UPT82, 1:100 UPTC21 or 1:500 PATH52 antibodies diluted in the same blocking buffer overnight at 4°C in a humidified chamber. The cells were washed three times for 5 min each in blocking buffer, and incubated in their corresponding secondary antibodies for one hour. The secondary antibody used in conjunction with UPT82 and PATH52 was an anti-rabbit IgG monoclonal antibody coupled with Texas Red (1:250) (Molecular Probes, Eugene, OR) and the secondary antibody used in conjunction with UPTC21 was an anti-chicken IgG monoclonal antibody coupled with fluorescein (1:4000) (Aves Labs. Inc., Tigard, OR). The cells were then washed again as before. To mount the cells for viewing, a drop of Vectashield mounting medium (Vector Laboratories, Burlingame, CA) supplemented with 0.4 µg/ml of the DNA-binding dye DAPI (Roche Diagnostics, Mannheim, Germany) was used. Immunofluorescence was visualized using a Zeiss Axiophot, Zeiss LSM410 laser scanning confocal microscope.

#### 1.3.1.7. PCR genotyping

*Dnmt1s-TG1* and *Dnmt1s-TG2* mice were genotyped using PCR primers designed to amplify transgene sequence (*Mtase44* 5' ACTGCATGAATTCCTGCAAACAGA 3' and (*Mtase45* 5' AAAGGGTGTCACTGTCCGACTT 3') of size 310 bp. PCR reactions were performed using approximately 0.1 mg of mouse genomic tail DNA in a 50 µl reaction containing, 1X PCR buffer (Invitrogen, Carlsbad, CA), 1.5 mM MgCl<sub>2</sub>, 0.1 mM of each primer, 200 mM dNTPs, and 1.25 Units of Taq Polymerase (Invitrogen, Carlsbad, CA). The cycling

conditions were as follows: 5 minutes at 94°C, followed by 30 cycles of 45 seconds at 94°C, 45 seconds at 58°C, and 45 seconds at 72°C, and a final extension of 10 minutes at 72°C. PCR reactions were resolved on a 1% agarose gel and visualized by ethidium bromide staining. The *Dnmt1*<sup>ts1lo</sup> mice were genotyped using the *Egg6* (5'AGGAAAACAGTGGAGGAAAC 3') and *Egg7* (5'TACTTGCACAGGGCTGTCCT 3') primers. Cycling conditions were similar as above. As shown in figure, presence of a 380 bp band indicated a *Dnmt1*<sup>ts/1o</sup> allele while a 480 bp band indicated a wildtype allele.

#### 1.3.1.8. DNA isolation

Most DNA samples were isolated by incubating the required tissues in proteinase K (Invitrogen, Carlsbad, CA) digestion buffer (10 mM Tris-HCl pH 7.5, 100 mM NaCl, 10mM EDTA, 0.5% SDS, and 0.2 mg Proteinase K) at 50°C for 3-4 hours, followed by phenol-chloroform extraction and ethanol precipitation. DNA samples were resuspended in TE (10 mM Tris-HCl pH 7.5, 1mM EDTA pH 8).

#### 1.3.1.9. Bisulfite genomic sequencing technique for DNA methylation analysis

To study the methylation patterns of 3 imprinted genes, *H19* (paternally methylated), *Snrpn* and *Peg3* (maternally methylated) in the E13.5 embryos or survivor mice obtained from the various strains of mutant mice relevant to this study we used the bisulfite genomic sequencing technique (Clark et al. 1994). These mice had been mated to CAST7 male mice since the CAST7 strain of mice have single-nucleotide polymorphisms for the *H19*, *Snrpn* and *Peg3*

genes, thus helping us differentiate between the maternal alleles and the paternal alleles (Mann et al. 2003)

The DNA to be analyzed for methylation is digested with *HindIII* and treated with 40.5% Sodium Bisulfite for 16 hours at 55°C (Zeschnick et al.1997). The Sodium Bisulfite converts all the cytosines without the methyl group attached to them into uracils which on PCR amplification will result in thymines. The cytosines which are protected by the methyl groups attached to them will remain as cytosines (Figure 10). Thus, while studying the alleles, presence of CpGs indicated that they are methylated while presence of CpA's indicated that they are unmethylated. The treated DNA is PCR amplified using specific primers to the *H19*, *Snrpn* and *Peg3* genes. For all three imprinted genes, the regions which were analyzed were part of their DMDs.

DNAs for bisulfite genomic sequencing were isolated from either E13.5 embryos obtained from the uterine horns of the female mice or the distal end of the tail obtained from the survivor mice by grinding in liquid nitrogen prior to proteinase K digestion. DNAs were digested overnight at 37°C with *HindIII*, phenol/chloroform extracted, and ethanol precipitated. DNA was resuspended in TE (10 mM Tris-HCl pH 7.5, 1mM EDTA pH 8) and denatured at a final concentration of 0.3 M NaOH at 42° C for 30 minutes. Denatured DNA was treated with sodium bisulfite (Sigma, St. Louis MO) at a final concentration of 3.06 M and hydroquinone (Sigma, St. Louis MO) at a final concentration of 0.05 mM in the dark at 55° C for 15 to 18 hours. DNA was purified using the GeneClean II kit (Invitrogen, Carlsbad, CA) and resuspended in TE. Treated DNA was desulphonated for 15 minutes at 37° C at a final concentration of 0.3 M NaOH, neutralized with 3M NH<sub>4</sub>OAc at a final concentration of 0.3 M, and ethanol precipitated.

DNA was resuspended in 100 ml TE and used for PCR analysis. DNA was stored in the dark at -20° C for up to two weeks.

The specific regions of the imprinted genes that were analyzed are given below:

*H19*, GenBank accession number U19616, nucleotides 1301-1732

*Snrpn*, GenBank accession number AF081460, nucleotides 2151-2562

*Peg3*, GenBank accession number AF105262, nucleotides 2773-3111

The *H19* region includes a G:A (FVB/N:Cast7) polymorphism at nt position 1566. The *Snrpn* promoter region includes a G:T polymorphism at nt position 2348. The *Peg3* region includes a C:T polymorphism at nt position 3070.

Specific PCR primers used for specific genes are listed below. Nested PCR reactions were necessary to produce enough product from the genomic DNA.

Genes	Outer pair of primers	Inner pair of primers
<i>H19</i>	5'GAGTATTTAGGAGGTATAAGAATT3' 5'ATCAAAAACCTAACATAAACCC3'	5'GTAAGGAGATTATGTTTATTTTGG3' 5'CCTCATTAATCCATAACTAT3'
<i>Snrpn</i>	5'TATGTAATATGATATAGTTTAGAAATTAG3' 5'AATAAACCCAAATCTAAAATATTTTAATC3'	5'AATTTGTGTGATGTTTGTAATTATTGG3' 5'ATAAAATACACTTTCACACTAAAATCC3'
<i>Peg3</i>	5'TGATAATAGTAGTTTGATTGGTAGGG3' TAATTCACACCTAAAACCCTAAAACC3'	5'TTTTGTAGAGGATTTTGATAAGGAGG3' 5'AAATACCACTTTAAATCCCTATCACC3'

As mentioned before, two rounds of PCR were performed. The first reaction contained 1-4 ml of treated DNA in a 25 ml reaction containing, 1X PCR buffer (Invitrogen, Carlsbad, CA), 1.5 mM MgCl<sub>2</sub>, 0.4 mM of each primer, 200 mM dNTPs, and 0.50 Units of Taq Polymerase (Invitrogen, Carlsbad, CA). Cycling conditions for the first round of PCR were: 2 cycles of 94° C for 4 minutes, 55° C for 2 minutes, and 72° C for 2 minutes, followed by 35 cycles of 94° C for 1 minute, 55° C for 2 minutes, and 72° C for 2 minutes, with a final extension of 72° C for 10 minutes. The nested round of PCR was performed with the same reaction conditions and contained 2 - 5 ml of the first reaction product. Cycling conditions were as follows: 5 minutes at 94° C followed by 35 cycles of 94° C for 1 minute, 55° C for 2 minutes, and 72° C for 2 minutes, with a final extension of 72° C for 10 minutes. PCR products were electrophoresed on a 1% agarose gel and isolated using the Qiagen fragment isolation kit (Qiagen, Valencia, CA). PCR fragments were subcloned into the TOPO-TA pCR2.1 vector (Invitrogen, Carlsbad, CA) and sequenced using the *M13 reverse* primer.

Statistical differences in methylation of CpG dinucleotides of imprinted genes among the various strains of mice analyzed in this study were evaluated using a paired Student T-test (Table 4).

#### 1.3.1.10. DNA sequence analysis

All DNA sequencing was performed on the ABI 3700 DNA Analyzer or the ABI 3100 DNA Analyzer (Applied Biosystems, Foster City, CA). DNA sequence analysis was performed using MacVector 6.5 software (Oxford Molecular, Atlanta, GA). AssemblyLIGN Software was used for DNA sequence alignments (Oxford Molecular, Atlanta, GA).

#### 1.3.1.11. Analysis of imprinted gene expression

The expression of *H19* and *Snrpn* genes were analyzed to see if there was a correlation between their observed methylation patterns and their expression. For the expression assays, the same embryos and survivor offspring used for methylation analysis were studied. RNA was extracted from embryos and tissues using the UltraSpec RNA extraction kit (Biotecx, Houston, TX) and cDNA was synthesized using the M-MLV kit (Promega, Madison, WI). All the assays were dependent on the presence of distinguishing polymorphisms between the parental alleles in the specific imprinted genes studied.

##### *H19* expression

For this assay either ground embryos or skeletal muscle tissue was used as *H19* is expressed during embryonic development and in adult skeletal muscle. The required region of the *H19* gene was PCR amplified using specific *H19* primers. dCTP's were incorporated during the PCR cycle. PCR cycling conditions were 29 cycles of 94°C for 1 minute, 55°C for 2 minutes and 72°C for 2 minutes (Tremblay et al. 1995). The PCR product, after phenol chloroform extraction, was digested with *Cac8I* for 3 hours at 37°C and run on a polyacrylamide gel. Bands were visualized using auto-radiography. The embryos and tissues studied by this method were obtained from FVB/N X CAST7 matings. If expression was from the CAST7 allele, PCR amplified cDNA had a restriction site for *Cac8I* and so the presence of a 148 bp band indicated expression from the CAST7 allele. If expression was from a FVB/N allele, there was no restriction site for *Cac8I*, so the presence of a 648 bp band, which is the size of the PCR product, indicated expression from the FVB/N allele. Thus we could distinguish expression from either parental allele.

### *Snrpn* expression using SNUPE assay

In this assay, either ground embryo or ground adult brain tissue was used as there is high expression of *Snrpn* in the adult brain. The *Snrpn* region was PCR amplified from the cDNA using specific primers. The PCR conditions were 40 cycles of 94°C for 30 seconds, 42°C for 30 seconds and 72°C for 2 minutes. The PCR product was extracted from an agarose gel using the Qiagen fragment isolation kit (Qiagen, Valencia, CA) and 10 ng of the isolated DNA fragment was mixed with 1uM of the SNUPE primer, the required PCR buffers and 2 uCi of either <sup>32</sup>PdGTP or <sup>32</sup>PdATP. The PCR cycling conditions consisted of one cycle of 94°C for 30 seconds, 42°C for 30 seconds and 72°C for 1 minute (Szabo and Mann 1995). After electrophoresis of the samples on a 15% denaturing gel, bands were visualized by autoradiography. The incorporation of dGTPs indicated the expression of FVB allele while the incorporation of dATPs indicated the expression of CAST7 allele (Figures 17 and 18).

The primers used for analyzing the expression of *H19* and *Snrpn* in the various strains of mice are given below:

Genes	Primers	Primer sequence
<i>H19</i>	<i>H19 forward</i>	5' CCTCAAGATGAAAGAAATGGT-3'
	<i>H19 reverse</i>	5'-AACACTTTATGATGGAAGTGC-3'
<i>Snrpn</i>	<i>Snrpn forward</i>	5' -TGCTGCTGTTG CTGCTACTG -3'
	<i>Snrpn reverse</i>	5' -GCAGTAAGAGGGGTCAAAGC-3'.
	<i>SNUPE primer</i>	5'-CAATTCACAAGAAGCATT-3'

#### 1.3.1.12. Methyltransferase activity assay

The assay was adapted from Issa et al. 1993. The MII stage oocytes were collected from the various strains of mice being studied in this project and lysed using the lysis buffer (50mM Tris.HCl pH7.8, 250mM NaCl, 10% Glycerol, 1mM EDTA, 1% Tween80, 0.01% NaN<sub>3</sub>, 1mM DTT, 60ug/ml PMSF, 100ug/ml RNase A). The oocyte protein was then incubated with 5ug of poly (dIdC) and 3uCi of <sup>3</sup>H-S-Adenosyl methyltransferase (SAM) (Sigma, St.Louis, MO) at 37°C for 2 hours. The reaction was then incubated with the STOP solution (1% SDS, 2mM EDTA, 3% 4-aminosalicylate.NaOH pH 7.5 5% Butanol, 125mM NaCl, 250ug/ml Sheared herring sperm DNA, 1mg/ml Proteinase K ) for 1 hour at 37°C. The reaction mix was extracted with phenol:chloroform by using phase-lock gels . The sample was ethanol- precipitated and treated with 0.3M NaOH to remove any RNA. The sample was then blotted on a GF/C glass microfibre filter paper and baked at 80°C. The filter paper was washed with 5% TCA and 70% ethanol and the radioactivity in the sample was measured using a liquid scintillation counter.

### 1.3.2. Cloning and methylation

#### 1.3.2.1. Production of cloned embryos

Cloned embryos were produced by Dr. Young Chung and Dr. Keith Latham at Temple University, Philadelphia, PA, using oocytes from (C57B6/J X DBA2/J) F<sub>1</sub> females as recipients and their cumulus cells as the source of donor nuclei (Wakayama et al. 1998; Chung et al. 2002).

## Preparation of Oocytes and Cumulus Cells

Recipient oocytes for all studies were from obtained from females superovulated by the injection of 5 IU of PMSG followed 48 h later by 5 IU of hCG. Oocytes were isolated at 13–15 h post-hCG injection in M2 medium, and cumulus cells were removed with 100 U/ml hyaluronidase (ICN Pharmaceuticals, Costa Mesa, CA). Oocytes were cultured in CZB medium. Oocytes were cultured at 37°C in an atmosphere of 5% CO<sub>2</sub> in air. Meiotic spindles were removed using a blunt, piezo-driven pipette to penetrate the zona pellucida. Spindle removal was performed in warm (37°C) Hepes-buffered CZB medium supplemented with 2.5g/ml cytochalasin B (Sigma, St.Louis, MO). The spindle-free oocytes were then washed extensively and returned to culture as above, for 1–2 h before injection. Cumulus cells were removed from oocytes using hyaluronidase at a concentration of 300 U/ml. Cumulus cells were maintained in this solution on ice until just before use, when they were collected by centrifugation, resuspended in a solution of CZB-G supplemented with 2%–3% polyvinyl pyrrolidone (PVP) (Sigma, St.Louis, MO), and dispersed in small quantities into microdrops on the injection chamber.

## Injection of Cumulus Cell Nuclei and Oocyte Activation

Cumulus cells were used as nuclear donor cells. Cumulus cells were isolated from cumulus-oocyte complexes following superovulation of (C57B6/J X DBA2/J) F1 females. Cumulus cell nuclei were isolated from individual cells by several rounds of trituration into the injection pipette. The pipette was then passed through the zona pellucida and the nuclei were injected into the spindle-free oocytes. Injections were performed at room temperature within 5–10 minutes on small groups of spindle-free oocytes in fully equilibrated CZB. The injected

oocytes were either activated immediately after injection (immediate activation) or 2-4 hours after injection (delayed activation). Activation of oocytes was induced by a 6-h incubation in calcium-free CZB supplemented with 10 mM SrCl<sub>2</sub> and 5g/ml cytochalasin B (Sigma, St.Louis, MO). Activated oocytes were extensively washed and cultured in CZB at 37°C in an atmosphere of 5% CO<sub>2</sub> in air.

#### Procurement of fertilized embryos

To obtain fertilized control embryos, (C57B6/J X DBA2J) F1 females were caged individually with stud males overnight and examined the next morning for the presence of a vaginal plug. One-cell fertilized embryos were recovered from the oviducts and cultured in the same media as the cloned embryos.

#### 1.3.2.2. Production of tetraploid embryos

Tetraploid embryos were constructed by transferring cumulus cell nuclei into unfertilized MII oocytes obtained from superovulated (C57B6/J X DBA2J) F1 females, in which the maternal chromosome-spindle complex was left in place, followed by 5 g/ml cytochalasin B treatment to maintain a diploid complement of maternal chromosomes and of the donor genome. The tetraploid embryos were cultured in the same media as the cloned embryos till the 8-cell stage.

#### 1.3.2.3. Production of Parthenogenetic embryos

Parthenogenetic embryos were obtained by immediate activation of intact MII oocytes obtained from superovulated (C57B6/J X DBA2/J) F1 females. Oocyte activation was by a 6-h

incubation in calcium-free CZB supplemented with 10 mM SrCl<sub>2</sub> and 5g/ml cytochalasin B. The embryos were cultured in CZB media at 37°C in an atmosphere of 5% CO<sub>2</sub> in air.

#### 1.3.2.4. Immunofluorescence analysis

Cloned, tetraploid and parthenogenetic embryos were fixed at the 1-cell through blastocyst stages, permeabilized, and processed for immunofluorescence using the techniques previously described (Chapter 1.3.1.6 and Ratnam et al. 2002). The fixed cells were incubated in either 1:100 UPT82, or in 1:100 UPTC21 or 1:500 PATH52. For double staining, simultaneous staining with both primary antibodies (UPT82 and UPTC21) followed by simultaneous staining with both their corresponding secondary antibodies was performed. Immunofluorescence was visualized using a Zeiss Axiophot, Zeiss LSM410 laser scanning confocal microscope (Carl Zeiss Microimaging, Thornwood, NY). All images were recorded under identical laser settings. Statistical differences in staining between embryo classes were evaluated using a Chi square test.

#### 1.3.2.5. Quantitative analysis of Dnmt1s staining in nuclei of 8-cell embryos

For each 8-cell embryo stained with either PATH52 or UPT82, confocal images through the middle of each nucleus were obtained. The intensity of staining of each nucleus was measured in these confocal sections using the National Institutes of Health Image program (<http://rsb.info.nih.gov/nihimage/>). The eight intensity values for each embryo were then calculated as a fraction of the maximum nuclear intensity value.

## 1.4. Discussion

### 1.4.1. Functional significance of the Dnmt1s and Dnmt1o proteins during mouse preimplantation development

The predominant DNA (cytosine-5)-methyltransferase in mammals is the Dnmt1 protein whose main role, or only role, in mammalian organisms is to maintain DNA methylation patterns on hemimethylated DNA following DNA replication. Dnmt1 has two isoforms, the Dnmt1s protein and the Dnmt1o protein. The Dnmt1o protein, which is only expressed in the oocytes and preimplantation embryos, maintains methylation patterns on imprinted genes during the 4<sup>th</sup> embryonic S-phase when the protein localizes to the 8-cell stage nuclei. Absence of Dnmt1o protein in the oocyte, leads to a 50% reduction in methylated alleles of imprinted genes which in turn leads to pre-natal lethality of these embryos. After implantation of the blastocyst, the Dnmt1s protein, which only differs from the Dnmt1o protein by a 118 amino acids at the N-terminus, is expressed in all cells of the post-implantation embryo and takes over the function of maintaining methylation patterns on hemimethylated DNA.

The reason for the use of two Dnmt1 isoforms is not clear, since they appear to have a similar function in somatic cells (Ding and Chaillet 2002). Dnmt1o when expressed in somatic cells, instead of Dnmt1s, maintained normal patterns of methylation. It is still to be determined if Dnmt1s can functionally replace Dnmt1o during oogenesis and preimplantation development. Also, ES cell lines expressing both isoforms of Dnmt1 revealed that Dnmt1o is much more stable than Dnmt1s (Ding and Chaillet 2002). It is probable that there is a difference in stability between the two isoforms during preimplantation development as well, and therefore one probable reason for Dnmt1o being used as a maternal effect protein is its increased stability.

To address these issues, mutant mouse lines were created that expressed Dnmt1s protein in the oocytes, either by means of a modified allele that encoded for an oocyte-specific *Dnmt1s* transcript (*Dnmt1<sup>1s/1o</sup>* mice) or by means of a transgene that exogenously expressed Dnmt1s during oogenesis. By our immunofluorescence assay, it was determined that the Dnmt1s protein trafficked to the nuclei in a similar manner to the Dnmt1o protein, that is, it trafficked to the nuclei only at the 8-cell stage of development where it can thus function to maintain methylation on imprinted genes specifically at the 4<sup>th</sup> S-phase of embryonic development.

From the *Dnmt1s-TG1*, *Dnmt1s-TG2* and *Dnmt1<sup>1s/1o</sup>* lines of mice it was determined that the presence of Dnmt1s protein during preimplantation development, along with the Dnmt1o protein, does not cause aberrant DNA methylation in the embryos. Analysis of offspring from these mice showed that there was no abnormal methylation on the parental allele of the imprinted gene that is normally unmethylated nor was there loss of any methylation from the parental allele that is usually methylated. Now the question arises to whether Dnmt1s protein could functionally replace Dnmt1o protein during preimplantation development. To address this issue the methylation patterns on a number of imprinted genes (*H19*, *Snrpn* and *Peg3*) in embryos and adult mice that had developed in the presence of the oocyte-derived Dnmt1s protein, instead of the Dnmt1o protein, were analyzed. The mouse lines that were used for this purpose were the *Dnmt1s-TG1/Dnmt1<sup>Δ1o</sup>* and *Dnmt1s-TG2/Dnmt1<sup>Δ1o</sup>* mice.

From our analysis it was clear that the degree to which imprinted gene methylation and expression was restored in the *Dnmt1s-TG1/Dnmt1<sup>Δ1o</sup>* mice was variable, ranging from a

complete restoration of imprinting, as seen in the survivors and some embryos, to a moderate restoration of imprinting, as seen in a few embryos. This variability was observed even though the amount and activity of the transgene-derived Dnmt1s protein in MII oocytes from the *Dnmt1s-TG1/Dnmt1<sup>Δ1o</sup>* mice was comparable to the normal amount and activity of the oocyte-derived Dnmt1o protein in wildtype oocytes. These findings indicate that a range of Dnmt1s protein levels are available to functionally replace the absent Dnmt1o protein, and we believe that this replacement takes place at the 4<sup>th</sup> embryonic S-Phase, as the Dnmt1o protein is normally found at the nucleus only in the 8-cell stage. It is possible that in the nuclei of certain 8-cell embryos there are adequate levels of Dnmt1s protein to maintain all the imprinted methylation patterns and it is these embryos that go on to develop into survivors. In the other 8-cell embryos there is probably insufficient levels of Dnmt1s protein to maintain all methylation and therefore there is incomplete restoration of genomic imprinting in these embryos. The results obtained from the *Dnmt1s-TG2/Dnmt1<sup>Δ1o</sup>* and heterozygous *Dnmt1<sup>Δ1o</sup>* mice also confirm the above hypothesis. Though the amount and activity of the transgene-derived Dnmt1s protein in MII oocytes from *Dnmt1s-TG2/Dnmt1<sup>Δ1o</sup>* females was comparable to the amount and activity of the oocyte-derived Dnmt1o protein in MII oocytes from heterozygous *Dnmt1<sup>Δ1o</sup>* females, no survivors were obtained from the *Dnmt1s-TG2/Dnmt1<sup>Δ1o</sup>* females. In contrast, the heterozygous *Dnmt1<sup>Δ1o</sup>* females gave rise to normal offspring.

The reason for this variability in Dnmt1s levels at the 8-cell stage where it is functionally required to maintain imprinted methylation patterns, could be its intrinsic instability during early preimplantation development. As has been observed from our analysis, there is a distinct decline in both the Dnmt1s and epitope-tagged Dnmt1s levels from the MII oocyte stage to the 8-cell

stage while the Dnmt1o protein maintains relatively constant levels. Since, the proteins measured during preimplantation development are all derived from oocyte-stores, and not from embryonic transcripts, the time course of protein levels during preimplantation development reflects the *in vivo* decay of the proteins. It is probable that during preimplantation development, there is an intrinsically determined decay mechanism at work that makes the Dnmt1s and epitope-tagged Dnmt1s proteins less stable than the Dnmt1o protein and therefore not available at the threshold level required to maintain methylation patterns at the 8-cell stage. Or the presence of the additional 118 amino acids in the Dnmt1s protein could make it a target of an extrinsic degradation pathway. The amino terminal domain of human DNMT1 is known to interact with the transcriptional repressor protein DMAP1 (Rountree et al. 2000). Presumably the mouse Dnmt1s also interacts with the mouse Dmap1 which might control the degradation of the Dnmt1s protein. The Dnmt1o protein, by virtue of its lacking the 118 amino acids at the N-terminus, would be excluded from this control and thus able to persist in high concentrations till the 8-cell stage of development, where it trafficks into the nuclei to maintain methylation patterns on hemimethylated DNA.

In summary, the Dnmt1s isoform can maintain genomic imprints in the absence of preimplantation Dnmt1o protein. However, the ability of Dnmt1s to maintain imprinting is critically dependant on the level of oocyte and preimplantation Dnmt1s. Both Dnmt1s and Dnmt1o have equivalent maintenance methyltransferase functions in oocytes but it appears that the Dnmt1s is less stable than Dnmt1o and therefore, at the 8-cell stage there is not the required level of Dnmt1s protein to maintain methylation of imprinted genes. Thus, the stability of the Dnmt1o protein appears to be a critically important feature in the Dnmt1o-dependent

maintenance of imprinted gene methylation patterns during preimplantation development, therefore leading to the evolution of two different isoforms of Dnmt1 protein during different stages of development.

### **The dynamics of Dnmt1s and Dnmt1o proteins in cloned mouse preimplantation embryos**

Mammalian cloning by somatic cell nuclear transfer is very inefficient leading to a very low rate of success in terms of obtaining cloned offspring. In fact, the majority of cloned embryos die before implantation, thus indicating a defect in essential, early events. Post-transcriptional gene regulatory mechanisms comprise some of the most critical mechanisms controlling early development during normal embryogenesis. These mechanisms are responsible for a number of key events, including DNA methylation and other forms of epigenetic information, that affect long-term viability and developmental potential. These events are probably regulated by the temporally correct production or activation of ooplasmic proteins, which efficiently interact with the embryonic genome.

From our previous data, we have seen that in normal embryos, maintenance of a correct DNA methylation pattern requires the expression of the correct, stage-specific Dnmt1 protein. Lack of expression of the Dnmt1o protein or misexpression of the Dnmt1s protein during preimplantation development leads to either embryonic lethality or fewer number of live births respectively due to lack of or partial maintenance of methylation. During somatic nuclear transfer, a somatic nucleus introduced into an enucleated oocyte contains the Dnmt1s isoform which is normally not present in early embryos. It is possible that the aberrant expression and localization of the Dnmt1 isoforms during preimplantation development of cloned embryos could lead to methylation defects such as those that have already been reported and subsequently

to developmental arrest at later stages of development. Therefore, to determine if cloned embryos exhibit a normal pattern of expression and cytoplasmic nuclear trafficking of Dnmt1 proteins we analyzed a number of cloned preimplantation embryos by our immunofluorescence assay with specific antibodies to Dnmt1 proteins.

The results presented in this study show that diploid cloned mouse embryos produced using adult cumulus cell nuclei aberrantly regulate the two forms of the Dnmt1 cytosine methyltransferase. We observe these defects at an early stage of development, when correct regulation of these proteins is essential to ensure correct DNA methylation patterns and normal viability at later stages. There was aberrant expression of the Dnmt1s protein in clones at the eight-cell stage, when this protein is normally not expressed until much later in development. Also, the Dnmt1s protein showed a mosaic pattern of expression where it was seen only in some nuclei of the 8-cell embryo. This aberrant expression of the Dnmt1s protein leads us to believe that cloned embryos lack the appropriate posttranscriptional gene regulatory mechanisms that normally prevent Dnmt1s protein expression in preimplantation embryos. Such a defect in regulating Dnmt1s mRNA translation or protein accumulation could reflect a broader defect in cloned embryos, affecting multiple maternal mRNAs and their proteins and such a defect would severely compromise cloned embryo viability.

We also found abundant cytoplasmic Dnmt1o in both normal and cloned eight-cell embryos but little or no nuclear uptake of Dnmt1o in cloned embryos. Thus, there appears to be a significant defect in the cytoplasmic-to-nuclear trafficking of Dnmt1o protein in clones. Indeed, the mosaic pattern of Dnmt1s nuclear localization may indicate defects in the trafficking of both

Dnmt1o and Dnmt1s into nuclei of eight-cell clones. This defect in cytoplasmic-nuclear protein trafficking could result from a failure of the somatic nucleus to express essential nuclear import proteins uniquely required in the early embryo or an incompatibility between somatic cell-derived chromatin or residual nuclear membrane components and embryonically expressed proteins. The defect in cytoplasmic-nuclear protein trafficking could affect nuclear reprogramming and contribute to the mosaic patterns of gene expression reported in cloned embryos.

One hypothesis about the expression of Dnmt1s in 8-cell cloned embryos is that Dnmt1s expression in these nuclei may be a consequence of the reduced nuclear abundance of Dnmt1o. Additional confirmation to this possibility comes from the measurement of Dnmt1s expression in fertilized embryos that lack the Dnmt1o protein because of their derivation from homozygous mutant *Dnmt1* <sup>$\Delta^{1o}$</sup>  oocytes. Intense UPT82 staining for Dnmt1s was seen in all nuclei of 4-cell, 8-cell, and 16-cell mutant embryos. This is consistent with the hypothesis that the absence of Dnmt1o in the nucleus leads to aberrant expression of Dnmt1s. Despite the expression of the Dnmt1s protein in these embryos, they remain nonviable and show a loss of methylation on imprinted genes, indicating a lack of functional compensation for the missing Dnmt1o protein. Based on this observation, the Dnmt1s protein in nuclei of eight-cell cloned embryos may also be unable to maintain methylation patterns on alleles of imprinted genes.

Thus, the failure of intracellular trafficking of Dnmt1o and the expression of Dnmt1s in the cloned embryos could contribute to defects in DNA methylation. From earlier data we have seen that Dnmt1s and Dnmt1o have similar maintenance methyltransferase activity. The Dnmt1s

form is, however, intrinsically less stable than the Dnmt1o form both in somatic cells and during preimplantation development. The relative instability of Dnmt1s, combined with the near absence of Dnmt1o from the nucleus, could lead to an overall reduction in Dnmt1 activity within cloned eight-cell blastomere nuclei and hence a loss of methylation at numerous sites, as occurs on alleles of imprinted genes in Dnmt1o-deficient embryos. Moreover, mosaic expression of Dnmt1s at the eight-cell stage could lead to heterogeneous DNA methylation patterns among blastomeres and eventually to heterogeneity in methylation patterns among the cells and tissues of an individual cloned animal or among cloned offspring.

Another interesting observation is that in cloned embryos, the observed nuclear Dnmt1s protein at the 8-cell stage appears to have been expressed by the embryo itself as opposed to being derived from the maternal store of the protein. In wildtype embryos, the Dnmt1o protein responsible for maintaining methylation of imprinted genes at the 8-cell stage, comes from the oocyte-store of the protein. One hypothesis is that the Dnmt1 proteins (both Dnmt1s and Dnmt1o) probably undergo conformational changes in the cytoplasm which enable them to translocate into the nucleus at the 8-cell stage. The amount of Dnmt1s protein in the cloned embryo also seems to be much lower than the amount of Dnmt1o protein in the wildtype embryos. This could probably be explained by the fact that Dnmt1s is intrinsically less stable than Dnmt1o, as we have shown.

We predict that increased amounts of Dnmt1s protein obtained from the cytoplasm of the oocyte might lead to an increase in the survival rate of clones. We therefore intend to introduce somatic nuclei obtained from the wildtype cumulus cells into the enucleated oocytes of *Dnmt1s-*

*TGI* mice or homozygous *Dnmt1*<sup>1s/1o</sup> mice which express high levels of Dnmt1s protein in their cytoplasm, and study the localization patterns of the Dnmt1 proteins, their effect on the methylation of the imprinted genes and their contribution to the overall success rate of obtaining clones.

In summary, our results reveal defects in the regulation of Dnmt1 gene expression and cytoplasmic-nuclear trafficking that precede any defects thus far reported for cloned embryos of any species. None of the cells examined in cloned embryos in this study appeared to express the correct pattern of nuclear Dnmt1 staining, and thus none of the cells appeared to have been reprogrammed correctly by this criterion. If defects in posttranscriptional gene regulation, cytoplasmic-nuclear protein trafficking, and expression of DNA methyltransferases also exist in clones of other species and are associated with similar blocks in reprogramming, then this would raise obvious concerns about the use of current cloning technologies for broader purposes such as therapeutic cloning.

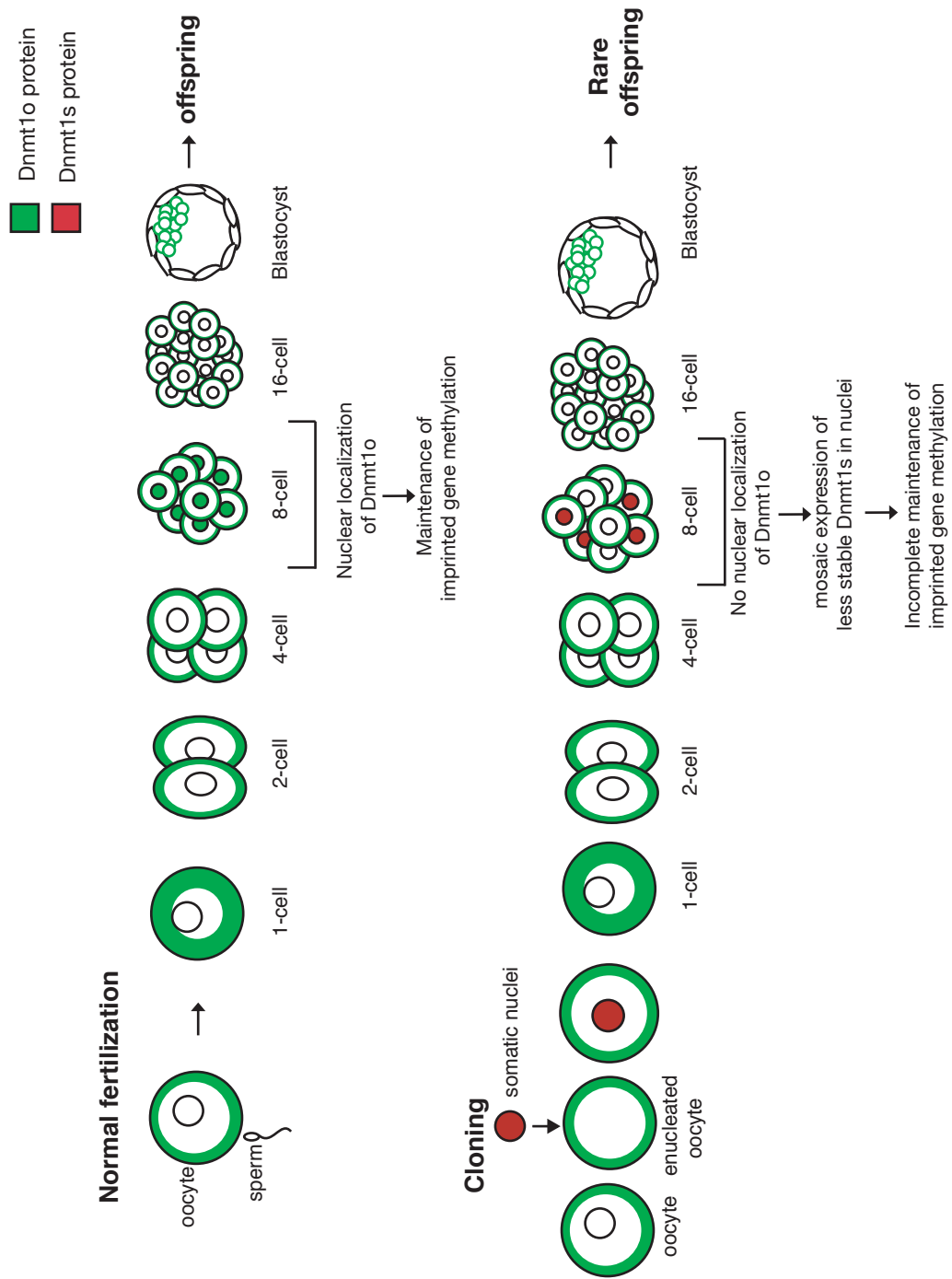


**Figure 29. Hypothesis to explain the dynamics of Dnmt1 proteins in cloned preimplantation development**

**Figure 29. Hypothesis to explain the dynamics of Dnmt1 proteins in cloned preimplantation development**

During normal mouse preimplantation development, the Dnmt1o protein which is expressed and stored in the MII oocyte translocates to the nuclei at the 8-cell stage where it maintains methylation of imprinted genes at that specific stage. There is no expression of the Dnmt1s protein during this period of mouse development. In cloned embryos the somatic nucleus that is injected into the enucleated oocyte expresses the Dnmt1s protein. From our data, it appears that the Dnmt1o protein present in the cytoplasm of the oocyte stays constant till the 8-cell stage, but unlike in the fertilized embryos, there is no uptake of the Dnmt1o protein into the nuclei at the 8-cell stage. Thus, there appears to be a significant defect in the cytoplasmic-to-nuclear trafficking of Dnmt1o protein in clones. This absence of the Dnmt1o protein in the 8-cell nuclei could lead to the mosaic expression of the embryonic Dnmt1s protein in the 8-cell nuclei. But due to the relative instability of the Dnmt1s protein, when compared to the Dnmt1o protein, there could be incomplete maintenance of imprinted gene methylation leading to low number of live births.

## **2. Role of Inpp4b and IP<sub>3</sub>R1 proteins in egg activation and formation of ovarian teratomas in mice**

### **2.1. Introduction**

#### **2.1.1. Oocyte maturation and egg activation**

In most animals the development of the immature oocyte into a fertilizable gamete, a process known as oocyte maturation, involves an arrest in the meiotic cell cycle while awaiting fertilization (Tunquist and Maller 2003). In vertebrate oocytes, maturation begins at the G<sub>2</sub>/M-phase border of meiosis I, and the arrest at the end of oocyte maturation occurs at metaphase of meiosis II. The mechanism of meiotic arrest still remains unclear as well as the molecular signal transduction pathways that operate during this stage of oogenesis. Masui and Markert (1971) described an activity in the cytoplasm of eggs from the leopard frog *Rana pipiens* that was able to initiate oocyte maturation when injected into immature G<sub>2</sub>-arrested oocytes. They termed this activity the maturation-promoting factor (MPF). They also discovered that microinjection of the same cytoplasm into one blastomere of a 2-cell embryo produced a cleavage arrest at metaphase in the injected blastomere. This led to the hypothesis that specific cytoplasmic factors are responsible for the inhibition of mitosis and cleavage at the metaphase II stage of the maturing oocyte. This factor was tentatively labeled cytostatic factor (CSF).

#### 2.1.1.1. Cytostatic factor in oogenesis and egg activation

CSF does not describe a single molecule or protein, but rather an activity found in the egg. Typically CSF activity occurs in the MII oocyte and metaphase arrest is established and maintained. CSF activity remains 30-40 minutes after fertilization before declining, but it never reappears in cleaving embryos. Many researchers have worked to uncover the molecular composition of CSF activity and candidate proteins which in turn need to fulfill three specific criteria to fit the definition of a cell cycle inhibitor. It must accumulate during oocyte maturation, it must be capable of functioning in meiosis II and must be inactivated on fertilization or parthenogenetic activation (Masui 2000; Kubiak and Ciemerych 2001). A few candidates have come to the fore, including the Mos protein where a sharp dose dependence for Mos-induced cleavage arrest suggested that a threshold amount of Mos protein is required for the arrest (Sagata et al. 1988; Sheets et al 1994). The Mos protein activates the MEK/MAPK/p90<sup>Rsk</sup> pathway which in turn leads to a Metaphase II arrest (Nebreda and Hunt 1993; Shibuya and Ruderman 1993). This CSF arrest is also dependent on the inhibition of the APC/C (Anaphase promoting complex/cyclosome) which is brought about by various pathways including the Mos/MAPK pathway (Lorka et al. 1998; Peter et al. 2001). But studies have shown that the Mos protein and APC/C inactivation is not sufficient for CSF, but is part of a larger pathway important for establishment of CSF arrest during meiosis II (Peter et al. 2001; Taieb et al. 2001). There may be other proteins involved which may be part of the Mos/MAPK pathway or acting independently to maintain CSF arrest. It is important to identify these proteins to have a better understanding of the molecular processes involved in egg activation.

#### 2.1.1.2. The role of $\text{Ca}^{++}$ signaling at fertilization

A series of  $\text{Ca}^{++}$  oscillations (periodic increase in ooplasmic  $\text{Ca}^{++}$  concentration) mediates many of the molecular events associated with fertilization and the entry into mitosis (Cantrell 2001; Mehlmann and Kline 1994; Carroll 2001). These include the transition of metaphase-arrested cells into interphase, and the exocytosis of cortical granules. The phosphatidylinositol (PtdIns) pathway appears to be primarily responsible for this increase in intracellular  $\text{Ca}^{++}$ . Here, one or more phospholipases hydrolyze phosphatidylinositol (4,5) biphosphate (PtdIns(4,5)P<sub>2</sub>) to diacylglycerol and inositol 1,4,5,-triphosphate (IP<sub>3</sub>). Soluble IP<sub>3</sub> diffuses throughout the cytoplasm, until it encounters 1,4,5-triphosphate receptor 1 (IP<sub>3</sub>R1) on the endoplasmic reticulum. This interaction results in the release of  $\text{Ca}^{++}$  and an increase in the concentration of cytoplasmic free  $\text{Ca}^{++}$  (Xu et al. 2002). The opening of IP<sub>3</sub>R1s is also regulated by the cytosolic  $\text{Ca}^{++}$  concentration, thus allowing the IP<sub>3</sub>R1s to act as calcium-induced calcium release channels.

Fertilization-induced  $\text{Ca}^{++}$  release via phosphatidylinositol metabolism is a process that is highly regulated from start to finish and many of the key players involved in this regulation are still unknown. For instance, the precise composition of the proximal part of this pathway, phospholipase C hydrolysis of PtdIns (4,5) P<sub>2</sub> is not clear (Saunders et al. 2002). It may involve a sperm surface ligand interacting with a receptor on the egg plasma membrane, in which a ligand-bound membrane receptor couples with an egg PLC to stimulate IP<sub>3</sub> production and  $\text{Ca}^{++}$  release, analogous to the signaling pathway found ubiquitously in somatic cells. Alternatively there may be a sperm factor, possibly the recently described phospholipase C $\zeta$  that is directly released into the egg cytosol at the time of fertilization (Saunders et al. 2002).

There are also other important events occurring that relate to changes in calcium release during meiotic maturation. During meiotic maturation oocytes become more responsive to stimuli that release  $\text{Ca}^{++}$  (Mehlmann and Kline 1994). That is, despite similar levels of stored calcium in all fully grown oocytes (GV and MII stages included) GV-stage oocytes release less  $\text{Ca}^{++}$  than MII oocytes when stimulated with  $\text{IP}_3$ , sperm or  $\text{Ca}^{++}$ . A likely explanation is that  $\text{Ca}^{++}$  release mechanisms undergo important changes during meiotic maturation. An example of this is the increase seen in  $\text{IP}_3\text{R}$  levels (Fissore et al. 1994). Another observation is that there is not the expected loss of plasma membrane  $\text{PtdIns}(4,5)\text{P}_2$  in the minutes following fertilization (Halet et al. 2002). Rather there is a paradoxical net increase that appears to be dependent on exocytosis of cortical granules. This finding suggests that cortical granule release stimulates an increase in plasma membrane  $\text{PtdIns}(4,5)\text{P}_2$  synthesis following fertilization, thus ensuring a continuing supply of  $\text{IP}_3$  to promote a long series of  $\text{Ca}^{++}$  oscillations.

It is interesting to note that many or all of the cellular events occurring as a consequence of fertilization-induced  $\text{Ca}^{++}$  oscillations can also be seen in unfertilized eggs. Fertilization of mouse eggs normally occurs during a window of 12-14 hours following the leutinizing hormone (LH) surge and leads to exit from Metaphase II and entry into interphase. If fertilization does not occur during this window, and unfertilized mouse eggs remain in the oviduct or are maintained in a suitable medium, a significant fraction of eggs will undergo spontaneous activation in a time-dependant manner (Xu et al. 1997). There is a time-dependant reduction in the density of cortical granules in eggs 13 to 22 hours after the controlled initiation of ovulation by administered hCG. *Cdc2/cyclin B* kinase and MAP kinase activities, events normally associated with the resumption of the cell cycle in fertilized eggs, steadily decrease from 13 to 22 hours

after hCG injection. Moreover, during this same time window, there is a marked increase in the percentage of eggs that can form pronuclei in response to microinjected IP<sub>3</sub>. Taken together, these findings are consistent with the notion that with increasing time after ovulation, the susceptibility of unfertilized eggs to being activated is increased due to the development of a partially activated state. One expected feature of eggs in this state is that many different stimuli could elevate intracellular Ca<sup>++</sup> and thus enhance the possibility of oocyte activation, leading to formation of ovarian teratomas (OTs).

### **2.1.2. Ovarian teratomas**

Teratomas are germ cell tumors that are found in men, women and certain susceptible mouse strains (Peterson et al. 1955, Stevens and Varnum 1974; Eppig et al 1977; Chaillet et al. 1996). A teratoma is a tumor composed of a bizarre arrangement of differentiated tissues that normally are found in other parts of the body. Virtually all teratomas contain a disorganized mixture of tissues of ectodermal, mesodermal and endodermal origin (Damjanov 1983; Gardner 1983). These structures are found in various proportions and stages of differentiation depending on the individual teratoma. Immature teratomas contain poorly differentiated carcinoma (EC) cells in addition to various blends of mature ectodermal, mesodermal and endodermal tissues.

#### **2.1.2.1. Origin of ovarian teratoma**

In 1946, Friedman and Moore proposed that an ovarian teratoma develops from an activated oocyte or its derivatives, such as cells of the blastocyst. There are a number of observations in human subjects that support this notion. First, OT's are usually found in, or

associated, with the ovary. Secondly, human teratomas are frequently found mixed with germ cell tumors (Damjanov 1993). Thirdly, the anatomical distribution of many teratomas is along the line of migration of primordial germ cells from the yolk sac to the genital ridge (Eddy et al. 1981). Lastly, convincing evidence for a germ cell origin of OT's is derived from their genotypes. Using chromosomal banding studies and chromosomal polymorphisms at or near the centromere Linder et al. in 1969 showed that many dermoid cysts are genetically haploid consistent with a parthenogenetic germ cell origin. This finding has since been confirmed in more extensive studies in which OT's were shown to originate from a variety of stages of oogenesis (Parrington et al. 1984)

#### 2.1.2.2. Genetic analysis of ovarian teratomas

Because oocytes progress through meiosis, a process involving genetic recombination and segregation of parental homologous chromosomes to different cells, OTs can be analyzed genetically by comparing the genotype of the tumor to the genotype of the tumor-bearing host. This approach was used by Linder et al. in 1969 to show parthenogenetic etiology in many human dermoid-cysts. Such an analysis can identify the latest meiotic stage reached in formation of an individual teratoma. Because this approach is analogous to identifying cancer-causing mutations by comparing the genotype of a tumor to the genotype of the tumor-bearing host, the various meiotic progressions of teratomas have been called types of errors. These errors, as outlined by Chakravarthy et al. 1989 and Surti et al. 1990, are listed in Table 6 with the expected genotype of an OT.

Based on the analysis of five mature teratomas using a limited number of genetic markers, the original studies by Linder et al. 1969 indicated that mature OTs arose from type 2 errors (oocytes that completed meiosis 1). In 1990, Surti et al. analyzed 89 mature OTs (mostly sporadic, non-familial) using only centromere markers and concluded that 65% were from a Type 2 or a Type 3 error and 35% were from Type 1 or a Type 4 error. The study by Deka et al. 1990 concluded that 21% of the 61 mature OTs analyzed were from a Type 2 error and 39% were from a Type 3 error. The conclusion from these studies is that human mature OTs can develop as a consequence of more than one type of meiotic error.

#### 2.1.2.3. Ovarian teratomas in genetically susceptible mouse strains

Although the developmental (meiotic) origin of individual OTs can be determined, little is known about the genetic predisposition to their formation. In humans, OTs occur spontaneously with no known genetic or environmental cause, and there are only a few reports suggesting a familial disposition to their formation. The development of mouse ovarian OTs, however is clearly genetically restricted. An example of this strong genetic influence is the high incidence of OTs in certain inbred strains of mice. Greater than 50% of inbred *LT/Sv* females develop OTs (Stevens 1983), and all or nearly all of these OTs are from oocytes that have completed meiosis 1 but have failed to complete the second meiotic division (Eppig et al. 1977; Eicher 1978). This singular origin of (singular error) for OT formation is not surprising since *LT/Sv* is an inbred strain and all the females are genetically identical (*LT/Sv* is a recombinant inbred strain derived from progenitor C58B6/J and BALB/c strains).

**Table 6. Types of errors that lead to formation of ovarian teratomas**

The table shows the type of errors that can occur in the progenitor germ cell of an OT and the expected genotype that would occur in an OT female who is heterozygous for centromeric and distal markers. It is very rare for a type 5 error to occur as two primordial germ cells must be present in a single Graafian follicle for them to fuse, and this is not a common occurrence.

**Table 6. Types of errors that lead to formation of ovarian teratomas**

Type of error	Error	Ovarian teratoma genotype	
		Centromeric markers	Distal markers
1	Failure to complete meiosis I or fusion of first polar body with oocyte	Heterozygous	Heterozygous or homozygous
2	Failure to complete meiosis II or fusion of second polar body with oocyte	Homozygous	Heterozygous or homozygous
3	Endoreduplication of mature ovum	Homozygous	Homozygous
4	Failure of primordial germ cell to enter meiosis	Heterozygous	Heterozygous
5	Fusion of two ova	Heterozygous or homozygous	Heterozygous or homozygous

#### 2.1.2.4. Role of strain-specific modifier genes in ovarian teratoma formation

Strain-specific modifier genes seem to play an important role in the development of *LT/Sv* OTs. West et al. in 1993 obtained evidence that a single codominant gene, *primary oocyte population (Poo)*, was responsible for metaphase arrest in *LT/Sv* oocytes. Fifty percent of (*C57B6/J* x *LT/Sv*) oocytes underwent spontaneous parthenogenetic activation and development to the blastocyst stage when cultured *in vitro* compared to 12% for *C57B6/J* and 88% *LT/Sv* oocytes (Eppig et al. 1996). These data suggest that a single *LT/Sv*-derived gene (not mapped) is responsible for the increased level of parthenogenetic development in (*LT/Sv* x *C57B6/J*) F1 and *LT/Sv* oocytes compared to *C57B6/J* oocytes.

One study provided the chromosomal location of a single *LT/Sv* determinant of OTs in *LT/Sv* mice (Lee et al. 1997). In this study, 8% of the (*C57B6/J* x *LT/Sv*) F2 females analyzed had an OT. A genome-wide scan identified the *ovarian tumorigenesis susceptibility 1 (Ots1)* gene on chromosome 6. Of the females analyzed with OTs, 23 females were homozygous for the *LT/Sv*-derived allele at both loci, 12 were heterozygous for both loci, one inherited a crossover between these two loci, and none were homozygous for *C57B6/J*-derived alleles at either locus. From these observations Lee and co-workers hypothesized that a single copy of the *LT/Sv Ots1* allele is necessary, but not sufficient, for OT formation (i.e., the *LT/Sv Ots1* allele is dominant to the *C57B6/J-Ots1* allele and not all individuals homozygous for the *LT/Sv-Ots1* allele develop an OT). Overall these analyses suggest that MI arrest, parthenogenetic activation and the *LT/Sv-Ots1* determinant are all necessary for OT development, but none alone are sufficient for ovarian teratoma formation.

Thus, it appears that there may be other genetic determinants involved, in addition to the *Ots1*, in the formation of OTs in mice. But not many candidates or mouse model systems have come to the fore to explain the other probable pathways that may be involved. There is also no direct evidence that changes in the dynamics of proteins involved in egg activation lead to OT formation in mice. The *Tgkd* line of mice produced by Chaillet et al. in 1996, however, seemed to have the potential to indeed add to our understanding of OT biology and the cell signaling pathways involved.

### **2.1.3. Ovarian teratomas in the *Tgkd* line**

In the course of studying the cis-acting requirements for genomic imprinting, Chaillet et al. produced the *Tgkd* transgenic line using the *RSVlgmyc* transgene (Chaillet et al. 1996). The *RSVlgmyc* transgene in the *Tgkd* line is genomically imprinted. However, it was also observed that this line has a high incidence of ovarian teratomas where approximately 20% of hemizygous *FVB-Tgkd* (inbred FVB/N mice that are hemizygous for *Tgkd* transgene) mice develop teratomas. The tumors are uni- or bi-lateral, of variable size, and some have evidence of metastases to the mesenteric lymph nodes and/or lungs. Upon dissection of the tumors, the central area was composed frequently of haemorrhagic and necrotic material. No other malignancies or morphological abnormalities were found in adults *FVB-Tgkd* mice. Interestingly cultured primary oocytes from *FVB-Tgkd* mice, like *LT/Sv* primary oocytes undergo spontaneous parthenogenetic activation and development to the blastocyst stage.

Histological examination of *FVB-Tgkd* teratomas revealed a malignant mixed germ cell phenotype (teratocarcinoma). The tumors contain areas of mature teratomous structures with well differentiated, keratinizing squamous epithelium, respiratory epithelium, cartilage, sebaceous glands, hair follicles, intestine, bone, fat, smooth muscle, and nerves. These structures are derivatives of all three embryonic germ layers typically represented in teratomas or teratocarcinomas: ectoderm, mesoderm, and endoderm. Other areas of the tumor are immature, composed mostly of undifferentiated mesenchymal cells with a high mitotic index, consistent with embryonal carcinoma cells. The tumors show embryoid bodies, Schiller-Duval bodies characteristic of endodermal sinus tumors, and malignant trophoblasts characteristic of choriocarcinoma. The larger tumors contained a significant amount of central necrosis. Tumors from all mice were histologically similar.

#### *Tgkd* allele as an insertional mutation

Three lines of evidence support the idea that the *Tgkd* allele functions as an insertional mutation. First, there is an absolute association between OTs and the presence of a *Tgkd* allele in the FVB/N strain. That is, all teratomas from hemizygous *FVB-Tgkd* females contain the transgene. Secondly, other transgenic lines produced with the same DNA construct as the *Tgkd* mice, but integrated at other chromosomal locations, did not develop tumors. Thirdly, hemizygous and homozygous *Tgkd* mice have distinct phenotypes where the hemizygous *Tgkd* mice, except for the frequent occurrence of ovarian teratomas, appear phenotypically normal, whereas homozygous *Tgkd* mice die around the time of birth. This was demonstrated by genotyping multiple offspring from various matings between hemizygous males and females at

different developmental times, using a DNA fragment that immediately flanked the transgene insertion and that distinguished wildtype from *Tgkd* alleles on Southern blots. The observed percentages of the different genotypes at embryonic days 8.5 and 10.5 were roughly equivalent to the expected percentages. However the observed percentages of homozygous transgenics at birth were approximately one-half of the expected value. At 3 weeks of age there were no identifiable homozygous *Tgkd* mice. These observations lead to the hypothesis that the expression of a gene neighbouring the insertion is altered in female germ cell, and this alteration leads to the development of ovarian teratomas. Under the assumption that indeed the ovarian teratomas were due to a *Tgkd*-mediated insertional mutation, Feng Ding and Richard Chaillet cloned the locus of integration of the transgene and identified the genes in the vicinity of the insertion.

As a first step in identifying a gene involved in the development of ovarian teratomas, genomic fragments flanking both sides of the *Tgkd* insertion were cloned. This was accomplished by first identifying single-copy junctional fragments on Southern blots probed with a variety of transgene fragments. Two junctional fragments, one from each side of the transgene insertion, were then cloned from sub-genomic libraries of *FVB-Tgkd* DNA. DNA sequencing of the junctional fragments and physical mapping of the flanking fragments to the mouse genome demonstrated that the transgene insertion resulted in small, approximately 1-kb deletion of genomic DNA. The sequence of DNA flanking the transgene insertion was used to determine the location of *Tgkd* within the sequence of the mouse genome. This placed the transgene insertion between two known chromosome 8 genes, *Inpp4b* and *Il15* (Figure 30), a location that is consistent with the previous map position determined from a panel of

recombinant-inbred strains. Because *Tgkd* inserted into a large, 200 kb interval between *Inpp4b* and *Il15*, there was a possibility that *Tgkd* disrupted an unidentified gene in this interval. Two lines of evidence indicate that this was unlikely. First extensive exon trapping of genomic sequences isolated from 60 kb of the genome surrounding the insertion site was performed, and no true exons were identified. These failed efforts included screening an ovary c-DNA library made from 10-day old mice with candidate exon sequences. Secondly no mouse or human ESTs have been identified in this interval between *Inpp4b* and *Il15*. Thus, it was predicted that either *Inpp4b* or *Il15* expression has been affected by *Tgkd*, and this effect has led to the development of ovarian teratomas.

Of the two genes on either side of *Tgkd*, alteration of *Inpp4b* would better account for the *FVB-Tgkd* phenotypes. Although little is known about the precise role of Inpp4b, its significant biological role is probably in modulating phosphatidylinositol signaling. As mentioned before, phosphatidylinositol signaling via IP<sub>3</sub> is known to play a role in egg activation. It is also known that the pathway of inositol metabolism that involved the production of PtdIns(3,4)P<sub>2</sub> (which, in turn, is responsible for an increase in IP<sub>3</sub> during egg activation) is regulated by phosphatases. It is therefore quite feasible that Inpp4b could be indirectly involved in egg activation as well. Altered Inpp4b activity could lead to an increase in IP<sub>3</sub> levels in MII oocytes and consequent Ca<sup>++</sup> release, which in turn, could lead to abnormal egg activation and teratomas. Moreover phosphatidylinositol signaling is an essential signal transduction system in mammalian cells, and disruption of a component in this pathway, namely Inpp4b, may well be associated with a perinatal lethality as seen in homozygous *Tgkd* mice. In contrast, homozygous null mutations in

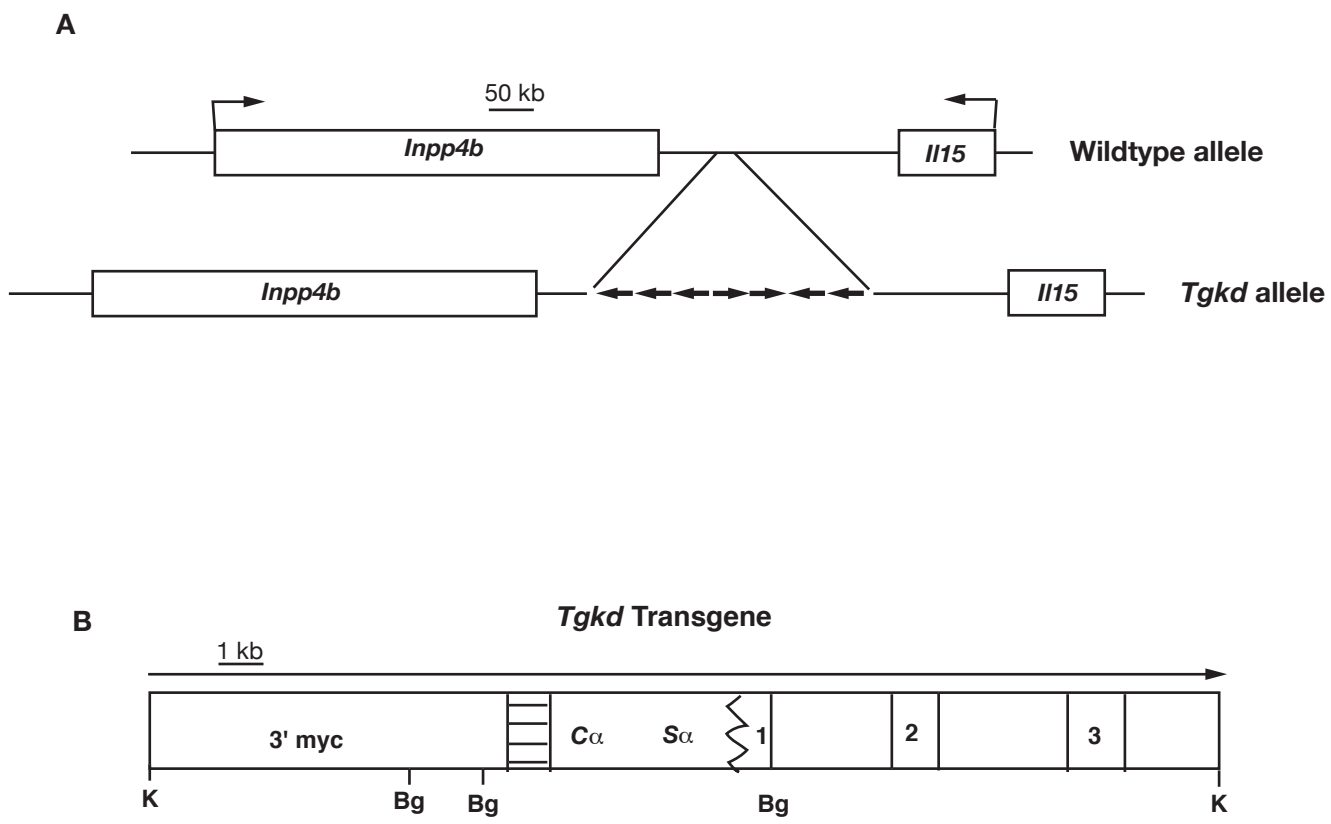


**Figure30.** Schematics of *RSVlgmyc* transgene and its insertion in *Tgkd* mice.

**Figure 30. Schematics of *RSVlgmyc* transgene and its insertion in *Tgkd* mice.**

A. Schematic of insertion of the *RSVlgmyc* transgene. From previous analysis, it was determined that *RSVlgmyc* inserted into a large, 200 kb interval between *Inpp4b* and *Il15* on chromosome 8

B. The *RSVlgmyc* transgene DNA construct. The main portion of the construct is derived from a Burkitt-like *IgA/c-myc* translocation (Chaillet et al. 1991). The 440-bp horizontally hatched region is a portion of the RSV-LTR. *C $\alpha$*  and *S $\alpha$*  are contiguous coding, intronic and switch regions of *IgA*. 1, 2, 3 are exons of *c-myc*. Exon 1 is truncated by *S $\alpha$* . The arrow above the construct refers to the orientation of a unit copy of the construct in the array of tandem copies

inserted between *Inpp4b* and *Il15*.

*I15* are viable and *I15*'s primary biological role appears to be in the development of the immune system, rather than in germ cell development (Ohteki et al. 2001).

#### 2.1.3.1. Strain-specific effects on *Tgkd* ovarian teratomas

The formation of the ovarian teratomas in the *Tgkd* females seemed to be dependant on the strain of the mice in which the transgene was present. As mentioned before, approximately 20% of hemizygous *FVB-Tgkd* mice develop teratomas while none of the C57B6/J or 129/Sv mice with the *Tgkd* transgene developed teratomas. F1 *Tgkd* mice produced by mating *FVB-Tgkd* mice to 129/Sv, DBA/2J or C57BL/6J(C57B6/J) mice, also do not develop OTs. These results suggest that, in addition to the gene disrupted by the *Tgkd* transgene, at least one additional FVB/N-derived gene is required for OTs to develop in *Tgkd* females. To test this hypothesis the following experiment was conducted by Dr. Eicher E (Jackson Laboratories, BarHarbour, ME). First, backcross generation females were produced by mating (*FVB-Tgkd* x C57B6/J)F1 *Tgkd* or (C57B6/J x *FVB-Tgkd*)F1 females to FVB/N males. At 120 days of age, the female were killed and scored for the presence or absence of an OT. 8% of the *Tgkd* females analyzed were OT positive whereas the remaining *Tgkd* females and all the non-*Tgkd* females were OT negative. This result suggests that an FVB/N-derived gene, other than the gene disrupted by the *Tgkd* transgene is required for OT development in *Tgkd* females. For simplicity, this gene was designated *Ots2* (*ovarian teratoma susceptibility 2*).

To map *Ots2*, a genome scan was performed using DNA isolated from the 31 *Tgkd* OT positive females. The only linkage noted, other than to the region of chromosome 8 containing the transgene insert, was to markers located on chromosome 6. This would imply that the *Ots2* gene is on chromosome 6. It was hypothesized that the FVB/N-derived *Ots2* gene is required for OT development in *Tgkd* females and homozygosity for the FVB/N-derived *Ots2* gene increases the probability of OT development. That is, a single copy of an FVB/N-derived *Ots2* gene is necessary but not sufficient, for OT formation in *Tgkd* females.

There is the possibility that *Ots1* and *Ots2* is the same gene. There is also the possibility that they are not the same gene but map to the same region on chromosome 6. To investigate the possibility that *Ots1* and *Ots2* are the same gene, *FVB-Tgkd* females were mated to *LT/Sv* males and F1 daughters were analyzed to determine if they developed an OT by 120 days of age. Females who contained an obvious abdominal growth before 120 days were killed and the presence of an OT was verified. At 120 days of age, normal appearing females were killed and checked for an OT. When each female was killed a tail biopsy was taken for later typing for the presence of *Tgkd*. Of the 48 *Tgkd* females analyzed, 43 were OT positive, whereas 0 of their 64 non-*Tgkd* female sibs were OT positive. This result suggests that *Ots1* and *Ots2* are indeed the same. A direct approach is needed, however to test for identity of *Ots1* and *Ots2*. If these two genes are the same, this will facilitate the ability to experimentally map the FVB *Ots2* and *LT/Sv Ots1* genes.

A strong candidate for the *Ots1* and *Ots2* genes on chromosome 6 is *Itpr1*, the gene encoding the IP<sub>3</sub>R1 protein. The level of IP<sub>3</sub>R1 protein increases almost two-fold during oocyte

maturation, and as mentioned before, it plays an important role in the release of  $\text{Ca}^{++}$  and an increase in the concentration of cytoplasmic free  $\text{Ca}^{++}$  following fertilization. The  $\text{IP}_3\text{R1}$  dynamics during oocyte maturation and fertilization suggest that strain variation in  $\text{IP}_3\text{R1}$  protein levels or minor sequence changes in the *Itp1* gene during these periods may influence the response to  $\text{IP}_3$  signalling and consequently the tendency to form ovarian teratomas.

#### 2.1.3.2. Type of Meiotic error

One hypothesis for the formation of ovarian teratomas in the *FVB-Tgkd* females is that these teratomas arise from oocytes that have undergone meiotic maturation. To begin to test this hypothesis, Richard Chaillet used a fragment flanking the *Tgkd* transgene to genotype a group of *FVB-Tgkd* teratomas that developed in the inbred FVB/N background, and compared their genotypes to those of their hemizygous *FVB-Tgkd* hosts. On southern blots of *BglII*-digested genomic DNA, this fragment distinguishes a wildtype FVB/N allele (7-kb band) from a *Tgkd* allele (12-kb band). Approximately one-half of the teratomas examined was hemizygous and the other half was homozygous. Notably, all teratomas contained at least one *Tgkd* allele. This finding effectively eliminates errors of type 3 (endoreduplication of a mature ovum) or type 4 (failure of a primordial germ cell to enter meiosis) as the underlying etiology of *FVB-Tgkd* teratomas. However because the genotyping of the teratomas was performed with a single distal heteromorphic marker located 33 cM from the centromere, the results could not distinguish among the remaining three possibilities (type 1-failure to complete meiosis; type 2-failure to complete meiosis II; type 5- fusion of two ova). A type 1 error would be consistent with *FVB-*

*Tgkd* oocytes that are physiologically abnormal early in germ cell development, whereas type 2 or 5 errors would suggest abnormalities during meiotic maturation or soon after its completion.

To distinguish among these possibilities, further genotyping of *Tgkd* teratomas that had developed in a mixed strain background was done, using many pericentromeric and distal heteromorphic markers. This analysis was done by Dr. Eva Eicher. DNA was isolated from 13 OTs obtained from 12 backcross females obtained by mating (*FVB-Tgkd/+* x *C57B6/J*) *Tgkd/+* F1 mice to *FVB/N* mice. Ten pericentric MIT markers were chosen for analysis such that each marker tagged a separate chromosome. First the 12 OT positive females were typed to determine if they were B/F (*C57B6/J/FVB/N*) or F/F for each marker (only markers that were B/F would be informative for analysis of their OT). With the exception of 3 MIT markers, the OT from a B/F female was B/B or F/F. For an OT to be B/B or F/F in a B/F female, MI must have been completed before the OT developed. It was thus concluded that the OTs present in *Tgkd* females are derived from germ cells that have completed MI and not MII. These results are similar to results obtained by females of the *LT/Sv* inbred strain. Taken together the preliminary observations suggest that the physiologic abnormality in *Tgkd* female germ cells is in a narrow window of meiotic maturation, after completion of meiosis I but before completion of meiosis II.

## 2.1.4. Specific Aims

### 2.1.4.1. Specific Aim 1

The *FVB-Tgkd* line of mice has a high incidence of ovarian teratomas, where approximately 20% of hemizygous *FVB-Tgkd* mice develop teratomas. From preliminary studies, there is strong evidence that *Tgkd* functions as an insertional mutation where the expression of a gene neighbouring the insertion is altered in female germ cell, and this alteration leads to the development of ovarian teratomas. One of the candidate genes whose expression could have been altered is the *Inpp4b* gene. The Inpp4b phosphatase is known to hydrolyze phosphatidylinositol lipids and inositol phosphates. We hypothesize that Inpp4b catalyzes the hydrolysis of IP<sub>3</sub>, and that disruption of Inpp4b expression could lead to higher IP<sub>3</sub> levels in oocytes, which in turn could lead to parthenogenetic activation of unfertilized eggs and formation of ovarian teratomas. There is also the possibility that Inpp4b could act as a cytostatic factor in MII oocytes to prevent cell division in unfertilized MII oocytes. Decreased Inpp4b protein levels could reduce the cytostatic activity in MII oocytes, thus leading to teratoma formation. To test these possibilities, Inpp4b protein levels will be measured in germinal vesicle stage oocytes, mature MII oocytes and preimplantation embryos from both FVB wildtype and *FVB-Tgkd* females. Inpp4b mRNA and Inpp4b enzymatic activity will also be measured in both wildtype and *Tgkd* females. The results of these experiments should clarify the role of Inpp4b in the development of ovarian teratomas in *FVB-Tgkd* females.

#### 2.1.4.2. Specific Aim 2

From preliminary studies it has been established that there is a strong FVB/N genetic determinant (*Ots2*) needed for OT development in *Tgkd* females. This determinant has been placed on chromosome 6, the same chromosome that contains *Ots1*, an *LT/Sv* genetic determinant of OT development. A good candidate for the *Ots2* gene is the *Itpr1* gene that encodes the IP<sub>3</sub>R1 protein. IP<sub>3</sub>R1 is responsible for mobilizing intracellular Ca<sup>++</sup> stores upon binding to IP<sub>3</sub> during egg activation. The IP<sub>3</sub>R1 dynamics during oocyte maturation and fertilization suggest that strain variation in IP<sub>3</sub>R1 protein levels or minor sequence changes in the *Itpr1* gene, during these periods may influence the response to IP<sub>3</sub> signalling and consequently the tendency to form ovarian teratomas. To analyze this hypothesis, the levels of IP<sub>3</sub>R1 protein will be analyzed in MII oocytes from 3 different strains, C57B6/J, FVB/N and 129/Sv. We will also analyze for sequence differences in the IP<sub>3</sub>R RNA between the various strains of mice including the *LT/Sv* mice. The outcome of this study will help us have a better understanding of the role of IP<sub>3</sub> and IP<sub>3</sub>R1 in OT development.

## 2.2. Results

### 2.2.1. Role of Inpp4b in the formation of ovarian teratomas

To confirm the possibility that lower levels of Inpp4b protein is a possible reason for formation of ovarian teratomas in the *FVB/Tgkd* females, we compared the levels of Inpp4b protein, mRNA and Inpp4b activity between the MII oocytes of wildtype FVB/N and *FVB-Tgkd* females. We also studied the dynamics of the Inpp4b protein during oogenesis to confirm its possible association as a cyostatic factor.

#### 2.2.1.1. Measurement of Inpp4b protein levels in wildtype and *Tgkd* oocytes

In FVB/N strain of mice

The notion that Inpp4b expression is altered in *FVB-Tgkd* oocytes was tested by measuring Inpp4b protein levels in MII oocytes from both *FVB-Tgkd* and FVB/N mice. Oocytes from both strains were collected at the same time following superovulation with PMS and hCG. Immunoblots from oocyte extracts were probed with two antibodies to Inpp4b (anti-Inpp4b (N-20) and anti-Inpp4b (F-13)). Surprisingly, the levels of Inpp4b were extraordinarily high in wildtype FVB/N oocytes. The 105-kD protein was easily detected in 1/4 of the extract from a single MII oocyte. The level of Inpp4b protein in *FVB-Tgkd* oocytes was approximately one half of that seen in FVB/N oocytes (Figure 31). The likely cause of this reduction in Inpp4b protein is that the *Tgkd* insertion in the 3' region of *Inpp4b* has generated a hypomorphic *Inpp4b* allele. Although the exact mechanism of this effect is unknown, the two likely possibilities are that the transgene's imprinting in the later stages of oogenesis has secondarily affected *Inpp4b*

transcription, or that a cis-acting regulatory element for *Inpp4b* transcription has been disrupted by the *Tgkd* insertion. Because of the lethal phenotype of *Tgkd* homozygous mice, the adverse effect of the *Tgkd* insertion would appear to apply to both parental alleles favoring the disruption of a cis-acting regulatory element.

In 129/Sv strain of mice

The levels of *Inpp4b* protein were also high in the MII oocytes from 129/Sv mice where the protein could be detected very easily from 1/4-1/2 of an oocyte (Figure 31). But the difference in the levels of protein between the wildtype 129/Sv oocyte and the 129/Sv-*Tgkd* oocyte was not as dramatic as the difference between the wildtype FVB and *FVB-Tgkd* oocytes. This outcome also coincides with the fact that ovarian teratomas develop only in the *FVB-Tgkd* mice and not in the 129/Sv-*Tgkd* mice, thus leading us to two conclusions. One is that the lower levels of *Inpp4b* protein could be directly related to the formation of ovarian teratomas. The second is that these levels of *Inpp4b* protein could be directly controlled by the *Ots2* gene and therefore differences in either the levels of the *Ots2* protein or sequences of the *Ots2* gene between the different strains of mice could lead to differences seen in the levels of *Inpp4b* protein in the *FVB-Tgkd* mice and the 129/Sv-*Tgkd* mice.

#### 2.2.1.2. Measurement of *Inpp4b* mRNA levels in wildtype and *Tgkd* oocytes

To further support our results from analyzing the protein levels of *Inpp4b*, a semi-quantitative RT-PCR technique was used to compare the levels of *Inpp4b* mRNA levels in MII

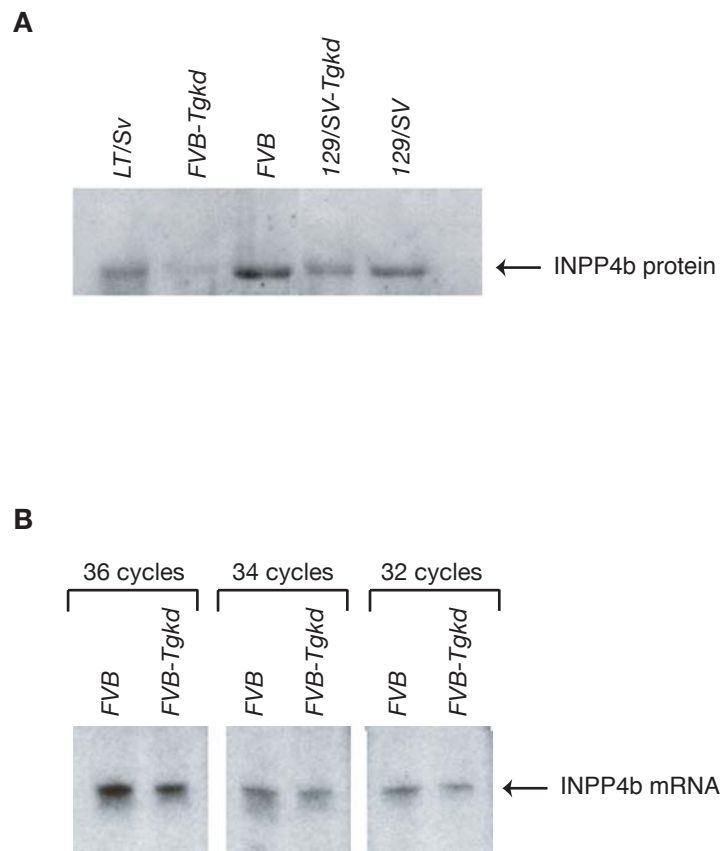


**Figure 31. Inpp4b expression in MII oocytes**

### Figure 31. Inpp4b expression in MII oocytes

A. Expression of Inpp4b protein in MII oocytes. Pools of 10 oocytes were obtained from *LT/Sv*, *FVB/N*, *FVB-Tgkd*, *129/Sv* and *129/Sv-Tgkd* strains of mice, lysed and run on a polyacrylamide gel. The amount of lysate run on the gel was equivalent to that of 1 oocyte. The samples were then transferred to an immunoblot, which was probed with the anti-Inpp4b (N-20) antibody to determine the levels of Inpp4b protein among the various strains of mice. A significant decrease in Inpp4b levels is seen between the wildtype *FVB/N* and *FVB-Tgkd* oocytes. But the difference in levels of protein between the wildtype *129/Sv* oocyte and the *129/Sv-Tgkd* oocyte is not as dramatic as the difference between the wildtype *FVB* and *FVB-Tgkd* oocytes. The level of Inpp4b protein in the *LT/SV* oocytes is comparable to the levels in the *129/Sv* oocytes. B. Expression of Inpp4b mRNA in MII oocytes. RNA was collected from 50 wildtype *FVB/N* and *FVB-Tgkd* oocytes and cDNA was obtained using reverse transcriptase. PCR for different number of cycles (32, 34 and 36) was performed on equal amounts of cDNA from *FVB* and *FVB-Tgkd* oocytes, using radiolabeled nucleoside triphosphates to detect by autoradiograms small amounts of PCR product during a linear phase of product accumulation. As seen in figure there is a slight decrease in the levels of *Inpp4b* mRNA in the MII oocytes from *FVB-Tgkd* mice when compared to oocytes from wildtype *FVB/N* females. But this difference is not as dramatic as the difference seen in the Inpp4b protein levels between the two strains of mice.

oocytes from FVB/N and *FVB-Tgkd* females. PCR for different numbers of cycles was performed on equal amounts of cDNA from FVB/N and *FVB-Tgkd* oocytes. Radiolabeled nucleoside triphosphates were used to detect small amounts of PCR product during a linear phase of product accumulation by autoradiograms. The mRNA for the *Innp4b- $\alpha$*  form is the predominant form in adult mouse ovaries (data not shown) and therefore the mRNA measured in the MII oocytes was also the *Innp4b- $\alpha$*  form. As shown in Figure 31, there was a slight decrease in the levels of *Innp4b* mRNA in the MII oocytes from *FVB-Tgkd* mice when compared to oocytes from wildtype FVB/N females. But this difference was not as dramatic as the difference seen in the Innp4b protein levels between the two strains of mice. There could be various reasons for this including the fact that the difference in Innp4b protein levels seen between the *FVB-Tgkd* mice and FVB/N mice could be due to a difference in post-transcriptional regulation of the protein. Or there could be a qualitative difference between *FVB-Tgkd* and FVB/N *Innp4b* transcripts that is not evident in the RT-PCR assay.

#### 2.2.1.3. Measurement of Innp4b activity in wildtype and *Tgkd* oocytes

Innp4b activity was measured in ovaries from *FVB-Tgkd* and FVB/N females to confirm that there is a direct consequence of lower Innp4b protein levels on phosphatidylinositol metabolism and egg activation. This was analyzed using radiolabeled [<sup>3</sup>H] 1,3,4 inositol triphosphate (gift from Norris A, Iowa State University, IA) as the substrate and the activity level was determined by the extent of conversion of the radiolabeled substrate to [<sup>3</sup>H] 1,3 inositol biphosphate. Ideally the Innp4b activity should have been measured in MII oocytes. However attempts to use oocytes were not successful, inspite of using 100 MII oocytes and allowing the

reaction to proceed for a wide range of time points. The reason for the lack of success could be that the number of oocytes was low or that the substrate used in this assay was not the right substrate for the activity of Inpp4b protein in the MII oocyte. To determine if a difference in Inpp4b activity could be seen in ovaries from *FVB-Tgkd* and *FVB/N* females, Inpp4b activity was measured in equal amount of ovary protein from the two strains. As seen in Table 7, there was a 10% decrease in the amount of Inpp4b activity in the ovaries from *FVB-Tgkd* females when compared to the ovaries from the *FVB/N* females. This decrease is not as significant as the difference seen in protein levels in the MII oocytes from *FVB-Tgkd* and *FVB/N* females. But the reason for this could be that the ovary is a more heterogenous mixture than the MII oocyte and there could be other phosphatases involved whose activity coincide with that of the Inpp4b protein and thus distort the results obtained from this assay. To obtain a much cleaner assay, it would be worthwhile to try measuring Inpp4b activity in pools of larger number of MII oocytes or using a different substrate other than the 1,3,4 inositol triphosphate.

#### 2.2.1.4. Inpp4b as a cytostatic factor

As mentioned before, there was a possibility that Inpp4b might be involved as a cytostatic factor to prevent egg-activation before fertilization or parthenogenetic activation. To prove this hypothesis, we decided to check if Inpp4b fit into some of the criteria required to be a cytostatic factor, i.e. it accumulates during oocyte maturation, it is capable of functioning in meiosis II and its level decreases on fertilization or parthenogenetic activation. GV stage oocytes and MII oocytes were collected from wildtype *FVB/N* females and *FVB-Tgkd* females following superovulation with PMSG and hCG. Immunoblots from oocyte extracts were probed with the

**Table 7. Measurement of Inpp4b activity in mouse ovary**

The assay used for the determination of Inpp4b in ovary extracts was modified from Majerus et al. 1990. The ovaries lysate collected from the mice were incubated with radiolabeled [<sup>3</sup>H] 1,3,4 inositol triphosphate as the substrate for 60 minutes at 37°C. The reaction product, [<sup>3</sup>H] 1,3 inositol biphosphate, which is presumably obtained due to the activity of Inpp4b in the ovaries, was eluted with 8 ml of 0.4M Ammonium formate, 0.1Formic acid, and radioactivity was measured by liquid scintillation spectroscopy as counts per minute (cpm).

Assay number	cpm per 5 ug of ovary protein	
	FVB/N	FVB/Tgkd
Assay 1	73	62
Assay 2	72.5	48

anti-Inpp4b antibody. Surprisingly, the levels of Inpp4b were significantly low in wildtype GV oocytes with the protein level being 1/10 of the level found in wildtype MII oocytes (Figure 32). Seemingly there was a 10-fold increase in the Inpp4b protein level during oocyte maturation leading to high amounts of the protein in the MII oocyte. This rise in Inpp4b concentration associated with meiotic maturation is greatly diminished in oocytes from hemizygous *Tgkd* females, such that the concentration in MII oocytes is, on average, less than one-half of that in wildtype oocytes.

To determine if there is also a fall in the protein level after oocyte fertilization, 1-cell and 2-cell embryos were collected from wildtype FVB/N females after mating them to wildtype males. MII oocytes were collected as previously described. Immunoblots with these oocyte and embryo extracts were probed with the anti-Inpp4b (N-20) antibody. There was a distinct decrease in the level of Inpp4b protein after fertilization and in the 2-cell stage embryos the protein was barely visible on the immunoblot (Figure 32). Thus, these findings are consistent with the notion that Inpp4b is a cytostatic factor that prevents spontaneous activation or cell division of unfertilized MII oocytes. Therefore, the low levels of Inpp4b proteins seen in the MII oocytes from FVB-*Tgkd* females would not be sufficient to prevent spontaneous activation and thus lead to ovarian teratoma formation.

#### 2.2.1.5. Localization of Inpp4b protein in the MII oocyte

Using the Inpp4b (N-20) antibody we analyzed the localization of the Inpp4b protein in the

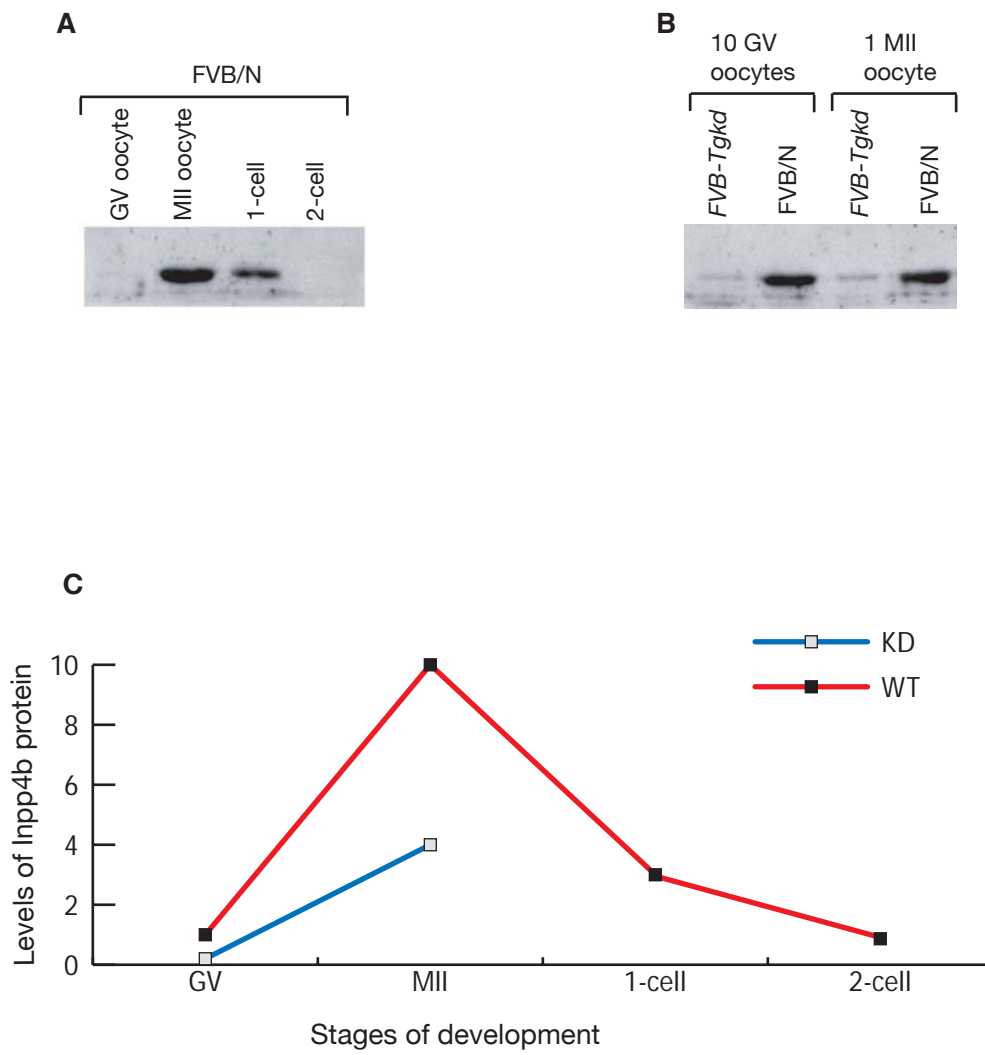


**Figure 32. Expression of Inpp4b protein during oogenesis and fertilization**

### **Figure 32. Expression of Inpp4b protein during oogenesis and fertilization**

A. Immunoblot of wildtype FVB/N embryos and wildtype FVB/N or FVB-Tgkd oocytes probed with the anti-Inpp4b antibody (N-20). 10 oocytes were used for the GV-stage (germinal vesicle stage) lanes and 1 oocyte or 1 embryo for each of the other lanes. 10 MII stage oocytes were pooled and 1/10th of this extract was loaded per lane. Similarly, 3 embryos were pooled and 1/3<sup>rd</sup> of this extract was loaded per lane. A significant increase in Inpp4b levels is seen from the GV stage to the MII stage of oogenesis. In contrast, a definite decrease is observed in the level of Inpp4b after fertilization. Also, a significant difference is observed between the FVB/N and FVB-Tgkd GV-stage oocytes just like in the MII stage oocytes. B. Graph depicting Inpp4b dynamics during oogenesis. The graph is a summary of the approximate changes in Inpp4b protein concentration per oocyte from GV stage oocytes to 2-cell stage embryos.

MII oocyte by immunofluorescence techniques. As seen in Figure 33 the Inpp4b protein seemed to localize to the cortical region of the oocyte. Considering our hypothesis that Inpp4b might have a role to play in the  $\text{Ca}^{++}$  transients, its localization to the oocyte cortex appears promising since the calcium channels involved in egg activation are present along the oocyte plasma membrane. This leads us to believe that there might be a physical interaction between the calcium channels and Inpp4b protein.

Taken together, the results from the studies so far seem to suggest that Inpp4b plays an important role in the formation, or rather, in the prevention of formation of ovarian teratomas from MII oocytes. Lower levels of Inpp4b protein coincide with the higher incidence of ovarian teratomas and the dynamics of Inpp4b protein during oogenesis correspond to the requirements for a cytostatic factor. Thus, it appears that Inpp4b could be part of a cytostatic factor that prevents spontaneous egg activation.

### **2.2.2. Role of IP<sub>3</sub>R1 in the formation of ovarian teratomas**

From preliminary data it was observed that the *Itp1* gene was a good candidate for the *Ots2* gene (the FVB/N genetic determinant needed for OT development in *Tgkd* females). As mentioned before, the IP<sub>3</sub>R1 dynamics during oocyte maturation and fertilization suggest that strain variation in IP<sub>3</sub>R1 protein levels, or minor sequence changes in the *Itp1* gene during these periods, may influence the response to IP<sub>3</sub> signalling and consequently the tendency to form ovarian teratomas. To analyze both aspects of this hypothesis two separate experiments were done. The level of IP<sub>3</sub>R1 protein was analyzed in MII oocytes from 3 different strains, C57B6/J,

MII oocyte stained with anti-Inpp4b antibody

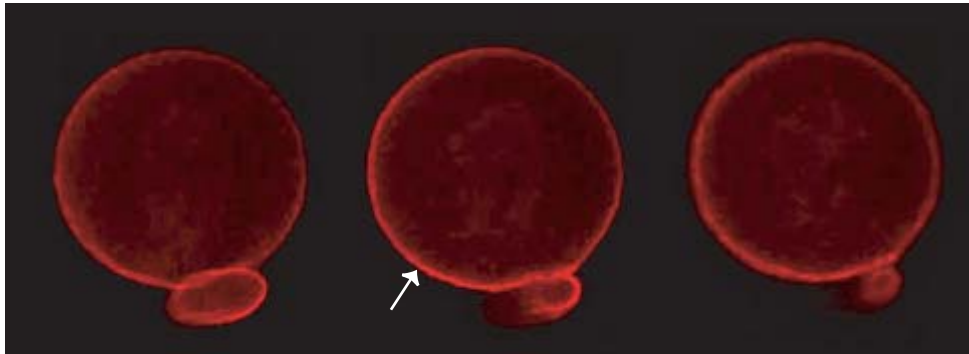


**Figure 33. Localization of Inpp4b protein in MII oocyte**

**Figure 33. Localization of Inpp4b protein in MII oocyte**

Using the anti-Inpp4b (N-20) antibody the localization of the Inpp4b protein in the MII oocyte was analyzed by immunofluorescence techniques. Three confocal sections through the MII oocyte are shown. The arrow indicates the localization of the Inpp4b protein to the cortical region of the MII oocyte.

FVB/N and 129/Sv. We also analyzed for sequence differences in the IP<sub>3</sub>R1 mRNA between the various strains of mice including the *LT/Sv* mice.

#### 2.2.2.1. Measurement of IP<sub>3</sub>R1 protein levels in the MII oocytes

To analyze the probability that there were differences in the levels of IP<sub>3</sub>R1 protein in oocytes from different strains of mice, MII oocytes from 3 different strains of mice, C57B6/J, FVB and 129/Sv, were collected at the same time following superovulation with PMSG and hCG. Immunoblots from these oocyte extracts were probed with the anti-IP<sub>3</sub>R1 antibody that could easily detect the 206 kD protein from an extract of 20 oocytes. As shown in Figure 34, there was no significant difference in the levels of IP<sub>3</sub>R1 protein between the MII oocytes from the three different strains. This result leads us to rule out the possibility that differences in the level of IP<sub>3</sub>R1 protein between the various strains of mice affect their individual susceptibility to formation of ovarian teratomas via their response to IP<sub>3</sub> signalling or their regulation by the *Inpp4b* protein. Therefore, it was important to consider the second possibility that differences in the sequence of the *Itp1* gene between the various strains could lead to differences in their tendency to form ovarian teratoma.

#### 2.2.2.2. Analysis of sequence differences in the *Itp1* gene among various strains of mice.

From the results described in the previous paragraph, it seemed that differences in the *Itp1* sequence could be a probable reason for the differences in the incidence of ovarian

Immunoblot probed with anti-IP<sub>3</sub>R1 antibody

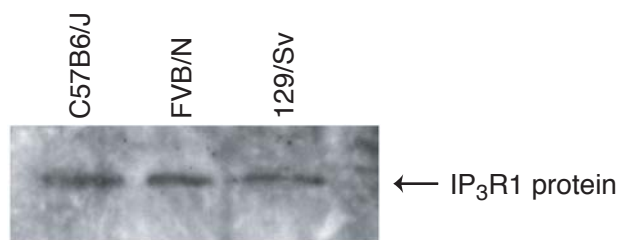


**Figure 34. Measurement of IP<sub>3</sub>R1 protein levels in MII oocytes**

**Figure 34. Measurement of IP<sub>3</sub>R1 protein levels in MII oocytes**

Pools of 25 oocytes were obtained from C57B6/J, FVB/N and 129/Sv strains of mice, lysed and run on a polyacrylamide gel. The samples were then transferred to an immunoblot, which was probed with the anti-IP<sub>3</sub>R1 antibody to determine the levels of the 260 kD IP<sub>3</sub>R1 protein among the various strains of mice. No significant difference in IP<sub>3</sub>R1 levels is seen between the different strains.

teratomas in the different strains. mRNA was collected from the ovaries of C57B6/J, FVB/N and *LT/Sv* mice and c-DNA was obtained using reverse transcriptase. 21 sets of primers were designed (Table 9) which covered the entire IP<sub>3</sub>R1 c-DNA. Using these primer sets, the IP<sub>3</sub>R1 c-DNA was PCR-amplified and the PCR products obtained were sequenced. Thus the sequence for the entire IP<sub>3</sub>R1 cDNA from the FVB/N ovary was obtained. This sequence was compared to the genomic sequence of the C57B6/J *Itp1* gene obtained from PubMed (GenBank Accession # NT\_039353). 11 single nucleotide polymorphisms (SNPs) were observed in various regions of the IP<sub>3</sub>R1 cDNA between FVB/N and C57B6/J (Table 8). Out of the 11 SNPs, 10 gave rise to silent mutations (no change in the amino acid sequence). But one of them (nucleotide #1323, GenBank Accession number NM\_010585) lead to a change in an amino acid (Table 8). Amino acid residue # 331 (GenBank Accession number NM\_010585) which was a serine in FVB/N strain was converted to a proline in the C57B6/J strain. The occurrence of these SNP's was confirmed by obtaining IP<sub>3</sub>R1 cDNA from C57B6/J and *LT/Sv* ovaries and the specific regions with the above mentioned SNP's were sequenced. It was observed that most of the SNP's obtained from the genomic sequence of the C57B6/J *Itp1* gene were true SNP's between the FVB/N and C57B6/J IP<sub>3</sub>R1 cDNA. But the SNP of interest, nucleotide #1323, was not a true SNP. Nucleotide #1323 was a thymine in all three strains of mice.

Thus, further analysis need to be done to determine if there are other changes in the IP<sub>3</sub>R1 protein among the oocytes from FVB/N, C57B6/J and *LT/Sv* strains of mice which might be responsible for the differences in their response to IP<sub>3</sub> signalling and consequently the tendency to form ovarian teratomas.

**Table 8. Single Nucleotide polymorphisms (SNPs) in *Itpr1* cDNA between different strains of mice**

To look for sequence differences in the IP<sub>3</sub>R1 mRNA between various strains of mice, cDNA was obtained from the ovaries of C57B6/J, FVB and *LT/Sv*. 21 sets of primers were designed (Table 8) which covered the entire IP<sub>3</sub>R1 c-DNA (Reference sequence number: NM\_010585 from NCBI). Using these primer sets the IP<sub>3</sub>R1 c-DNA was PCR-amplified and the PCR products obtained were sequenced. Thus, the sequence for the entire IP<sub>3</sub>R1 cDNA from FVB/N was compared to the genomic sequence of C57B6/J (Reference sequence number: NT\_039353 from NCBI) and a total of 11 different single nucleotide polymorphisms (SNP's) were obtained. In the table, the nucleotides in red are the nucleotide differences seen among the different strains. The single amino acid change observed occurred at amino acid # 331, where the serine residue in FVB/N and *LT/Sv* was converted to a proline residue in C57B6/J. But on confirmation by our cDNA analysis, this SNP of interest, nucleotide #1323, was not a true SNP. This nucleotide was a thymine in all three strains of mice.

**Table 8. Single Nucleotide polymorphisms (SNPs) in *Itp1* cDNA between different strains of mice**

Codons			Nucleotide number	Amino acid change
FVB/N	C57BL/6J	LT/Sv		
AAT	AAC	AAT	762	No change
TTT	TTC	TTT	825	No change
GAC	GAT	GAC	1023	No change
TGT	TGC	TGT	1087	No change
ACG	ACA	ACG	1147	No change
TCT	TCC	TCT	1162	No change
TCA	CCA	TCA	1323	S → P (amino acid # 331)
ACC	ACA	ACC	1719	No change
GAT	GAC	GAC	4348	No change
GTG	GTA	GTG	7225	No change
CTC	CTT	CTT	7261	No change

## **2.3. Materials and Methods**

### **2.3.1. Collection of oocytes and preimplantation embryos**

Germinal vesicle (GV) stage oocytes were obtained by puncture of ovarian follicles of 7-12 week-old-females in MII medium (Sigma, St.Louis, MO), as previously described (Clarke et al. 1992). Metaphase II (MII) oocytes were collected from 7-week-old females that were superovulated by injection of 7.5 IU of pregnant mares' serum gonadotropin, PMSG (CalBioChem, LaJolla, CA), followed 44 to 48 hours later by 5 IU of human chorionic gonadotropin, hCG (CalBioChem, LaJolla, CA). These oocytes were recovered from the oviducts 20 hours post-hCG and the cumulus cells were dispersed with 1 mg/ml hyaluronidase (Roche Diagnostics, Mannheim, Germany), as described (Hogan et al. 1986).

Preimplantation embryos were obtained as previously described (Clarke et al. 1992). Superovulated females were caged individually with stud males overnight, and examined for the presence of a vaginal plug the next morning. One-cell embryos were recovered from the oviducts at E0.5 and 2-cell embryos at E1.5 in Hepes-buffered CZB medium (Erbach et al., 1994) and the cumulus mass dispersed as described above.

For all isolation procedures, healthy-looking oocytes and preimplantation embryos were collected in a 35 mm Petri dish using a mouth-controlled micropipette and washed free of any adhering somatic cells by transfer through two dishes of culture medium. Oocytes and embryos were either processed immediately for immunofluorescence or stored at  $-80^{\circ}\text{C}$  in lysis buffer for immunoblotting; or stored at  $-80^{\circ}\text{C}$  in culture medium for RNA isolation.

### **2.3.2. Role of Inpp4b in ovarian teratoma formation**

#### 2.3.2.1. Immunoblot analysis

To study the levels of Inpp4b protein in the oocytes and preimplantation embryos collected from FVB/N, *FVB-Tgkd*, 129/Sv and *129/Sv-Tgkd* females, we used the immunoblot technique. The antibodies used for this technique were the Inpp4b (N-20) or the Inpp4b (F13) antibodies (Santa Cruz Biotechnology, SantaCruz, CA). These antibodies were generated to different epitope regions of the Inpp4b protein. Both antibodies gave similar results when used to analyze the Inpp4b protein in the FVB/N and *FVB-Tgkd* oocytes.

Oocytes or preimplantation embryos were collected manually from washings of oviducts or uteri and pooled and lysed in 5% SDS, 2.5% glycerol, 2.5%  $\beta$ -mercaptoethanol, 0.01% bromophenol blue, 0.025M Tris-HCl, pH 6.8 (1X sample buffer). All samples were denatured by heating at 95°C for 5 minutes, and then separated by electrophoresis on SDS-5% polyacrylamide gels at 4°C. Afterwards they were transferred to PVDF membranes (Millipore Corporation, Bellerica, MA). Membranes were blocked in 5% Carnation dry skim milk in 10 mM Tris-HCl (pH 8.0), 140 mM NaCl, for a least one hour and probed with either Inpp4b (N-20) or Inpp4b (F-13) diluted 1:10,000 in blocking buffer for 3 hours. Following three washes of 5 minutes each in 0.1% Tween-20 TBS, the membrane were incubated for one hour at room temperature in biotinylated rabbit anti-goat IgG (Jackson ImmunoResearch Laboratories, Inc., West Grove, PA) diluted 1:30,000 in blocking buffer and washed as above. Bound antibody was detected by chemiluminescence (ECL Plus, Amersham, Piscataway, NJ).

### 2.3.2.2. Immunofluorescence analysis

To study the localization of the Inpp4b protein in the oocytes from wildtype FVB/N females we used the Inpp4b (N-20) antibody that has been described in the previous paragraph.

Denuded oocytes were freed of the zona pellucida using acidified (pH 2.5) Tyrode's medium (Hogan et al. 1986), and fixed for 10 to 15 minutes at room temperature in 3.7% formaldehyde in PBS. All solutions for immunofluorescence of Inpp4b were prepared in PBS and procedures carried out at room temperature. The fixed cells were blocked for at least one hour in blocking buffer (3% BSA, 0.1% Triton X-100) and then incubated in either 1:100 preimmune serum or 1:100 Inpp4b (N-20) antibody diluted in the same blocking buffer overnight at 4°C in a humidified chamber. The oocytes were washed three times for 5 min each in blocking buffer, and incubated in an anti-goat IgG monoclonal antibody coupled with Alexa Fluor (1:250) (Molecular Probes, Eugene, OR) for an hour at room temperature. The cells were then washed again as before. To mount the cells for viewing, a drop of Vectashield mounting medium (Vector Laboratories, Burlingame, CA) supplemented with 0.4 µg/ml of the DNA-binding dye DAPI (Roche Diagnostics, Mannheim, Germany) was used. Immunofluorescence was visualized using a Zeiss Axiophot, Zeiss LSM410 laser scanning confocal microscope.

### 2.3.2.3. RT-PCR assay

To study the RNA levels of Inpp4b in the FVB/N and *FVB-Tgkd* females, a semi-quantitative RT-PCR technique was used (Ding and Chaillet 2001). RNA was collected from 50 MII oocytes using the Rneasy mini kit (Qiagen, Valencia, CA) and cDNA was obtained from

this mRNA using the M-MLV Reverse Transcriptase kit (Promega, Madison, WI). PCR for different number of cycles (32, 34 and 36 cycles) was performed on equal amounts of cDNA from FVB and *FVB-Tgkd* oocytes, using radiolabeled oligonucleotides (<sup>32</sup>P dCTPs). PCR reactions were performed using approximately cDNA from 50 MII oocytes in a 10 ml reaction containing, 1X PCR buffer (Invitrogen, Carlsbad, CA), 1.5 mM MgCl<sub>2</sub>, 10uM of the Innp4b (Forward) and Inpp4b (Reverse) primers, 200 mM dNTPs, <sup>32</sup>P dCTPs and 1.25 Units of Taq Polymerase (Invitrogen, Carlsbad, CA). The cycling conditions were as follows: 5 minutes at 94°C, followed by 32, 34 or 36 cycles of 45 seconds at 94°C, 45 seconds at 58°C, and 45 seconds at 72°C, and a final extension of 10 minutes at 72°C. The Innp4b- $\alpha$  form, with a hydrophilic C-terminus is the form predominantly expressed in adult mouse ovaries (data not shown). The RT-PCR assay measured just the  $\alpha$  form under the assumption that this is very likely the predominant form in the MII oocytes as well. 4ul of the PCR product obtained was run on a polyacrylamide gel and bands were visualized using autoradiography. Thus, a series of PCR products from a range of amplification cycles was obtained and the results of an FVB/N series were compared to that of an *FVB-Tgkd* series.

The PCR primers used for the RT-PCR assay were as follows:

*Innp4b(forward)* 5'ACACCGACCACATCACAACA 3'

*Inpp4b (reverse)* 5' TACGAAGACCACCGTTCTTG 3'

#### 2.3.2.4. Innp4b activity assay

The assay used for the determination of Innp4b in ovary extracts from FVB/N and *FVB-Tgkd* females, was modified from Majerus et al. 1990. The ovaries collected from the mice were

ground in liquid nitrogen and lysed in 0.5 ml of 2% Triton X-100, 20mM Hepes, 10mM EDTA, 10ug of Leupeptin/ml, and 1mM of Protease inhibitor (Roche Diagnostics, Mannheim, Germany). The lysate was incubated with radiolabeled [<sup>3</sup>H] 1,3,4 inositol triphosphate (gift from Norris A, Iowa State University, IA) as the substrate in 25ul or 50ul containing 50mM MES (pH 6.5) and 5mM EDTA for 60 minutes at 37°C. Reactions were stopped by dilution to 1ml with cold water and poured onto a 0.4ml Dowex formate column (BioRad Laboratories, Hercules, CA). The reaction product, [<sup>3</sup>H] 1,3 inositol biphosphate was eluted with 8 ml of 0.4M Ammonium formate, 0.1M Formic acid, and radioactivity was measured by liquid scintillation spectroscopy.

### **2.3.3. Role of IP<sub>3</sub>R1 in ovarian teratoma formation**

#### **2.3.3.1. Immunoblot analysis**

To look for differences in the levels of IP<sub>3</sub>R1 protein in MII oocytes from 3 different strains of mice, MII oocytes were collected from the oviducts of C57B6/J, FVB/N and 129/Sv strains of mice and lysed in 1X sample buffer as has been described before. The immunoblot assay is very similar to what has already been described for studying the Inpp4b protein levels in section. The antibody used in this assay was the anti-IP<sub>3</sub>R1 antibody (Affinity BioReagents, Golden, CO) diluted 1:1000 in blocking buffer and the PVDF membrane with the oocyte extracts was probed with this antibody for 3 hours. The secondary antibody used was the biotinylated donkey anti-rabbit IgG (Amersham, Piscataway, NJ) diluted 1:3,000 in blocking buffer. Bound antibody was detected by chemiluminescence as described earlier.

#### 2.3.3.2. Analysis of c-DNA for sequence differences in *Itpr1* gene

To look for sequence differences in the IP<sub>3</sub>R1 mRNA between various strains of mice, mRNA was collected from the ovaries of C57B6/J, FVB/N and *LT/Sv* mice using the RNA UltraSpec kit (Biotecx, Houston, TX) and c-DNA was obtained using the M-MLV reverse transcriptase kit (Promega, Madison, WI). 21 sets of primers were designed (Table 9) which covered the entire IP<sub>3</sub>R1 c-DNA. These primers were designed on the basis of the IP<sub>3</sub>R1 cDNA obtained for the ICR strain of mice (GenBank Accession number NM\_01085). Using these primer sets the IP<sub>3</sub>R1 c-DNA was PCR-amplified using the *Pfu*-Turbo Polymerase and the PCR products obtained were sequenced. Thus the sequence for the entire IP<sub>3</sub>R1 cDNA from the FVB/N ovary was obtained. This sequence was compared to the genomic sequence of the C57B6/J *Itpr1* gene obtained from PubMed (GenBank Accession # NT\_039353). A total of 11 different single nucleotide polymorphisms (SNP's) were obtained along the entire cDNA.

The comparison of the IP<sub>3</sub>R1 cDNA sequence from the different strains of mice was performed using AssemblyLIGN Software (Oxford Molecular, Atlanta, GA). The translation of the cDNA sequence into its corresponding IP<sub>3</sub>R1 amino acid sequence was done using MacVector 6.5 software (Oxford Molecular, Atlanta, GA).

**Table 9. Primers to analyze *Itp1* c-DNA for SNPs**

21 sets of primers were designed which covered the entire IP<sub>3</sub>R1 cDNA. These primers were designed on the basis of the IP<sub>3</sub>R1 cDNA sequence from the ICR strain of mice (GenBank Accession number: NM\_010585).

**Table 9. Primers to analyze *Itp1* c-DNA for SNPs**

<b>Forward primers</b>	<b>Reverse primers</b>	<b>Region amplified</b>
atcctaacggaacgagctcc	gctgtacaacacaacgggtca	region 21 nt:129-449
ggatttatcagcaccttagg	tggccagcattgacaggatt	region 20 nt:401-900
ttacaagcttcgctccatcg	ccaggcattcttctcaaag	region 19 nt:826-1310
tggctacagggcattacttg	ttccaactcccagcgatg	region18 nt:1251-1712
ctttgccaatgatgccagca	tttccggtgtgtggagca	region17 nt:1660- 2140
ttggcttcatgcagaagcag	gacacatccttcaaagagg	region16 nt:2061- 2561
gacatcctcagctactacag	ggttaatcggagaaggctcag	region15 nt:2510- 2992
gagggtgtgaacttagccag	cacattactggcccttct	region 14 nt:2921- 3400
ataggatctcctgcctctgt	tcatcgggaccttggccttt	region13 nt:3291-3750
cattgtggagaagtctgagc	tgaagatgtgctgcatcgtc	region 12 nt:3700- 3719
tgtttctcaagccagggatc	tgagtgaccacacgaacgat	region 11 nt:4110-4560
atccatctggtggagctctt	tcttggtacgtcagagagca	region 10 nt:4451-4961
gctgatgccgagccaaaag	ttcttccatagcctctgtc	region 9 nt:4897-5400
ataccaagcaactgctggag	tggaatactcggctactgga	region 8 nt:5301-5790
caacctggatcatgatctca	taggctgcatgatggtgatg	region 7 nt:5740-6230
cctgatgaccattaccagtc	cttccatgatggccagtagca	region 6 nt:6131-6630
tggacctggtgttagaactg	gagcgcaggaagaagtcattga	region 5 nt:6570-7065
attacaccagagcgggaa	gaactccacatccagaacca	region 4 nt:7008-7502
ctgctgggagcttcaatgtct	ctcacactgtgttcgttatcc	region 3 nt:7391-7912
atgtgtgcagggtagagacg	tccttcacttcaccagcac	region 2 nt:7809-8280
gtgctggtgaaagtgaagga	cacatgtacccttagtgggcaa	region 1 nt:8197-8218

## 2.4. Discussion

An ovarian teratoma (OT) is a benign tumor originating in the ovary from a female germ cell. The incidence of ovarian teratomas in women is high. Early studies suggest that an OT is derived from outgrowths of activated, mature oocytes. Although the developmental (meiotic) origin of individual OTs can be determined in humans, little is known about the genetic predisposition to their formation. The two mouse OT models are the *LT/Sv* strain and the *Tgkd* transgene in the inbred FVB/N strain (*FVB-Tgkd* strain) and the analysis of these two strains of mice may lead us to the identification of genes that are related to the formation of ovarian teratomas.

One hypothesis for the formation of ovarian teratomas in the *FVB-Tgkd* females is that these teratomas arose from oocytes that have undergone meiotic maturation. This hypothesis was confirmed by Dr. Eva Eiker (The Jackson Laboratory, Bar Harbor, ME), who genotyped the *Tgkd* teratomas that had developed in a mixed strain background using many heteromorphic markers. From her analysis, it was concluded that the OTs present in *Tgkd* females are indeed derived from germ cells that have completed MI and not MII. These results are similar to results obtained from females of the *LT/Sv* inbred strain.

#### 2.4.1. Role of *Inpp4b* disruption on the formation of *Tgkd* ovarian teratomas

From earlier analyses, it was concluded that the *Tgkd* allele functioned as an insertional mutation. The hypothesis was that the expression of a gene neighbouring the insertion is altered in female germ cell, and this alteration lead to the development of ovarian teratomas. From work done by Feng Ding and Richard Chaillet, it was concluded that the transgene inserted between two known chromosome 8 genes, *Inpp4b* and *Il15*. Of the two genes on either side of *Tgkd*, alteration of *Inpp4b* would better account for the *FVB-Tgkd* phenotypes as its significant biological role is probably in modulating phosphatidylinositol signaling which is known to play a role in egg activation. Here, one or more phospholipases hydrolyze phosphatidylinositol (4,5) biphosphate (PtdIns(4,5)P<sub>2</sub>) to diacylglycerol and inositol 1,4,5,-triphosphate (IP<sub>3</sub>). Soluble IP<sub>3</sub> diffuses throughout the cytoplasm, where it associates with 1,4,5-triphosphate receptor (IP<sub>3</sub>R1). This interaction results in an increase in the concentration of cytoplasmic free Ca<sup>++</sup> and thus leads to egg activation. It is possible that *Inpp4b* could be one of the components of the pathway involved in the production of PtdIns(4,5)P<sub>2</sub> and therefore, altered *Inpp4b* activity would lead to abnormal egg activation and teratomas.

From our analyses it was determined that indeed the *Inpp4b* protein levels in the *FVB-Tgkd* females was lowered in comparison to the wildtype *FVB/N* oocytes. It is possible that this reduction is due to the *Tgkd* transgene insertion in the 3' region of *Inpp4b*, which in turn, might have generated a hypomorphic *Inpp4b* allele. Although the exact mechanism of this effect is not known, one likely possibility is that a cis-acting regulatory element for *Inpp4b* transcription has been disrupted by the *Tgkd* insertion. Also, the lethal phenotype of *Tgkd/Tgkd* homozygous

mice, leads us to believe that the adverse effect of the *Tgkd* insertion would apply to both parental alleles thus favoring the disruption of a cis-acting regulatory element. Surprisingly, there was no significant difference in the level of Inpp4b protein between the 129/Sv and 129/Sv-*Tgkd* oocytes. This result will be discussed in detail in later paragraphs.

To confirm our results from analyzing the protein levels of Inpp4b, a semi-quantitative RT-PCR technique was used to compare the levels of Inpp4b mRNA levels in MII oocytes from FVB/N and *FVB-Tgkd* females. There was a slight decrease in the levels of *Inpp4b* mRNA in the MII oocytes from *FVB-Tgkd* mice when compared to oocytes from wildtype FVB/N females. But this difference was not as dramatic as the difference seen in the Inpp4b protein levels between the two strains of mice. There could be various reasons for this including the fact that the difference in Inpp4b protein levels seen between the *FVB-Tgkd* mice and FVB/N mice could be due to a difference in post-transcriptional regulation of the protein. Or there could be a qualitative difference between *FVB-Tgkd* and FVB/N Inpp4b transcripts that is not evident in the RT-PCR assay. Also, Inpp4b activity was measured in ovaries from *FVB-Tgkd* and FVB/N females to confirm that there is a direct consequence of lower protein levels on phosphatidylinositol metabolism. A 10% decrease in the amount of Inpp4b activity was recorded in the ovaries from *FVB-Tgkd* females when compared to the ovaries from the FVB/N females. This decrease is not as significant as the difference seen in protein levels in the MII oocytes from *FVB-Tgkd* and FVB/N females. But the reason for this could be that the ovary is a more heterogenous mixture than the MII oocyte and there could be other active phosphatases involved that distort the results obtained from this assay or the substrate used was not the right substrate for the activity of Inpp4b protein in the MII oocyte or ovary. Further analysis will be

necessary, to measure Inpp4b activity in pools of large number of MII oocytes or using a different substrate other than the 1,3,4 inositol triphosphate.

There is also the possibility that Inpp4b could act as a cytostatic factor in MII oocytes to prevent cell division in unfertilized MII oocytes. Few candidates have been discovered so far that could be involved in CSF activity, including the Mos protein, but it is clear that there are other proteins involved which may be part of the Mos/MAPK pathway or could be acting independently to maintain CSF arrest. If Inpp4b is indeed a candidate involved as a cytostatic arrest of MII oocytes, it needs to fulfill three specific criteria to fit the definition of a cell cycle inhibitor. It must accumulate during oocyte maturation, it must be capable of functioning in meiosis II and must be inactivated on fertilization or parthenogenetic activation. To test this hypothesis, the dynamics of Inpp4b protein was analyzed during oogenesis and preimplantation development. The levels of Inpp4b were significantly low in wildtype GV oocytes with the protein level being  $1/10^{\text{th}}$  of the level found in wildtype MII oocytes. Seemingly there was a 10-fold increase in the Inpp4b protein level during oocyte maturation leading to high amounts of the protein in the MII oocyte. This rise in Inpp4b concentration associated with meiotic maturation is diminished in oocytes from *FVB-Tgkd* females, and so the concentration in MII oocytes is lower than that in wildtype oocytes. Also, there was a dramatic decrease in the level of Inpp4b protein after fertilization and in the 2-cell stage embryos. Thus, these findings are consistent with the notion that Inpp4b is a cytostatic factor that prevents spontaneous activation or cell division of unfertilized MII oocytes. Therefore the low levels of Inpp4b proteins seen in the MII oocytes from *FVB-Tgkd* females would not be sufficient to prevent spontaneous activation, and thus lead to ovarian teratoma formation.

Taken together, the results from the studies so far seem to suggest that Inpp4b seems to play an important role in the prevention of ovarian teratoma formation from MII oocytes. Lower levels of Inpp4b protein coincide with the higher incidence of ovarian teratomas and the dynamics of Inpp4b protein during oogenesis correspond to the requirements for a cytostatic factor. Thus, it appears that Inpp4b could be part of a cytostatic factor that prevents spontaneous egg activation and therefore lower levels of this protein could lead to ovarian teratoma formation

To confirm the results from our analyses that reduction in Inpp4b levels is indeed responsible for teratoma formation in *FVB-Tgkd* females, an independent transgenic experiment will be undertaken to phenocopy the *Tgkd* teratoma phenotype. Interfering, double stranded *Inpp4b* RNA will be expressed specifically in MII oocytes using the *zona pellucida 3* (*ZP3*) promoter (Stein et al. 2003). These transgenic lines will then be analyzed for the formation of ovarian teratomas.

Another experiment to test the role of Inpp4b reduction in the formation of teratomas in *FVB-Tgkd* females is the re-establishment of Inpp4b protein levels in the *FVB-Tgkd* oocytes. This will be done by expressing wildtype Inpp4b protein levels in maturing *FVB-Tgkd* oocytes, from a *ZP3-Inpp4b* transgene (Lira et al. 1990). The expected outcome is that the forced expression of Inpp4b in *FVB-Tgkd* oocytes will preclude the development of ovarian teratomas.

#### 2.4.2. IP<sub>3</sub>R1 as a probable candidate for control of spontaneous egg activation

The formation of the ovarian teratomas in the *Tgkd* females seemed to be dependant on the strain of the mice in which the transgene was present. As mentioned before, only the hemizygous *FVB-Tgkd* mice develop teratomas while none of the C57B6/J or 129/Sv mice with the *Tgkd* transgene developed teratomas. F1 *Tgkd* mice produced by mating *FVB-Tgkd* mice to 129/Sv, DBA/2J or C57B6/J mice, also do not develop OTs. These results suggest that, in addition to the gene disrupted by the *Tgkd* transgene, at least one additional FVB/N-derived gene (*Ots2*) is needed for OT development in *Tgkd* females and this determinant has been placed on chromosome 6, the same chromosome that contains *Ots1*, an *LT/Sv* genetic determinant of OT development. A good candidate for the *Ots2* gene is the *Itp1* gene that encodes for the IP<sub>3</sub>R1 protein that, in turn, is responsible for mobilizing intracellular Ca<sup>++</sup> stores upon binding to IP<sub>3</sub> during egg activation. The IP<sub>3</sub>R1 dynamics during oocyte maturation and fertilization suggest that strain variation in IP<sub>3</sub>R protein levels or minor sequence changes in the *Itp1* gene, during these periods may influence the response to IP<sub>3</sub> signalling and consequently the tendency to form ovarian teratomas.

To analyze this hypothesis, the levels of IP<sub>3</sub>R1 protein were analyzed in MII oocytes from 3 different strains, C57B6/J, FVB/N and 129/Sv. There was no significant difference in the levels of IP<sub>3</sub>R1 protein between the MII oocytes from the three different strains. This result lead us to rule out the possibility that differences in the level of IP<sub>3</sub>R1 protein between the various strains of mice affect their individual susceptibility to formation of ovarian teratomas via their response to IP<sub>3</sub> signalling or their regulation of the Inpp4b protein. Therefore, we considered the

second possibility, that differences in the sequence of the *Itp1* gene between the various strains could lead to differences in their tendency to form ovarian teratoma.

When we analyzed for sequence differences in the IP<sub>3</sub>R1 mRNA among the three strains of mice, C57B6/J, FVB/N and *LT/Sv*, it was observed that there were 10 different SNPS but none of them gave rise to an amino acid change. It is therefore necessary to further analyze the IP<sub>3</sub>R1 protein for other possible differences that might lead to strain specificity for OT formation. Preliminary data (data not shown) indicate that there are two different forms of the IP<sub>3</sub>R1 cDNA in the ovary. The only difference between the two isoforms seems to be the lack of a single exon in one of them. It would be worthwhile to determine which isoform is present in the oocyte and if there is a difference in this isoform among the different strains.

Thus, from our results, it is possible to build a hypothesis to explain the role of Inpp4b and IP<sub>3</sub>R1 proteins during egg activation. In most vertebrates the development of the immature oocyte into a fertilizable gamete, a process known as oocyte maturation involves an arrest at metaphase of meiosis II. This arrest is brought about by the cytostatic factor (CSF) present in high levels in the MII oocyte. From our studies it appears that the Inpp4b could be one of the cytostatic factors as it shows a 10-fold increase in concentration from the GV stage of oogenesis to the MII stage, that stage of oogenesis where the specific function of the CSF is called upon (i.e., maintenance of Metaphase II arrest). At this stage, the high levels of Inpp4b, probably act on the PtdIns(4,5)P<sub>2</sub>'s, either directly or indirectly, converting them to monophosphates and thus keeping the concentration of the PtdIns(4,5)P<sub>2</sub>'s under the minimum levels required for egg activation. On fertilization by sperm or parthenogenetic activation, the levels of Inpp4b fall

dramatically, leading to a net increase in the PtdIns(4,5)P<sub>2</sub>'s, as has been observed by Halet et al. 2002. One or more phospholipases hydrolyze the PtdIns(4,5)P<sub>2</sub>'s to diacylglycerol and IP<sub>3</sub>. Soluble IP<sub>3</sub> interacts with IP<sub>3</sub>R1, and this interaction results in a series of Ca<sup>++</sup> oscillations which in turn mediates many of the molecular events associated with fertilization and the entry into mitosis and cell division. The Inpp4b could also act directly on the IP<sub>3</sub> at the MII stage, keeping their levels under the minimum level required for activation or it could associate with the IP<sub>3</sub>R1 and thus prevent the IP<sub>3</sub>-IP<sub>3</sub>R1 interaction that would otherwise lead to egg activation (Figure 35).

In the *FVB-Tgkd* mice, the low levels of Inpp4b in the MII oocytes probably lead to an increase in the PtdIns(4,5)P<sub>2</sub>'s during maturation and these in turn are acted upon by the phospholipases leading to the release of IP<sub>3</sub>. IP<sub>3</sub> associates with IP<sub>3</sub>R1 resulting in the Ca<sup>++</sup> oscillations which ultimately lead to oocyte activation and ovarian teratomas. It is also possible that low levels of Inpp4b could lead to an increase in IP<sub>3</sub> levels or IP<sub>3</sub>-IP<sub>3</sub>R1 interaction, thus leading to oocyte activation.

To confirm that Inpp4b levels are indeed associated with egg activation, it would be necessary to analyze the activation state of GV-stage and MII oocytes from FVB/N and *FVB-Tgkd* mice. These will include a number of measures like change in cortical granule content, time of pronucleus appearance and the number and amplitude of Ca<sup>++</sup> transients. The activation state of the oocytes will be induced by incubation in SrCl<sub>2</sub> and IP<sub>3</sub> injections. These experiments will be done by Dr. Norris A., Iowa State University, IA. If the oocytes from *FVB-Tgkd* mice indeed show a higher activation state than those from the wildtype mice, then it would confirm

our hypothesis that decreased levels of Inpp4b protein are indeed associated with physiological abnormalities of *FVB-Tgkd* germ cells.

Another factor to consider is the strain specificity that is seen in the occurrence of ovarian teratomas due to the transgene. Surprisingly, there is no dramatic decrease in the levels of Inpp4b protein in the MII oocytes from *129/Sv-Tgkd* mice when compared to the wildtype *129/Sv* mice, in spite of the insertion of the transgene. One hypothesis is that the FVB-derived *Ots2* gene, which is required for the formation of the *FVB-Tgkd* ovarian teratomas, is also responsible for the maintenance of Inpp4b levels. If it is confirmed that *Itp1* is indeed the *Ots2* gene, then it is possible that a variant form of the IP<sub>3</sub>R1 protein seen in the *C57B6/J-Tgkd* and probably in the *129/Sv-Tgkd* strains of mice, is able to bring back the level of Inpp4b protein back to the level seen in the wildtype mice and thus able to keep oocyte activation in check. In contrast, the IP<sub>3</sub>R1 protein variant seen in the *FVB-Tgkd* and *LT/Sv* mice is unable to maintain the Inpp4b levels and thus leads to ovarian teratoma formation.

Thus from our experiments, we have been able to shed some light on the role of Inpp4b and IP<sub>3</sub>R1 as potential genetic determinants for controlling spontaneous activation of unfertilized oocytes. These studies have brought our attention to new signaling pathways that could be involved in ovarian teratoma formation and further studies are necessary to elucidate the exact mechanism involved.

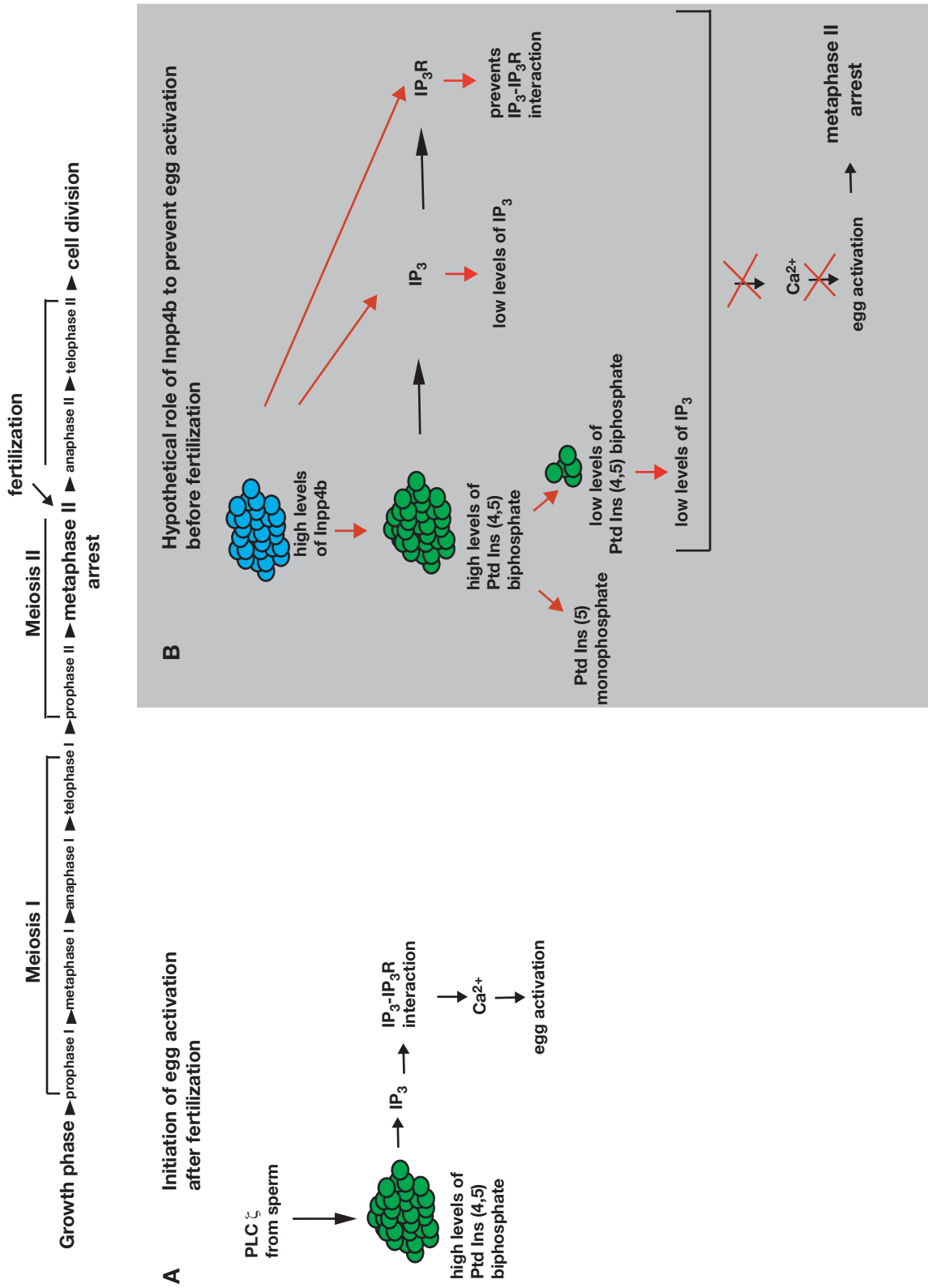


**Figure 35. Hypothetical role of Inpp4b during MII stage of oogenesis**

**Figure 35. Hypothetical role of Inpp4b during MII stage of oogenesis**

A. Initiation of egg activation after fertilization. A series of  $\text{Ca}^{++}$  oscillations mediates many of the molecular events associated with fertilization and the entry into mitosis (Cantrell 2001; Mehlmann and Kline 1994; Carroll 2001). The phosphatidylinositol (PtdIns) pathway appears to be primarily responsible for this increase in intracellular  $\text{Ca}^{++}$ . Here, one or more phospholipases (including phospholipase  $\text{C}\zeta$ ) hydrolyze  $\text{PtdIns}(4,5)\text{P}_2$  to DAG and  $\text{IP}_3$ . Soluble  $\text{IP}_3$  diffuses throughout the cytoplasm, until it encounters  $\text{IP}_3\text{R1}$  on endoplasmic reticulum. This interaction results in the release of  $\text{Ca}^{++}$  and an increase in the concentration of cytoplasmic free  $\text{Ca}^{++}$  (Xu et al. 2002). B. Hypothetical role of Inpp4b to prevent egg activation before fertilization. At the MII stage, the high levels of Inpp4b, probably act on the  $\text{PtdIns}(4,5)\text{P}_2$ , either directly or indirectly, converting them to monophosphates and thus keeping the concentration of the  $\text{PtdIns}(4,5)\text{P}_2$ 's under the minimum levels required for egg activation. The Inpp4b could also act directly on the  $\text{IP}_3$  at the MII stage, keeping their levels under the minimum level required for activation or it could associate with the  $\text{IP}_3\text{R1}$  and thus prevent the  $\text{IP}_3$ - $\text{IP}_3\text{R1}$  interaction which would otherwise lead to egg activation. Thus, through any of these pathways, Inpp4b could prevent the series of  $\text{Ca}^{++}$  oscillations which is responsible for the resumption of Meiosis II and cell division and thus prevent abnormal egg activation before fertilization

## BIBLIOGRAPHY

- Abbott, A. L., R. A. Fissore, et al. (1999). "Incompetence of preovulatory mouse oocytes to undergo cortical granule exocytosis following induced calcium oscillations." Dev Biol 207(1): 38-48.
- Andersen, C. B., R. A. Roth, et al. (1998). "Protein kinase B/Akt induces resumption of meiosis in *Xenopus* oocytes." J Biol Chem 273(30): 18705-8.
- Bansal, V. S., K. K. Caldwell, et al. (1990). "The isolation and characterization of inositol polyphosphate 4-phosphatase." J Biol Chem 265(3): 1806-11.
- Behboodi, E., W. Groen, et al. (2001). "Transgenic production from in vivo-derived embryos: effect on calf birth weight and sex ratio." Mol Reprod Dev 60(1): 27-37.
- Bestor, T. H. (2000). "The DNA methyltransferases of mammals." Hum Mol Genet 9(16): 2395-402.
- Bird, A. (2002). "DNA methylation patterns and epigenetic memory." Genes Dev 16(1): 6-21.
- Bourc'his, D., D. Le Bourhis, et al. (2001). "Delayed and incomplete reprogramming of chromosome methylation patterns in bovine cloned embryos." Curr Biol 11(19): 1542-6.
- Campbell, K. H., J. McWhir, et al. (1996). "Sheep cloned by nuclear transfer from a cultured cell line." Nature 380(6569): 64-6.
- Cantrell, D. A. (2001). "Phosphoinositide 3-kinase signalling pathways." J Cell Sci 114(Pt 8): 1439-45.
- Caplen, N. J., S. Parrish, et al. (2001). "Specific inhibition of gene expression by small double-stranded RNAs in invertebrate and vertebrate systems." Proc Natl Acad Sci U S A 98(17): 9742-7.
- Cardoso, M. C. and H. Leonhardt (1999). "DNA methyltransferase is actively retained in the cytoplasm during early development." J Cell Biol 147(1): 25-32.
- Carlson, L. L., A. W. Page, et al. (1992). "Properties and localization of DNA methyltransferase in preimplantation mouse embryos: implications for genomic imprinting." Genes Dev 6(12B): 2536-41.

- Carroll, J., K. Swann, et al. (1994). "Spatiotemporal dynamics of intracellular  $[Ca^{2+}]_i$  oscillations during the growth and meiotic maturation of mouse oocytes." Development 120(12): 3507-17.
- Carroll, J. (2001). "The initiation and regulation of  $Ca^{2+}$  signalling at fertilization in mammals." Semin Cell Dev Biol 12(1): 37-43.
- Cattanach, B. M. and M. Kirk (1985). "Differential activity of maternally and paternally derived chromosome regions in mice." Nature 315(6019): 496-8.
- Cattanach, B. M., J. A. Barr, et al. (1992). "A candidate mouse model for Prader-Willi syndrome which shows an absence of Snrpn expression." Nat Genet 2(4): 270-4.
- Cattanach, B. M. a. B., C.V. (1997). Genomic imprinting in the mouse: Possible final analysis in genomic imprinting. Frontiers in molecular biology. W. a. S. A. Reik, IRL Press: 118-141.
- Chaillet, J. R., T. F. Vogt, et al. (1991). "Parental-specific methylation of an imprinted transgene is established during gametogenesis and progressively changes during embryogenesis." Cell 66(1): 77-83.
- Chaillet, J. R. (1994). "Genomic imprinting: lessons from mouse transgenes." Mutat Res 307(2): 441-9.
- Chaillet, J. R., D. S. Bader, et al. (1995). "Regulation of genomic imprinting by gametic and embryonic processes." Genes Dev 9(10): 1177-87.
- Chakravarti, A., P. P. Majumder, et al. (1989). "Gene-centromere mapping and the study of non-disjunction in autosomal trisomies and ovarian teratomas." Prog Clin Biol Res 311: 45-79.
- Chung, Y. G., M. R. Mann, et al. (2002). "Nuclear-cytoplasmic "tug of war" during cloning: effects of somatic cell nuclei on culture medium preferences of preimplantation cloned mouse embryos." Biol Reprod 66(4): 1178-84.
- Chung, Y. G., S. Ratnam, et al. (2003). "Abnormal regulation of DNA methyltransferase expression in cloned mouse embryos." Biol Reprod 69(1): 146-53.
- Clarke, H. J., C. Oblin, et al. (1992). "Developmental regulation of chromatin composition during mouse embryogenesis: somatic histone H1 is first detectable at the 4-cell stage." Development 115(3): 791-9.
- Colledge, W. H., M. B. Carlton, et al. (1994). "Disruption of c-mos causes parthenogenetic development of unfertilized mouse eggs." Nature 370(6484): 65-8.
- Crooijmans, R. P., R. J. Dijkhof, et al. (2001). "The gene orders on human chromosome 15 and chicken chromosome 10 reveal multiple inter- and intrachromosomal rearrangements." Mol Biol Evol 18(11): 2102-9.

- Damjanov, I. K., bb;Solter,d (1983). the human teratomas: experimental and clinical biology. the pathology of human teratomas. i. Damjanov. Clifton, NJ, Hunana: 23-66.
- Dean, W., F. Santos, et al. (2001). "Conservation of methylation reprogramming in mammalian development: aberrant reprogramming in cloned embryos." Proc Natl Acad Sci U S A 98(24): 13734-8.
- DeChiara, T. M., E. J. Robertson, et al. (1991). "Parental imprinting of the mouse insulin-like growth factor II gene." Cell 64(4): 849-59.
- Deka, R., A. Chakravarti, et al. (1990). "Genetics and biology of human ovarian teratomas. II. Molecular analysis of origin of nondisjunction and gene-centromere mapping of chromosome I markers." Am J Hum Genet 47(4): 644-55.
- Dennis, K., T. Fan, et al. (2001). "Lsh, a member of the SNF2 family, is required for genome-wide methylation." Genes Dev 15(22): 2940-4.
- Ding, F. and J. R. Chaillet (2002). "In vivo stabilization of the Dnmt1 (cytosine-5)-methyltransferase protein." Proc Natl Acad Sci U S A 99(23): 14861-6.
- Dong, A., J. A. Yoder, et al. (2001). "Structure of human DNMT2, an enigmatic DNA methyltransferase homolog that displays denaturant-resistant binding to DNA." Nucleic Acids Res 29(2): 439-48.
- Dorward, A. M., K. L. Shultz, et al. (2003). "High-resolution genetic map of X-linked juvenile-type granulosa cell tumor susceptibility genes in mouse." Cancer Res 63(23): 8197-202.
- Ducibella, T., E. Anderson, et al. (1988). "Quantitative studies of changes in cortical granule number and distribution in the mouse oocyte during meiotic maturation." Dev Biol 130(1): 184-97.
- Ducibella, T., S. Kurasawa, et al. (1990). "Precocious loss of cortical granules during mouse oocyte meiotic maturation and correlation with an egg-induced modification of the zona pellucida." Dev Biol 137(1): 46-55.
- Eddy, E. C., JM; Gong,D; Fenderson,BA (1981). "origin and migration of primordial germ cells in mammals." gamete research 4: 333-362.
- Eggan, K., H. Akutsu, et al. (2001). "Hybrid vigor, fetal overgrowth, and viability of mice derived by nuclear cloning and tetraploid embryo complementation." Proc Natl Acad Sci U S A 98(11): 6209-14.
- Eicher, E. M. (1978). "Murine ovarian teratomas and parthenotes as cytogenetic tools." Cytogenet Cell Genet 20(1-6): 232-9.
- Eppig, J. J., L. P. Kozak, et al. (1977). "Ovarian teratomas in mice are derived from oocytes that have completed the first meiotic division." Nature 269(5628): 517-8.

- Eppig, J. J., K. Wigglesworth, et al. (1996). "Genetic regulation of traits essential for spontaneous ovarian teratocarcinogenesis in strain LT/Sv mice: aberrant meiotic cell cycle, oocyte activation, and parthenogenetic development." Cancer Res 56(21): 5047-54.
- Fafalios, M. K., E. A. Olander, et al. (1996). "Ovarian teratomas associated with the insertion of an imprinted transgene." Mamm Genome 7(3): 188-93.
- Fafalios, M. K., E. A. Olander, et al. (1996). "Ovarian teratomas associated with the insertion of an imprinted transgene." Mamm Genome 7(3): 188-93.
- Fairburn, H. R., L. E. Young, et al. (2002). "Epigenetic reprogramming: how now, cloned cow?" Curr Biol 12(2): R68-70.
- Fissore, R. A., F. J. Longo, et al. (1999). "Differential distribution of inositol trisphosphate receptor isoforms in mouse oocytes." Biol Reprod 60(1): 49-57.
- Gardner, R. (1983). "Teratomas in perspective." cancer surveys 2: 1-19.
- Gluzman, Y. (1981). "SV40-transformed simian cells support the replication of early SV40 mutants." Cell 23(1): 175-82.
- Groudine, M. and H. Weintraub (1981). "Activation of globin genes during chicken development." Cell 24(2): 393-401.
- Gurdon, J. B. (1962). "Adult frogs derived from the nuclei of single somatic cells." Dev Biol 4: 256-73.
- Halet, G., R. Tunwell, et al. (2002). "The dynamics of plasma membrane PtdIns(4,5)P(2) at fertilization of mouse eggs." J Cell Sci 115(Pt 10): 2139-49.
- Hashimoto, N., N. Watanabe, et al. (1994). "Parthenogenetic activation of oocytes in c-mos-deficient mice." Nature 370(6484): 68-71.
- Hata, K., M. Okano, et al. (2002). "Dnmt3L cooperates with the Dnmt3 family of de novo DNA methyltransferases to establish maternal imprints in mice." Development 129(8): 1983-93.
- Hehl, S., B. Stoyanov, et al. (2001). "Phosphoinositide 3-kinase-gamma induces Xenopus oocyte maturation via lipid kinase activity." Biochem J 360(Pt 3): 691-8.
- Hermann, A., S. Schmitt, et al. (2003). "The human Dnmt2 has residual DNA-(cytosine-C5) methyltransferase activity." J Biol Chem 278(34): 31717-21.
- Hogan, B. B., DP; Tilly, R (1983). "F9 teratocarcinoma cells as a model for the differentiation of parietal and visceral endoderm in the mouse embryo." Cancer Surveys 2: 115-140.
- Hogan, B., Constantini, F., Lacy, E. (1986). Manipulating the Mouse Embryo: A laboratory Manual. Cold Spring Harbor, Cold Spring Harbor Laboratory Press.

- Howell, C. Y., T. H. Bestor, et al. (2001). "Genomic imprinting disrupted by a maternal effect mutation in the Dnmt1 gene." Cell 104(6): 829-38.
- Humpherys, D., K. Eggan, et al. (2001). "Epigenetic instability in ES cells and cloned mice." Science 293(5527): 95-7.
- Ilgren, E. V., DJT (1983). "The comparative pathology of teratomas." Cancer Surveys 2(209-215).
- Issa, J. P., P. M. Vertino, et al. (1993). "Increased cytosine DNA-methyltransferase activity during colon cancer progression." J Natl Cancer Inst 85(15): 1235-40.
- Jacobs, P. A., C. M. Wilson, et al. (1980). "Mechanism of origin of complete hydatidiform moles." Nature 286(5774): 714-6.
- Jellerette, T., C. L. He, et al. (2000). "Down-regulation of the inositol 1,4,5-trisphosphate receptor in mouse eggs following fertilization or parthenogenetic activation." Dev Biol 223(2): 238-50.
- Kajii, T. and K. Ohama (1977). "Androgenetic origin of hydatidiform mole." Nature 268(5621): 633-4.
- Kaneko-Ishino, T., Y. Kuroiwa, et al. (1995). "Peg1/Mest imprinted gene on chromosome 6 identified by cDNA subtraction hybridization." Nat Genet 11(1): 52-9.
- Kang, Y. K., D. B. Koo, et al. (2001). "Aberrant methylation of donor genome in cloned bovine embryos." Nat Genet 28(2): 173-7.
- Kang, Y. K., D. B. Koo, et al. (2001). "Typical demethylation events in cloned pig embryos. Clues on species-specific differences in epigenetic reprogramming of a cloned donor genome." J Biol Chem 276(43): 39980-4.
- Kato, Y., A. Yabuuchi, et al. (1999). "Developmental potential of mouse follicular epithelial cells and cumulus cells after nuclear transfer." Biol Reprod 61(4): 1110-4.
- Kimura, T., A. Suzuki, et al. (2003). "Conditional loss of PTEN leads to testicular teratoma and enhances embryonic germ cell production." Development 130(8): 1691-700.
- Kubiak, J. Z. and M. A. Ciemerych (2001). "Cell cycle regulation in early mouse embryos." Novartis Found Symp 237: 79-89; discussion 89-99.
- Latham, K. E. (1999). "Mechanisms and control of embryonic genome activation in mammalian embryos." Int Rev Cytol 19: 71-124.
- Lee, G. H., J. M. Bugni, et al. (1997). "Genetic dissection of susceptibility to murine ovarian teratomas that originate from parthenogenetic oocytes." Cancer Res 57(4): 590-3.

- Lei, H., S. P. Oh, et al. (1996). "De novo DNA cytosine methyltransferase activities in mouse embryonic stem cells." Development 122(10): 3195-205.
- Li, E., T. H. Bestor, et al. (1992). "Targeted mutation of the DNA methyltransferase gene results in embryonic lethality." Cell 69(6): 915-26.
- Li, E., C. Beard, et al. (1993). "Role for DNA methylation in genomic imprinting." Nature 366(6453): 362-5.
- Linder, D. (1969). "Gene loss in human teratomas." Proc Natl Acad Sci U S A 63(3): 699-704.
- Linder, D., B. K. McCaw, et al. (1975). "Parthenogenic origin of benign ovarian teratomas." N Engl J Med 292(2): 63-6.
- Lira, S. A., R. A. Kinloch, et al. (1990). "An upstream region of the mouse ZP3 gene directs expression of firefly luciferase specifically to growing oocytes in transgenic mice." Proc Natl Acad Sci U S A 87(18): 7215-9.
- Liu, K., Y. F. Wang, et al. (2003). "Endogenous assays of DNA methyltransferases: Evidence for differential activities of DNMT1, DNMT2, and DNMT3 in mammalian cells in vivo." Mol Cell Biol 23(8): 2709-19.
- Lorca, T., A. Castro, et al. (1998). "Fizzy is required for activation of the APC/cyclosome in Xenopus egg extracts." Embo J 17(13): 3565-75.
- Lyon, M. F. (1992). "Some milestones in the history of X-chromosome inactivation." Annu Rev Genet 26: 16-28.
- Mahler, J. F., W. Stokes, et al. (1996). "Spontaneous lesions in aging FVB/N mice." Toxicol Pathol 24(6): 710-6.
- Majerus, P. W., T. S. Ross, et al. (1990). "Recent insights in phosphatidylinositol signaling." Cell 63(3): 459-65.
- Maleszewski, M. Y., R (1995). "Spontaneous and sperm-induced activation of oocytes in LT/Sv strain of mice." Developmental and Growth Differentiation 37: 679-685.
- Martin, G. R. (1980). "Teratocarcinomas and mammalian embryogenesis." Science 209(4458): 768-76.
- Martin, G. R. (1981). "Isolation of a pluripotent cell line from early mouse embryos cultured in medium conditioned by teratocarcinoma stem cells." Proc Natl Acad Sci U S A 78(12): 7634-8.
- Masui, Y. and C. L. Markert (1971). "Cytoplasmic control of nuclear behavior during meiotic maturation of frog oocytes." J Exp Zool 177(2): 129-45.

- Masui, Y. (2000). "The elusive cytotostatic factor in the animal egg." Nat Rev Mol Cell Biol 1(3): 228-32.
- McGrath, J. and D. Solter (1984). "Inability of mouse blastomere nuclei transferred to enucleated zygotes to support development in vitro." Science 226(4680): 1317-9.
- Meehan, R. R., S. Pennings, et al. (2001). "Lashings of DNA methylation, forkfuls of chromatin remodeling." Genes Dev 15(24): 3231-6.
- Meehan, R. R. (2003). "DNA methylation in animal development." Semin Cell Dev Biol 14(1): 53-65.
- Mehlmann, L. M. and D. Kline (1994). "Regulation of intracellular calcium in the mouse egg: calcium release in response to sperm or inositol trisphosphate is enhanced after meiotic maturation." Biol Reprod 51(6): 1088-98.
- Mertineit, C., J. A. Yoder, et al. (1998). "Sex-specific exons control DNA methyltransferase in mammalian germ cells." Development 125(5): 889-97.
- Mintz, B. and R. A. Fleischman (1981). "Teratocarcinomas and other neoplasms as developmental defects in gene expression." Adv Cancer Res 34: 211-78.
- Monk, M., M. Boubelik, et al. (1987). "Temporal and regional changes in DNA methylation in the embryonic, extraembryonic and germ cell lineages during mouse embryo development." Development 99(3): 371-82.
- Morison, I. M. and A. E. Reeve (1998). "A catalogue of imprinted genes and parent-of-origin effects in humans and animals." Hum Mol Genet 7(10): 1599-609.
- Nebreda, A. R. and T. Hunt (1993). "The c-mos proto-oncogene protein kinase turns on and maintains the activity of MAP kinase, but not MPF, in cell-free extracts of Xenopus oocytes and eggs." Embo J 12(5): 1979-86.
- Nicholls, R. D. and J. L. Knepper (2001). "Genome organization, function, and imprinting in Prader-Willi and Angelman syndromes." Annu Rev Genomics Hum Genet 2: 153-75.
- Norris, F. A. and P. W. Majerus (1994). "Hydrolysis of phosphatidylinositol 3,4-bisphosphate by inositol polyphosphate 4-phosphatase isolated by affinity elution chromatography." J Biol Chem 269(12): 8716-20.
- Norris, F. A., R. C. Atkins, et al. (1997). "The cDNA cloning and characterization of inositol polyphosphate 4-phosphatase type II. Evidence for conserved alternative splicing in the 4-phosphatase family." J Biol Chem 272(38): 23859-64.
- O'Neill, G. T. and M. H. Kaufman (1987). "Ovulation and fertilization of primary and secondary oocytes in LT/Sv strain mice." Gamete Res 18(1): 27-36.

- Ohama, K., K. Nomura, et al. (1985). "Origin of immature teratoma of the ovary." Am J Obstet Gynecol 152(7 Pt 1): 896-900.
- Ohara, O., R. L. Dorit, et al. (1989). "One-sided polymerase chain reaction: the amplification of cDNA." Proc Natl Acad Sci U S A 86(15): 5673-7.
- Ohgane, J., T. Wakayama, et al. (2001). "DNA methylation variation in cloned mice." Genesis 30(2): 45-50.
- Ohteki, T., K. Suzue, et al. (2001). "Critical role of IL-15-IL-15R for antigen-presenting cell functions in the innate immune response." Nat Immunol 2(12): 1138-43.
- Okano, M., S. Xie, et al. (1998). "Cloning and characterization of a family of novel mammalian DNA (cytosine-5) methyltransferases." Nat Genet 19(3): 219-20.
- Okano, M., D. W. Bell, et al. (1999). "DNA methyltransferases Dnmt3a and Dnmt3b are essential for de novo methylation and mammalian development." Cell 99(3): 247-57.
- Oswald, J., S. Engemann, et al. (2000). "Active demethylation of the paternal genome in the mouse zygote." Curr Biol 10(8): 475-8.
- Parrington, J. M., L. F. West, et al. (1984). "The origin of ovarian teratomas." J Med Genet 21(1): 4-12.
- Patel, S., S. K. Joseph, et al. (1999). "Molecular properties of inositol 1,4,5-trisphosphate receptors." Cell Calcium 25(3): 247-64.
- Peter, M., A. Castro, et al. (2001). "The APC is dispensable for first meiotic anaphase in *Xenopus* oocytes." Nat Cell Biol 3(1): 83-7.
- Peterson, W. P., EC; Edmunds, FT; Hundley, JM; Morris FK (1955). "Benign cystic teratomas of the ovary: a clinico-statistical study of 1,007 cases with a review of the literature." American Journal of Obstetrics and Gynecology 70: 368-382.
- Peterson, W. (1957). "Malignant degeneration of benign cystic teratomas of the ovary: a collective review of the literature." Obstet. Gynecol Surv 12: 793-830.
- Philpott, C. C., M. J. Ringuette, et al. (1987). "Oocyte-specific expression and developmental regulation of ZP3, the sperm receptor of the mouse zona pellucida." Dev Biol 121(2): 568-75.
- Polejaeva, I. A., S. H. Chen, et al. (2000). "Cloned pigs produced by nuclear transfer from adult somatic cells." Nature 407(6800): 86-90.
- Ratnam, S., C. Mertineit, et al. (2002). "Dynamics of Dnmt1 methyltransferase expression and intracellular localization during oogenesis and preimplantation development." Dev Biol 245(2): 304-14.

- Reik, W. and W. Dean (2001). "DNA methylation and mammalian epigenetics." Electrophoresis 22(14): 2838-43.
- Renard, J. P., S. Chastant, et al. (1999). "Lymphoid hypoplasia and somatic cloning." Lancet 353(9163): 1489-91.
- Richards, E. J. and S. C. Elgin (2002). "Epigenetic codes for heterochromatin formation and silencing: rounding up the usual suspects." Cell 108(4): 489-500.
- Roy, P. H. and A. Weissbach (1975). "DNA methylase from HeLa cell nuclei." Nucleic Acids Res 2(10): 1669-84.
- Sagata, N., M. Oskarsson, et al. (1988). "Function of c-mos proto-oncogene product in meiotic maturation in *Xenopus* oocytes." Nature 335(6190): 519-25.
- Sanford, J. P., H. J. Clark, et al. (1987). "Differences in DNA methylation during oogenesis and spermatogenesis and their persistence during early embryogenesis in the mouse." Genes Dev 1(10): 1039-46.
- Saunders, C. M., M. G. Larman, et al. (2002). "PLC zeta: a sperm-specific trigger of Ca(2+) oscillations in eggs and embryo development." Development 129(15): 3533-44.
- Sheets, M. D., C. A. Fox, et al. (1994). "The 3'-untranslated regions of c-mos and cyclin mRNAs stimulate translation by regulating cytoplasmic polyadenylation." Genes Dev 8(8): 926-38.
- Shibuya, E. K. and J. V. Ruderman (1993). "Mos induces the in vitro activation of mitogen-activated protein kinases in lysates of frog oocytes and mammalian somatic cells." Mol Biol Cell 4(8): 781-90.
- Spemann, H. (1938). Embryo Development and Induction. New Haven, CT, Yale University Press.
- Stein, P., P. Svoboda, et al. (2003). "Transgenic RNAi in mouse oocytes: a simple and fast approach to study gene function." Dev Biol 256(1): 187-93.
- Stevens, L. C. (1973). "A new inbred subline of mice (129-terSv) with a high incidence of spontaneous congenital testicular teratomas." J Natl Cancer Inst 50(1): 235-42.
- Stevens, L. C. and D. S. Varnum (1974). "The development of teratomas from parthenogenetically activated ovarian mouse eggs." Dev Biol 37(2): 369-80.
- Stevens, L. (1983). "Testicular, ovarian and embryo-derived teratomas." cancer surveys 2: 75-91.
- Stoger, R., P. Kubicka, et al. (1993). "Maternal-specific methylation of the imprinted mouse *Igf2r* locus identifies the expressed locus as carrying the imprinting signal." Cell 73(1): 61-71.

- Surani, M. A., S. C. Barton, et al. (1986). "Nuclear transplantation in the mouse: heritable differences between parental genomes after activation of the embryonic genome." Cell 45(1): 127-36.
- Surti, U., L. Hoffner, et al. (1990). "Genetics and biology of human ovarian teratomas. I. Cytogenetic analysis and mechanism of origin." Am J Hum Genet 47(4): 635-43.
- Szabo, P. E. and J. R. Mann (1995). "Biallelic expression of imprinted genes in the mouse germ line: implications for erasure, establishment, and mechanisms of genomic imprinting." Genes Dev 9(15): 1857-68.
- Taieb, F. E., S. D. Gross, et al. (2001). "Activation of the anaphase-promoting complex and degradation of cyclin B is not required for progression from Meiosis I to II in *Xenopus* oocytes." Curr Biol 11(7): 508-13.
- Tamashiro, K. L., T. Wakayama, et al. (2000). "Postnatal growth and behavioral development of mice cloned from adult cumulus cells." Biol Reprod 63(1): 328-34.
- Tanaka, S., M. Oda, et al. (2001). "Placentomegaly in cloned mouse concepti caused by expansion of the spongiotrophoblast layer." Biol Reprod 65(6): 1813-21.
- Tang, L. Y., M. N. Reddy, et al. (2003). "The eukaryotic DNMT2 genes encode a new class of cytosine-5 DNA methyltransferases." J Biol Chem 278(36): 33613-6.
- Trasler, J. M., D. G. Trasler, et al. (1996). "DNA methyltransferase in normal and *Dnmtn/Dnmtn* mouse embryos." Dev Dyn 206(3): 239-47.
- Tremblay, K. D., J. R. Saam, et al. (1995). "A paternal-specific methylation imprint marks the alleles of the mouse H19 gene." Nat Genet 9(4): 407-13.
- Tunquist, B. J. and J. L. Maller (2003). "Under arrest: cytostatic factor (CSF)-mediated metaphase arrest in vertebrate eggs." Genes Dev 17(6): 683-710.
- Van den Wyngaert, I., J. Sprengel, et al. (1998). "Cloning and analysis of a novel human putative DNA methyltransferase." FEBS Lett 426(2): 283-9.
- Waddington, C. H. (1957). The strategy of the genes. London, Allen and Unwin.
- Wakayama, T., A. C. Perry, et al. (1998). "Full-term development of mice from enucleated oocytes injected with cumulus cell nuclei." Nature 394(6691): 369-74.
- Wakayama, T. and R. Yanagimachi (2001). "Effect of cytokinesis inhibitors, DMSO and the timing of oocyte activation on mouse cloning using cumulus cell nuclei." Reproduction 122(1): 49-60.
- Walsh, C. P., J. R. Chaillet, et al. (1998). "Transcription of IAP endogenous retroviruses is constrained by cytosine methylation." Nat Genet 20(2): 116-7.

- Weintraub, H. (1985). "Assembly and propagation of repressed and depressed chromosomal states." Cell 42(3): 705-11.
- West, J. D., S. Webb, et al. (1993). "Inheritance of a meiotic abnormality that causes the ovulation of primary oocytes and the production of digynic triploid mice." Genet Res 62(3): 183-93.
- Wigler, M. H. (1981). "The inheritance of methylation patterns in vertebrates." Cell 24(2): 285-6.
- Willadsen, S. M. (1979). "A method for culture of micromanipulated sheep embryos and its use to produce monozygotic twins." Nature 277(5694): 298-300.
- Wilmut, I., A. E. Schnieke, et al. (1997). "Viable offspring derived from fetal and adult mammalian cells." Nature 385(6619): 810-3.
- Xu, Z., A. Abbott, et al. (1997). "Spontaneous activation of ovulated mouse eggs: time-dependent effects on M-phase exit, cortical granule exocytosis, maternal messenger ribonucleic acid recruitment, and inositol 1,4,5-trisphosphate sensitivity." Biol Reprod 57(4): 743-50.
- Xu, G. L., T. H. Bestor, et al. (1999). "Chromosome instability and immunodeficiency syndrome caused by mutations in a DNA methyltransferase gene." Nature 402(6758): 187-91.
- Xu, Z., C. J. Williams, et al. (2003). "Maturation-associated increase in IP3 receptor type 1: role in conferring increased IP3 sensitivity and Ca<sup>2+</sup> oscillatory behavior in mouse eggs." Dev Biol 254(2): 163-71.
- Yanagimachi, R. (2002). "Cloning: experience from the mouse and other animals." Mol Cell Endocrinol 187(1-2): 241-8.
- Yoder, J. A., R. W. Yen, et al. (1996). "New 5' regions of the murine and human genes for DNA (cytosine-5)-methyltransferase." J Biol Chem 271(49): 31092-7.
- Yoder, J. A., N. S. Soman, et al. (1997). "DNA (cytosine-5)-methyltransferases in mouse cells and tissues. Studies with a mechanism-based probe." J Mol Biol 270(3): 385-95.
- Young, L. E., K. Fernandes, et al. (2001). "Epigenetic change in IGF2R is associated with fetal overgrowth after sheep embryo culture." Nat Genet 27(2): 153-4.
- Zeschnigk, M., B. Schmitz, et al. (1997). "Imprinted segments in the human genome: different DNA methylation patterns in the Prader-Willi/Angelman syndrome region as determined by the genomic sequencing method." Hum Mol Genet 6(3): 387-95.